CREATION RESEARCH SOCIETY

QUARTERLY

Volume 61 Winter 2025 Number 3

- FOSSIL CROCODYLIANS GREW LARGER AND LONGER AND LIVED LONGER
- THE NORTH AMERICAN MIDCONTINENT AND THE GENESIS FLOOD PART II: RIFTING AND THE FLOOD
- ORIGINAL POLYPLOIDY AS A CONTRIBUTOR TO DIVERSIFICATION
- DOES THE MATURE CREATION CONCEPT EXPLAIN THE SOLAR SYSTEM'S CREATION?
- NUMERICAL EVALUATION OF POST-FLOOD FORMATION OF TRANSVERSE DRAINAGES (WATER GAPS)
- ABSTRACTS OF THE CREATION RESEARCH SOCIETY ANNUAL CONFERENCE 2024

CREATION RESEARCH SOCIETY
QUARTERLY
Volume 61
Number 3 | Winter 2025

Articles

Fossil Crocodilians Grew Larger and Longer, and Lived Longer than Extant Crocodilians ... 172
Jake Hebert

Original Polyploidy as a Contributor to Diversification ... 189
Harry Sanders

Numerical Evaluation of Post-Flood Formation of Transverse Drainages (Water Gaps) ... 202
Nathan W. Mogk

Does the Mature Creation Concept Explain the Solar System's Creation? ... 213
Jerry Bergman

The North American Midcontinent and the Genesis Flood Part II: Rifting and the Flood ... 221
John K. Reed, Michael J. Oard, Peter Klevberg

Departments

Conference Abstracts: 11th Annual CRS Conference Review ... 239

Letter to the Editor: Structure of the Cosmos ... 250

Media Review ... 253

Instructions to Authors ... 255

Membership/Subscription Application and Renewal Form ... 257

Order Blank for Past Issues ... 258

CREATION RESEARCH SOCIETY
QUARTERLY

Volume 61
Number 3 | Winter 2025

Haec Credimus

*For in six days the Lord made heaven and earth, the sea,
and all that in them is, and rested on the seventh. —Exodus 20:11*

Cover by Michael E. Erkel, Afton, Virginia

Design services by Cindy Blandon,
cblandon@aol.com

The *Creation Research Society Quarterly* is published by the Creation Research Society, 1 W. Firestorm Way #145, Glendale, AZ 85306, and it is indexed in the *Christian Periodical Index* and the *Zoological Record.*

Send papers on all subjects to the Editor:
CRSQeditor@creationresearch.org or to
Tim Clarey, 1806 Royal Lane, Dallas, TX 75229.

Send book reviews to the Book Review Editor:
Mary Beth Kaiser, Book Review Editor,
marybethd4@gmail.com.

ISSN 0092-9166

Printed in the United States of America

Creation Research Society Quarterly 2025 61:172–188

Fossil Crocodilians Grew Larger and Longer, and Lived Longer than Extant Crocodilians

Jake Hebert

Abstract

Whatever factor or factors enabled extreme human longevity in the pre- and immediate post-Flood worlds likely also affected the animal kingdom. Thus, direct or indirect evidence for greater past animal longevity is also *de facto* evidence for greater past human longevity. The field of skeletochronology is making it possible to deduce information about the ontogenetic growth trajectories of giant fossil crocodilians such as *Deinosuchus riograndensis* (alternately, *D. hatcheri*) and *Sarcosuchus imperator*. Their growth curves indicate that these crocodilians grew for at least 50–60 years, a duration significantly greater than even the total typical 30-year lifespan of extant crocodilians. Moreover, a smoothed *Deinosuchus* growth curve published in the mainstream evolutionary literature suggests this age of 50 years likely significantly underestimates the true age at maturity. Given the evidence from longevity studies linking both larger adult body sizes and greater ages at maturation to greater longevity, the large adult body sizes of *Deinosuchus* and *Sarcosuchus* and their prolonged maturation intervals are indirect evidence of lifespans greater than extant crocodilians. Other giant fossil crocodilians, some of which may be direct ancestors of extant crocodilians, were also likely experiencing greater longevity. Moreover, the similarity of giant crocodilian body sizes in Cretaceous, Miocene, and Pliocene strata suggest that these crocodilians obtained their giant sizes under similar environmental conditions. This could suggest they all lived in the pre-Flood world and would be another argument for a 'high' Cenozoic Flood/post-Flood boundary.

Key Words: crocodilians, *Deinosuchus, Euthecodon brumpti,* fossils, giantism, *Gryposuchus croizati,* longevity, ontogeny, pre-Flood, *Purussaurus brasiliensis, Rhamposuchus, Sarcosuchus imperator,* von Bertalanffy growth curves

---

Accepted for publication March 21, 2024

Introduction

Creation researchers have long noted (e.g., Taylor, 1987; Morris, 1993, Woetzel, 2013; Nelson, 2017; and Coppedge, 2023) that extant animals are often represented by much larger and more massive fossil ancestors. This trend extends to the crocodilians, members of the order Crocodylia (or Crocodilia). The order Crocodylia is composed of three extant families, Crocodylidae, Alligatoridae, and Gavialidae. The family Crocodylidae is composed of true crocodiles, while the Alligatoridae consists of alligators and caimans. The Gavialidae consists of gharials and false gharials.

Crocodilians generally have similar body shapes (Figure 1) but vary in size and especially in the shape of their snouts. The gharial and false gharial have long, narrow snouts compared to most crocodilians. Likewise, the jaws of alligators and caimans tend to be more 'U'-shaped than the 'V'-shaped jaws of crocodiles, and a greater number of teeth are visible in the mouths of crocodiles than in alligators (Hennigan, 2008). As a matter of nomenclature, the name 'crocodilian' is used as a generic term for all crocodile/alligator/gharial-like animals, extant and extinct, whereas 'crocodile' is used to indicate only true crocodiles in the family Crocodylidae.

Of particular relevance to this study are the giant fossil crocodilians *Deinosuchus riograndensis* (or *Deinosuchus hatcheri*) and *Sarcosuchus imperator*. Their fossils are found in Cretaceous strata, stratigraphically below the K-Pg (or K-T) boundary, which means they must date from the Flood, regardless of whether one holds to a 'high' or 'low' Cenozoic boundary between Flood and post-Flood rocks.

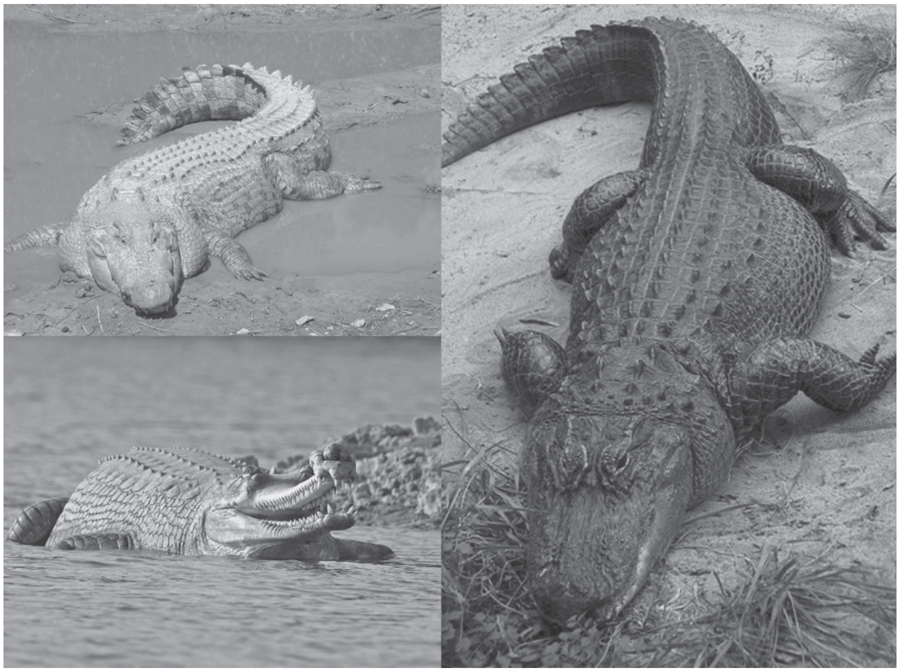

Figure 1. Representatives of the three families in the order Crocodilia: Crocodylidae, Alligatoridae, and Gavialidae. Clockwise, starting from top-left of image: the saltwater crocodile (*Crocodylus porosus*), the American alligator (*Alligator mississippiensis*), and the gharial (*Gavialis gangeticus*). Image credits: Composite Image: Little Jerry, CC BY-SA 4.0. https://creativecommons.org/licenses/by-sa/4.0/. Saltwater crocodile image credit: Molly Ebersold of the St. Augustine Alligator Farm (public domain). American alligator image credit: Postdlf, CCA-SA 3.0 Unported. https://creativecommons.org/licenses/by-sa/3.0/deed.en. Gharial image credit: Charles J. Sharp; sharpphotography.co.uk. CCA-SA 4.0 International. https://creativecommons.org/licenses/by-sa/4.0/deed.en.

Deinosuchus Background Information

The suffix *suchus* is the Latin form of the Greek word *soukhos*, which refers to a *crocodile* (Sibley 2023). Of course, *deino* is Greek for "terrible" (e.g., *dinosaur* means "terrible lizard"). Thus the name *Deinosuchus* means (Figure 2) 'terrible crocodile' or 'terror crocodile,' but it has been described as an 'alligatoroid,' more closely related to alligators than to crocodiles (Cossette and Brochu, 2020; Diaz, 2020).

Deinosuchus expert David Schwimmer (2002, p. 13) wrote that "to the casual observer, a *Deinosuchus* would appear to be a cross between a huge alligator and a huge crocodile" and stated that it would be "almost indistinguishable" from living crocodilians (Broom, 2018). Nevertheless, Schwimmer has said that he is not comfortable describing *Deinosuchus* as an alligator or crocodile *per se* (Schwimmer, 2002, p. viii). *Deinosuchus* had some noticeable anatomical differences between it and extant crocodilians, particularly its bulbous snout that is absent from extant crocodilians. Hence, it may have belonged to a different Genesis kind than the kind or kinds to which extant crocodilians belong.

Deinosuchus was enormous. Most body length estimates range from the more conservative 8–10 meters (Erickson and Brochu, 1999) to more generous estimates of 10.6 to 13.7 meters (Broom, 2018). An 8-to-10-meter-long

Deinosuchus would have an estimated body mass of between 2500 and 5000 kilograms (Erickson and Brochu, 1999).

A well-known painting by R.D. Martin depicts a *Deinosuchus* lunging from a body of water, preparing to take a bite out of a startled *Albertosaurus*. Given the likely fearsomeness of this creature, Thomas and Biddle (2023) have suggested *Deinosuchus* as a candidate for the Biblical Leviathan described in Job 41.

By evolutionary reckoning, *Deinosuchus* lived about 83 to 74 million year ago, during the Late Cretaceous. Schwimmer (2002, pp. 48, 107) has noted that *D. hatcheri* and *D. riograndensis* specimens from the American west and southwest (e.g., Texas and Montana) tend to be larger but less numerous than the *D. schwimmeri* (formerly *D. rugosus*) specimens from the eastern United States (Mississippi, Alabama, Georgia, and North Carolina). Or to put it another way, *Deinosuchus* specimens on the western side of the so-called Late Cretaceous Western Interior Seaway are larger and less numerous than those on the eastern side. Schwimmer (2002) estimates the eastern variety to be about 8 meters long, but the west-southwestern variety to be possibly as long as 12 meters. One possible explanation for the difference in body sizes could be CET (continuous environmental tracking) adaptations to different environments (Guliuzza and Gaskill, 2018). Another possibility is that larger adults panicked during the Flood, leaving behind the more numerous but smaller and slower juveniles, so that they were physically separated during the chaos of the Flood.

Figure 2. Reconstruction of *Deinosuchus hatcheri* in the Natural History Museum of Utah. Image credit: Daderot. CC0 1.0 Universal Public Domain Dedication. https://creativecommons.org/publicdomain/zero/1.0/deed.en.

There has been some controversy regarding the naming of *Deinosuchus*. The first *Deinosuchus* fossils were found in Montana by T. W. Stanton and J. B. Hatcher in 1903 and were reported by W. J. Holland six years later (Holland, 1909; Schwimmer, 2002). Holland named the species *Deinosuchus hatcheri* in Hatcher's honor. The fossils comprising this holotype (name-bearing) specimen consisted of two large vertebrae, some ribs, and about 25 bony scutes called osteoderms.

However, it was a well-known American Museum of Natural History reconstruction of a giant crocodilian jaw from the Rio Grande region of Texas that brought *Deinosuchus* to the attention of the general public. The reconstructed specimen was originally named *Phobosuchus riograndensis,* but the name was changed to *Deinosuchus riograndensis* in 1979 (Schwimmer, 2002). It is now recognized that this famous reconstruction was inaccurate in some respects.

Giant crocodilian fossil teeth were found in North Carolina in 1858. They were originally designated as *Polyptychodon rugosus*, but the name was later changed to *D. rugosus*. *Deinosuchus* species from the eastern United States were later renamed as *D. schwimmeri* in David Schwimmer's honor (Cossette and Brochu, 2020).

Because the *D. riograndensis* fossil material is more abundant than that associated with *D. hatcheri*, Cossette and Brochu (2020) proposed making *D. riograndensis* the type species, rather than *D. hatcheri*.

Sarcosuchus imperator Background Information

Sarcosuchus imperator has been described as a giant crocodile (or 'super croc') but with a snout similar to that of a gharial. As in the case of *Deinosuchus*, *suchus* refers to a *crocodile*. *Sarco-* comes from the Greek σομχος, meaning 'flesh,' and *imperator* is Latin for *commander*. Thus *Sarcosuchus imperator* is the "flesh crocodile emperor." By evolutionary reckoning, it lived in

Africa and South America in the Early Cretaceous, roughly 113 million years ago (Rigby, 2021). Sereno et al. (2001) estimated it to have a length between 11 and 12 meters, but this length estimate was later revised downward to between 9 and 9.5 meters (O'Brien et al., 2019). Booker (2005) has suggested *S. imperator* as a candidate for the Biblical Leviathan.

Like *Deinosuchus*, some aspects of the anatomy of *S. imperator* are distinct from those of extant crocodilians. For instance, *S. imperator* did not have the ball-and-socket (procoelous) vertebrae joints typical of extant crocodilians (Sereno et al., 2001). Like *Deinosuchus*, it had a somewhat bulbous snout. Hence, it is possible that *S. imperator* may, like *Deinosuchus*, represent a distinct created Genesis kind.

The Physiological Importance of Body Mass

Theodosius Dobzhansky (1973) famously wrote in an anti-creationist essay, "Nothing in biology makes sense except in the light of evolution." Many years later, C.A. Brassey and J.D. Gardiner (2015) turned this phrase to say, "Nothing in biology makes sense except in the light of [body mass]." They went on to say (p. 1), "Body mass is arguably the most fundamental property of an organism, and key evolutionary concepts within the fields of ecology, physiology, and biomechanics can only be understood within its context." Although we creationists would disagree with Brassey and Gardiner's evolutionary viewpoint, I believe they are correct when they describe the great importance of body mass in understanding physiology and biomechanics.

Creation researchers have long noted (e.g., Taylor 1987, Morris 1993, Woetzel 2013, Nelson 2017, and Coppedge 2023) that extant animals are often represented by much larger and more massive fossil ancestors. In 1982 creation researcher Donald W. Patten (1982, p. 40) suggested that the Genesis patriarchs were larger, lived longer, and took longer to mature than extant humans:

> Besides the decline in lifespans as seen in Genesis after the flood, there was also a decline in the age of the patriarchs at the time of their firstborn son, hence a decline in age of arrival at sexual maturity, and presumably skeletal maturity. Hence the smallness of contemporary animals compared to fossil ones.

Although I am not confident that the sons listed in Genesis 5 and 11 are all firstborn, I think Patten was absolutely correct that the Genesis historical data (particularly in Genesis 5) *strongly* imply delayed sexual maturation, and probably delayed skeletal maturation, as well. Creation researcher Greg Beasley (1990, p. 5) later wrote:

> The fossilised remains of both flora and fauna are, as a rule, significantly larger in the past than in their extant counterparts. One possible explanation for this 'shrinkage' over time is that the growth potential of living organisms has been impeded through *earlier maturation and declining longevity*; a consequence of changes in the prevailing biospheric conditions during the earth's recent past. It is proposed that these changes were brought about by, and as a consequence of, geophysical, atmospheric and biological changes, initiated during the Flood. The writer proposes that morphological shrinkage is **primarily a phenomenon of the post-Flood period, as was declining longevity and earlier skeletal maturation**. [italics mine, boldface his]

The deduction that ancient humans might have been larger than extant humans was fairly obvious, given the widespread giantism in the fossil record. However, Patten and Beasley's deduction that long-lived creatures in general and humans in particular should take longer to mature is particularly noteworthy, as it appears to have been deduced almost entirely, if not entirely, from the Scriptural data *alone*. Although some references published in the 1980s (Lindstedt and Calder 1981, Calder 1984, and Schmidt-Nielsen 1986) discussed the idea that biological timescales (including lifespan and maturation times) are mass-dependent, neither Patten nor Beasley appears to have been aware of these references, as they do not cite them.

Testing a Creationist Prediction

In essence, Patten and Beasley predicted that longer-lived creatures should be larger and take longer to mature than creatures with shorter lifespans (Figure 3). At the time, there were very little data available to test that hypothesis. However, that is beginning to change. Multiple studies published in the last 20 years or so show positive correlations between larger body mass and greater longevity, as well as between larger body

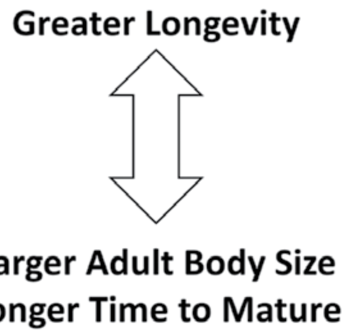

Figure 3. Studies of extant animals have shown that larger adult body sizes and longer maturation times are generally positively correlated with greater longevity.

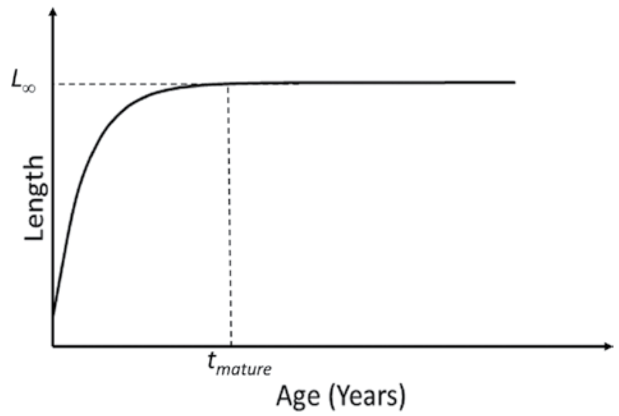

Figure 4. The von Bertalanffy growth curve, showing an organism's length or height as a function of time since birth or hatching. Growth effectively, if not completely, stops when the organism reaches skeletal maturity at time t_{mature}.

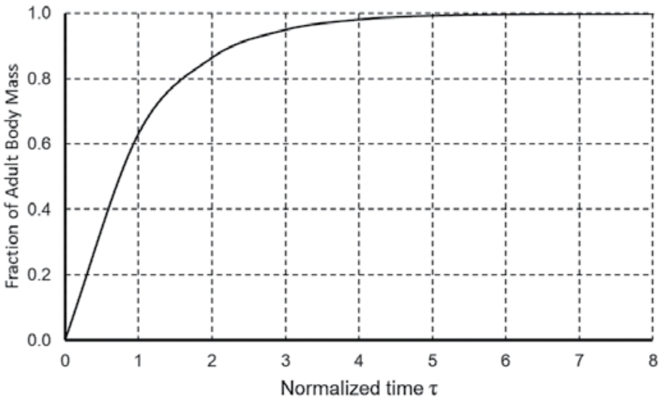

Figure 5. Theoretical mass-versus-age growth curve derived by West, Brown, and Enquist (2001), showing the manner in which fraction of adult body mass varies as a function of (normalized) time τ since birth or hatching. Reproduced from Figure 7 of Hebert (2023b). Used by permission of Cedarville University and the International Conference on Creationism.

mass and greater ages at maturation. In short, larger creatures tend to live longer and take longer to mature than smaller creatures. Admittedly, most of these studies span higher taxonomic categories (classes, orders, and families), but some show these correlations even within a single genus or species (see Sato, 1994; Genade et al., 2005; Lee et al., 2013). Overviews of these studies, including apparent contrary evidence, are provided in Hebert (2023b) and Hebert, Overman, and Sherwin (2024).

Moreover, the field of sclerochronology is now making it possible to test this 42-year-old creationist prediction by comparing the lifespans, sizes, and maturation times of fossil organisms to those of their extant, living counterparts. Sclerochronology (Moss, Ivany, and Jones, 2021) is the study and counting of periodic features in the skeletal portions of animals that grow by accretion, such as the shells of bivalves like clams and oysters. Paleontologists are using similar techniques to also count periodic growth structures in other taxa such as fishes, gastropods (Jones, Arthur, and Allard, 1989; Jambura and Kriwet, 2020; Shimada et al., 2021), and reptiles (Erickson and Brochu, 1999; Erickson, Rogers, and Yerby, 2001; Woodward, 2005). The use of growth increments in bones to determine age is called skeletochronology (Hutton, 1986).

Ontogenetic Growth Curves

The von Bertalanffy (1938) growth function (VBGF), depicted graphically in Figure 4, is often used to describe the ontogenetic growth of various organisms. The organism's length L as a function of time t is given by:

$$L(t) = L_\infty \left(1 - e^{-k(t-t_0)}\right) \qquad (1)$$

In Equation (1), time t is measured in years, as is the time t_0, the theoretical time at which the organism has a body length of zero. The parameter k (with units of years^{-1}) controls the relative speed with which the organism reaches an adult body length of L_∞. It should be noted that k is not a growth rate *per se*, although it is a proxy for growth rate. Lower and higher k values are associated with slower and faster growth, respectively.

Theoretically, Equation (1) describes indeterminate (never-ceasing) growth, since for any finite time t the organism's growth never quite stops. As a practical matter, however, it is often used to model both indeterminate and determinate growth, since one can treat the age at skeletal maturity as the time at which the slope of the function becomes arbitrarily small. However, Day and Taylor (1997) have criticized the use of the VBGF, particularly for modeling determinate growth, stating that the VBGF "often fails to provide an appropriate description of prematurity growth" (pp. 381–382). They argue that two separate equations, one for younger ages and a second for older ages close to maturity, are needed to accurately model ontogenetic growth. However, we are here most concerned with correctly modeling growth closer to ages at maturity, and the VBGF seems to do this reasonably well. Thus, most researchers ignore this complication, as we do here. The VBGF is used by commercial fisheries to model fish growth, and it is the growth curve most often used to model the growth of bivalves, like clams and oysters (Moss et al, 2021). Relevant to our purposes here, most studies of crocodilian ontogenetic growth use the VBGF (Viotto, Navarro, and Piña, 2020).

It should be noted that the VBGF is ideally obtained from length-versus-age data for a population. As such, L_∞ is the *average* size of organisms in the population that live long enough to reach maturity. Hence, some members of the population will have adult body sizes greater than L_∞, and some will have adult body sizes less than L_∞. When fitting a VBGF to length-versus-age data for a population, a computer program uses nonlinear least squares regression to find the values of k, t_0, and L_∞ that give the best overall fit to the data.

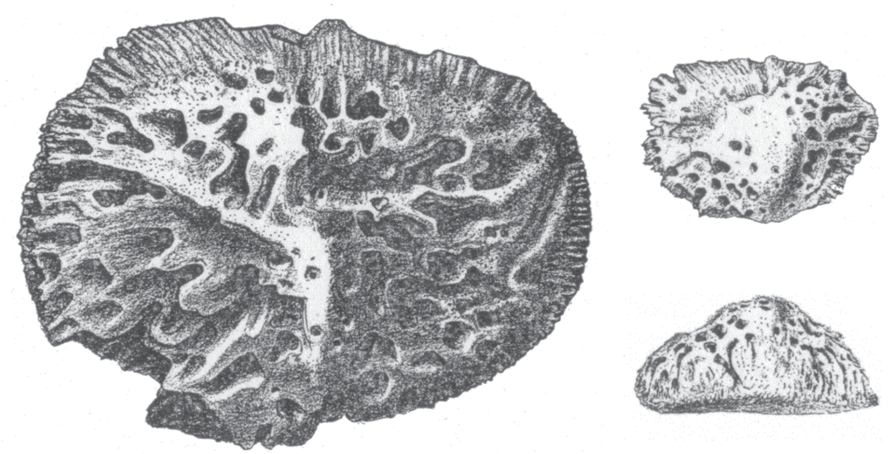

Figure 6. W. J. Holland sketches of overhead (left and upper right) and lateral (lower right) views of *Deinosuchus hatcheri* osteoderms. Public Domain. Wikimedia Commons.

West, Brown and Enquist (2001) have developed a metabolic theory of ontogenetic growth, in which the organism's mass m as a function of time t is given by

$$\left(\frac{m}{M}\right)^{1/4} = 1 - \left[1 - \left(\frac{m_0}{M}\right)^{1/4}\right] e^{-\frac{1}{4} a t M^{-1/4}} \tag{2}$$

In Equation (2), M is the adult body mass, m_0 is the mass at time $t = 0$, and a is a taxon-specific constant. A generalized form of Equation (2) is shown in Figure 5. In Figure 5, the fraction of adult body mass is plotted as a function of a dimensionless time parameter τ. Hence, Equation (2) and Figure 5 are general results that may be applied to a wide array of organisms. With some algebraic manipulation (West, Brown, and Enquist, 2001; Hebert, 2023b), it is possible to show that an organism's adult body mass M is proportional to the fourth power of its age at skeletal maturity, t_{mature} :

$$M = k \cdot t_{mature}^4 \tag{3}$$

The value of k is taxon-dependent. Thus, we might expect larger, more massive versions of creatures within a biblical kind to take longer to mature. However, it should be noted that k in Equation (3) may also depend on ambient conditions, which certainly have changed after the Flood. Thus one likely cannot safely assume, until demonstrated otherwise, that the proportionality 'constant' k for a particular taxon would have necessarily remained the same before and after the Flood.

Inferring Crocodilian Ages from Dorsal Osteoderms

Hutton (1986, p. 333) showed that growth in Nile crocodiles from Zimbabwe was "strictly confined" to the hot season (late October to mid-March), when water temperatures were highest. This makes sense in light of the fact that crocodilians are poikilothermic ("cold-blooded"). Hence their rates of bone growth and deposition vary with ambient temperatures (Schwimmer, 2002, p. 62). During these periods of rapid growth, broad "zones" of rapid bone deposition formed within crocodile bones. During the cool season, narrow "annuli," indicative of slow bone growth, were deposited. Hutton noticed that these seasonal laminations were most numerous and distinct within the crocodiles' long bones and within bony scutes called *osteoderms* (Figure 6).

Presumably, these seasonal laminations could be used to construct size-versus-age growth curves for living crocodilians. However, a complication is that the oldest laminations within long bones are sometimes "re-modeled." This complicates the counting process, necessitating some means of estimating the number of older laminae that have been remodeled and are no longer visible within the long bone. This re-modeling process is less of an issue in reptiles than it is in mammals. This is one of the reasons that crocodilians are considered an 'excellent' choice for the study of morphological changes throughout ontogeny (Cossette et al., 2022, p. 2905).

However, Hutton noted that the laminae within osteoderms were also numerous, distinct, and were less subject to remodeling. Although it is not readily apparent from Figure 6 how or where these growth laminations are located, Erickson and Brochu (1999) seem to imply (see the caption to their Figure 2b) that the counted growth laminations are visible on the ventral (bottom) portions of osteoderms taken from the dorsal neck region. However, Figure 6 only depicts the dorsal (overhead) and lateral (side) views of an osteoderm, This is apparently the reason that the growth laminations are not evident in Figure 6.

Hutton conducted longitudinal studies and found that he could use the growth laminations within these anterior neck osteoderms to construct age-versus-length growth curves for crocodiles. He validated his method for male and non-breeding female crocodiles with ages as high as 46 years, and found that his method could 'predict' lengths at a given age with no more than 9–15% error.

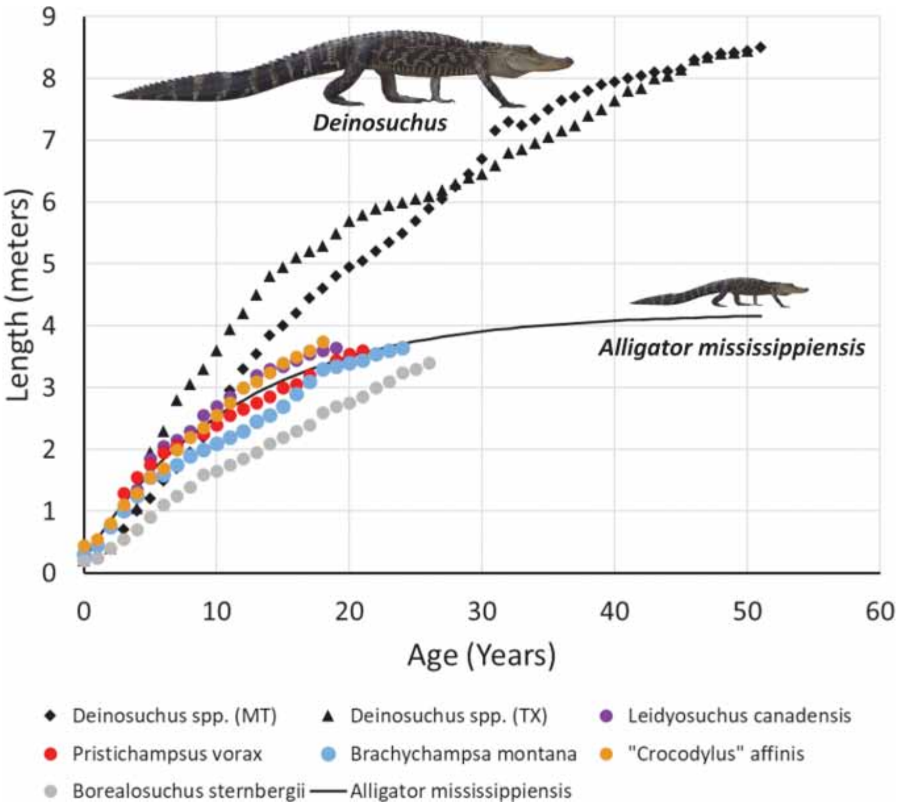

Figure 7. Length-versus-age growth curves for the American alligator (*Alligator mississippiensis*) and multiple species of fossil crocodilians, after Figure 2a in Erickson and Brochu (1999). Alligator image credit: Gareth Rasberry, CC BY-SA 3.0. https://creativecommons.org/licenses/by-sa/3.0/. Reproduced from Figure 10 of Hebert (2023b), used by permission of Cedarville University and the International Conference on Creationism.

Deinosuchus Ontogenetic Growth Curves

Erickson and Brochu (1999) used Hutton's osteoderm method and *Deinosuchus* specimens from Texas and Montana to construct growth curves for *Deinosuchus*, five other non-gavialoid fossil crocodilians, the American alligator *Alligator mississippiensis*, and the saltwater crocodile *Crocodylus porosus*. As Erickson and Brochu were not sure whether or not the Montana and Texas specimens were the same species, they designated both the Texas and Montana specimens as *Deinosuchus* spp. I emailed Erickson and Brochu, hoping to obtain their raw data, but I did not hear back from them. I reconstructed the seven fossil growth curves from their Figure 2a to the best of my ability. I had difficulty plotting all the data points close to the origin due to the overlap of the multiple different curves in that part of the chart. I also included in my chart the inferred VBGF from an American alligator catch-tag-and-release study (Chabreck and Joanen, 1979), to provide a comparison between extinct and extant crocodilians. These eight reconstructed growth curves are shown in Figure 7.

At the time Erickson and Brochu did their analysis, no complete *Deinosuchus* fossils were available, so they had to use allometric relationships to estimate the total *Deinosuchus* body length. In extant crocodilians, head length is strongly correlated with total body length (Schwimmer, 2002, p. 47), and the equation

$$TBL = -4.39 + 7.49THL \qquad (4)$$

is sometimes used to estimate total body length (*TBL*) when total head length (*THL*) is known. In Eq. (4) *TBL* and *THL* are both measured in inches. Erickson and Brochu used an allometric formula similar to that of Eq. (4) to estimate total body lengths of between 8.43 and 9.10 meters for their Texas and Montana *Deinosuchus* specimens.

From Figure 7 it seems that *Deinosuchus* spp. was much larger and took much longer to mature than extant crocodilians. Although I extended my *Alligator mississippiensis* growth curve in Figure 7 out to an age of 51 years to match the lengths of the two *Deinosuchus* growth curves, Erickson and Brochu's VBGR curve for the American alligator extended only to 25 years. Likewise, a 'typical' growth curve for extant crocodiles in Figure 1 of Padian, Horner, and de Ricqlés (2004) only extends to ~27 years. The AnAge database (https://genomics.senescence.info) reports that some crocodiles have been reported to attain ages as high as 40 to 70 years, but these were animals living in captivity, not the wild. As Erickson and Brochu noted (1999, p. 205), "[e]xtant crocodylians rarely live this long [~50 years] in the wild." Thus, these growth curves show that *Deinosuchus* had a lifespan significantly longer than extant crocodilians. A popular-level account (Connor, 1999) summarizing their research said:

> Scientists have solved the mystery of a giant prehistoric crocodile which was so big that it could make a meal of a dinosaur.
>
> Deinosuchus was five times the size [in weight, J. H.] of the biggest crocodiles alive today and researchers have now discovered why—it lived far longer than its present-day cousins.
>
> Unlike the dinosaurs, which became giants by putting on weight quickly, Deinosuchus grew slowly and became gigantic simply by continuing to get bigger while living to a relatively great age….
>
> The scientists studied the growth rings of Deinosuchus bones and found that the reptiles must have lived for at least 50 years, about 20 years more than living crocodiles, and considerably longer than the dinosaurs alive at the time.

Note that this last statement implies that a longevity of ~30 years is typical of today's crocodilians. Although it is often claimed that 50 years represents *Deinosuchus* longevity, 50 years is not necessarily the full lifetime potential of *Deinosuchus*. Rather, 50 years is simply the approximate ages of these two *Deinosuchus* specimens when they died.

In passing, I do not necessarily agree that (large) dinosaurs grew rapidly. Myhrvold (2013) has criticized studies purporting to show that dinosaurs grew rapidly, citing an inability to replicate their results, as well as methodological and statistical fallacies (see Hebert, 2023b, for a brief discussion). The only two studies Myhrvold did not criticize implied much slower rates of sauropod dinosaur growth (Woodward, 2005; Lehman and Woodward, 2008).

Are the Laminations Annual?

Based on their published results, mainstream paleontologists clearly think growth bands in fossil crocodilians most likely represent yearly or seasonal variations. However, Schwimmer (2002) gives two reasons for questioning this assumption. First, mainstream paleontologists think the Cretaceous climate was quite warm with less-pronounced seasonality (and creationists would probably agree with this description of the pre-Flood climate). In such a climate, would temperature variations be sufficiently pronounced to result in annual growth bands, as in today's world? Second, the growth curve of the Texan *Deinosuchus* is very similar to that of the Montana specimen, even though the Montana specimen apparently lived farther north, with presumably more pronounced high-latitude seasonal differences.

Actually, the second objection is answered by the first. Latitudinal temperature differences would have been less-pronounced in a warmer climate with less-pronounced seasons.

As to the first objection, seasonal variations of some sort would still seem to be the most likely cause of the growth bands, even if some factor other than temperature was the true cause. Schwimmer suggests prey migrations, wet-dry seasonal differences, or changes in ocean circulation or nutrient availability as possible causes, but notes that these too, could be annual. He states (2002, p. 63), "At present, this line of reasoning [from the *Deinosuchus* growth curves] is an interesting and reasonable argument for the size of *Deinosuchus* and its growth. There are no good alternative explanations currently proposed, and the question is still wide open for study." As of this writing, most paleontologists still seem to think these growth bands are annual.

Also, in a (presumably) stable pre-Flood climate, one would expect non-seasonal variations in temperature or other variables to be mild, with the largest fluctuations resulting from seasonal variation. It is indeed possible that these seasonal variations may not have always been sufficiently large to stimulate annual growth rings in fossil crocodilians. But in that case, each growth band, on average, would represent *more* than one year, and the age estimates discussed below are too low. Hence, within a creationist framework, the ages discussed below could be minimum ages, with the true ages being even greater.

Still Growing at Time of Death?

In a 2004 discussion, Padian, Horner, and de Ricqlés (2004, p. 560, their Figure 4) *assume* that the Montana and Texas specimens used to construct the growth curves had reached 100% of their adult size, which Erickson and Brochu (1999, p. 206) estimated at 8.43 to 9.10 meters. However, there are reasons to suspect that these Montana and Texas *Deinosuchus* specimens were still growing when they died.

First, the American alligator (*Alligator mississippiensis*) has been shown to exhibit determinate growth. This means, contrary to popular misperception, American alligators stop growing before they die of natural causes. This was demonstrated by a 35-year capture-tag-and-release study (Wilkinson et al., 2016). Wilkinson et al. defined determinate growth (p. 843) as growth that continued for some time after an organism reached reproductive maturity, but which stopped before the organism became senescent. Hence, growth of the American alligator slows down and ceases, with the slope of the growth curve "leveling off" and approaching zero prior to natural death. The Wilkinson et al. study included alligators with ages as young as 14.6 years and as old as 68.6 years. The growth curves obtained by Wilkinson et al. (2016) implied that male alligators stopped growing at 43 years, and females stopped growing at 31 years.

Although not certain, it seems reasonable that other extant and fossil crocodilians would *also* exhibit determinate growth. Wilkinson et al. (2016, p. 843) stated their research "adds to a growing list of studies suggesting crocodilians as a group exhibit this growth pattern rather than indeterminate growth." They noted that indeterminate growth for crocodilians seems to have merely been assumed, partly because of a scarcity of data for the largest and oldest specimens. Yet a more recent study by Woodward, Horner, and Farlow (2011) shows that a kind of bone microstructure called an *external fundamental system* (EFS) is present in the long bones of skeletally mature American alligators, and it has also been found in the long bones of some dinosaur fossils. The presence of an EFS would be evidence that the Montana and Texas *Deinosuchus* specimens had stopped growing, but Erickson and Brochu did not mention or describe an EFS in their 1999 paper. Indeed, long bones may not have even been part of their two fossil samples.

The growth curves in Figure 7 seem to have not yet "levelled off," which would indicate that *Deinosuchus* spp. was still growing at 50 years of age.

Second, within a creationist framework, all animals, including crocodilians, must have been originally designed by God to exhibit determinate growth (Hebert, 2023b). In a pre-Fall world without any death, continuous growth without limit would have been physically untenable.

A third reason to suspect that these *Deinosuchus* specimens were still growing at time of death is that most adult length estimates for *Deinosuchus riograndensis* are considerably longer than 9 meters. Indeed, Schwimmer (2002, pp. 47–48) noted that a *Deinosuchus* skull from the Big Bend region of Texas, the same locale from which Erickson and Brochu obtained their Texas specimen, had a total head length of ~1.31 meters (51.6 inches). Inserting this total head length (*THL*) into Eq. (4) implies a total body length (*THL*) of 382 inches, or 9.7 meters. Interestingly, an online article on the website of the journal *Science* (Schilthuizen, 1999) published the same month as the 1999 Erickson and Brochu *Nature* paper, states that *Deinosuchus* measured "well over 10 meters from head to tail."

Schwimmer (2002, p. 13) states that the largest *Deinosuchus* specimens were at least 11 meters, and possibly 12 meters long. In a newspaper article, he was quoted as saying (Broom, 2018), "The most conservative [*Deinosuchus* length] estimate among my peers is 35 feet, and the most optimistic is 45 feet. Forty feet is a good round number." Converting these estimates into meters yields a lower length estimate of 10.7 meters, an upper limit of 13.7 meters, and an intermediate estimate of 12.2 meters. Although Schwimmer did not explicitly say so, this is probably a length estimate for the larger *D. riograndensis* specimens from the American West and Southwest, as he estimates the adult length of the eastern variety to be ~8 meters.

Moreover, Cossette and Brochu (2020) strongly imply in the very first sentence of their abstract that 10 meters is a minimum length estimate for *Deinosuchus*: "*Deinosuchus* is a lineage of giant (≥10 m) Late Cretaceous crocodylians from North America." Interestingly, in that same paper they cite the 1999 Erickson and Brochu paper, using it as evidence that the length of *Deinosuchus* approached 10 meters, despite the lower original reported length estimate of 8.43 to 9.10 meters in Erickson and Brochu (1999).

Teasing Out Additional *Deinosuchus* Ontogenetic Information

If determinate growth did indeed characterize fossil crocodilians, *none* of the fossil crocodilians whose growth curves are shown in Figure 7 have yet reached skeletal maturity, including *Deinosuchus* spp. Again, Erickson and Brochu (1999) did not mention the observation of an EFS in any of the long bones belonging to the fossil specimens used to construct their two *Deinosuchus* growth curves. Apparently, no long bones were present in their fossil samples. In fact, it isn't even clear what particular fossil data they used. The caption to Figure 2 in their 1999 paper states that the "specimen [catalog] numbers are available from the authors on request." I did email Erickson and Brochu, hoping to acquire this information, but I did not hear back from them.

The growth curves of the other fossil crocodilians shown in Figure 7 are probably too short to justify attempting to fit VBGFs to them. However, in the case of *Deinosuchus*, we have a sufficient amount of ontogenetic data that we can reasonably attempt to do so. Given an estimated adult body length of ~10 meters, the Deinosuchus specimens whose growth curves are shown in Figure 7 had likely already achieved more than 80% of their total adult body length. A VBGF would give us a better idea of how long it would take *D. riograndensis* to reach skeletal maturity.

As noted earlier, Erickson and Brochu (1999) did not provide their length-versus-age data in tabular form, but I reconstructed their data to the best of my ability, as shown in Figure 7 (see also Figure 10 in Hebert 2023b). However, Padian, Horner, and de Ricqlés (2004) *did* include a smoothed version of Erickson and Brochu's *Deinosuchus* growth curve in their Figure 1. Careful examination shows that the Padian et al. growth curves for *Deinosuchus* and 'Typical crocodiles' do not extend all the way back to an age of $t = 0$ years. Their 'Typical crocodiles' curve begins at $t \sim 3.5$ years, and the *Deinosuchus* curve begins at $t \sim 2$ years. Padian et al. probably truncated their smoothed curves because of the inability of a VBGF to accurately model the inflection in the growth curves at the earliest states of ontogeny, with ages close to $t = 0$.

They did not provide VBGF equations for these two smoothed curves, but it is possible to learn them. I was able to reproduce their smoothed curves by carefully reading off their Figure 1 length and age values that were, with three exceptions, equally spaced at five-year intervals. The reason for the exceptions is that I made sure to include the 'end points' of their smoothed curves, which did not always fall on even multiples of five years. Seven data points were used to re-construct the 'Typical crocodile' growth curve, and eleven data points were used to re-construct the *Deinosuchus* growth curve (see Tables I and II). I then used the IDL function mpfitexpr.pro (Markwardt, 2009) to perform a nonlinear least squares regression to obtain best-fit VBGFs for these two curves.

I should note that here I am *not* attempting to find the best-fitting smoothed curve to the raw *Deinosuchus* data in Erickson and Brochu (1999). Rather, I am simply taking Padian et al.'s published 2004 curve at face value and trying to find the equation that describes it. Obviously, they thought their smoothed curve was reasonable, or they would not have published it. I just want to find the *equation* of this curve in order to estimate how long, based on the assumption of determinate growth, it would take an "average" *Deinosuchus* to reach skeletal maturity.

This method requires a specified functional form, trial values for the parameters to be found, and estimated errors (one standard deviation) in the dependent variable values. When finding the overall best fit, the method gives greater weight to data points with smaller uncertainties. Because I am only attempting to reproduce the two smoothed curves from Figure 1 in Padian et al., I assumed *equal uncertainty* in each data point, rather than the 15% length error estimated by Hutton (1986). This is because the error in this exercise is *not* the uncertainty in an allometric length estimate. Rather, it is the uncertainty in reading data points off an already-published plot. Since it is presumably equally difficult for me to read one data point off Padian et al.'s Figure 1 as it is any other data point, I assumed equal uncertainty in all the data points. Since I was reasonably, but not absolutely, confident that I could read data points to within a precision of 0.10 meters, I took the 2-sigma estimated uncertainty to be 0.10 meters, with the corresponding 1-sigma error of 0.05 meters.

Table I. Reconstructed age and length values from the smoothed 'Typical crocodile' growth curve shown in Figure 1 in Padian, Horner, and de Ricqlès (2004).

Age (Years)	Length (meters)
3.5	1.3
5	1.7
10	2.6
15	3.2
20	3.6
25	3.8
27	3.85

Table II. Reconstructed age and length values from the smoothed *Deinosuchus* growth curve shown in Figure 1 in Padian, Horner, and de Ricqlès (2004).

Age (Years)	Length (meters)
2	0.55
5	1.9
10	3.4
15	4.4
20	5.3
25	6.05
30	6.7
35	7.1
40	7.7
45	8.0
50	8.4

All data values and trial parameters were inputted as double-precision.

For the 'Typical crocodile' curve, I used starting values of $L_\infty = 4.0$ meters, $k = 0.1$ years^{-1}, and $t_0 = -0.5$ years. In five iterations, the code converged to values of $L_\infty = 4.183$ meters, $k = 0.0937$ years^{-1}, and $t_0 = -0.4957$ years.

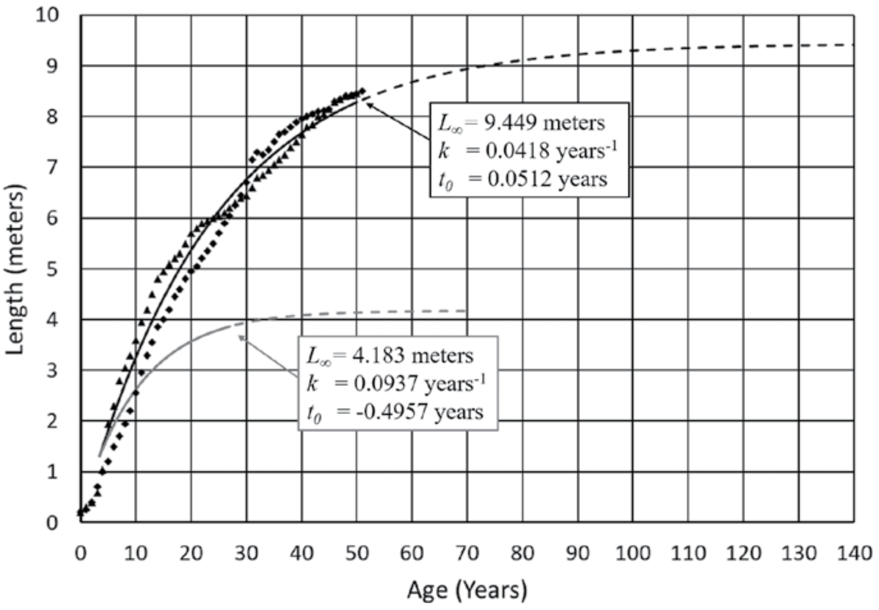

Figure 8. A smoothed von Bertalanffy growth curve for 'Typical crocodiles' (solid and dashed gray line) and for *Deinosuchus* spp. (solid and dashed black line). The smoothed *Deinosuchus* growth curve fits the reconstructed *Deinosuchus* length-versus-age data (black triangles and diamonds) quite well, despite being derived from Figure 1 in Padian, Horner, and de Ricqlés (2004), rather than Figure 2a in Erickson and Brochu (1999).

For the *Deinosuchus* growth curve, I used starting trial values of $L_\infty = 9.50$ meters, $k = 0.05$ years^{-1}, and $t_0 = -0.50$ years. Within six iterations, the code converged to best-fit VBGF values of $L_\infty = 9.449$ meters, $k = 0.0418$ years^{-1}, and $t_0 = 0.0512$ years. Given that *Deinosuchus* surely had a positive body length at hatching, t_0 should technically be a negative value. However, this issue is moot, since we used only age values of 2 years or greater in our fitting. Also, it may seem odd that the fitted values of t_0 imply that the gestation time for the giant *Deinosuchus* (0.051years) is actually less than that of an extant smaller 'Typical crocodile' (0.496 years), but this too is likely due to our exclusion of data near $t = 0$.

I also experimented with other starting values and constraints, such as minimum allowed final lengths of 10 and 11 meters. The result shown in Figure 8 is the most conservative result, having the smallest value of L_∞ and the shortest time to reach skeletal maturity.

In Figure 8, I have overlaid my reconstructed smoothed *Deinosuchus* and 'Typical crocodiles' growth curves on top of my reconstructed *Deinosuchus* data from Figure 7. Note that the *Deinosuchus* growth curve does a good job of matching the reconstructed data and 'splitting the difference' between the Montana and Texas data sets, even though they were both obtained from the smoothed curve in Figure 1 in Padian, Horner, and de Ricqlés (2004) and *not* from 'raw' data in Erickson and Brochu's Figure 2.

Implications of Their Smoothed Growth Curve

The smoothed growth curve of Padian, Horner, and de Ricqlés (2004), under the assumption of determinate growth described by a VGBF, implies that *Deinosuchus* probably took *considerably* longer than 50 years to reach skeletal maturity. As noted earlier, one could define t_{mature} as the age at which the slope of the growth curve becomes arbitrarily small. If one defines this as the age at which growth drops to less than 1 cm per year, the implied age of *Deinosuchus* skeletal maturity is 89 years. If one defines it as the age at which growth drops to less than 1 mm per year, then it is 144 years (!). Some papers in the technical literature (Taylor, 1958; Natanson et al., 2006) define "longevity" as the age at which an organism typically reaches 95% of its final adult body length. This definition doesn't really make sense to me, as longevity, as most people understand it, can greatly exceed the time to reach maturity. In any case, according to this definition, *Deinosuchus* spp. reached maturity at 72 years.

This smoothed curve gives an additional reason to suspect that growth had not yet ceased at 50 years of age. The dashed black line in Figure 8 implies a growth rate of just under 5 cm per year at age 50. Would growth then completely stop at age 51, or is it more likely that growth would continue, but at a decelerated rate, until the growth rate became negligible?

Thus, Padian et al.'s (2004) smoothed *Deinosuchus* growth curve could imply that *Deinosuchus* age at skeletal maturity was ~70 years, or greater. However, it's not possible to say too much beyond this, as the informal nature of the smoothed curve in Padian, Horner, and de Ricqlés (2004) makes a rigorous statistical analysis impossible. A more rigorous statistical analysis of the two original *Deinosuchus* spp. curves in Figures 7 and 8 might be possible. However, such an analysis is complicated by the fact that the data points in each of the two curves don't meet the requirements for a 'simple' non-linear regression. For instance, attempting to fit a VBGF to the Texas *Deinosuchus* data (triangles) in Figures 7 and 8 will result in residuals that are consistently positive for one part of the VBGF curve and consistently negative for another part of the curve. The same will be true for the Montana *Deinosuchus* data (diamonds) in Figures 7 and 8.

Nevertheless, because longevity studies have shown a positive correlation between greater longevity and larger adult body sizes and greater ages at maturation, these *Deinosuchus* growth curves constitute both direct and indirect evidence that *Deinosuchus* longevity was considerably greater than that of today's crocodilians.

Ontogenetic Growth Inferences for *Sarcosuchus imperator*

Sereno et al. (2001) performed a similar study using Lower Cretaceous *S. imperator* fossils from the Sahara. Because no complete *S. imperator* fossil was available, they used skull lengths of the extant saltwater crocodile (*Crocodylus porosus*) and the gharial (*Gavialis gangeticus*) to estimate the total body length of *S. imperator*, since "[i]n extant crocodylians, skull and total body lengths of subadult and adult individuals are strongly correlated and show negligible sexual variation" (Sereno, 2001, p. 1517). Their plot of *C. porosus* and *G. gangeticus* total body lengths against skull lengths showed that, for a given skull length, body lengths fell within a narrow range of values. Their allometric regression (see their Figure 4B) implied that the *S. imperato*r's skull length of 1.6 meters would be accompanied by a total body length of about 11.8 meters. Their length estimate of 11–12 meters was later revised downward to between 9 and 9.5 meters by O'Brien et al. (2019).

Sereno et al. counted about 40 (presumably annual) growth rings within the trunk osteoderms of a subadult *S. imperator* specimen whose total length was estimated to be about 80% of this total adult length. A femur was present in the fossil material, but Sereno et al. did not mention an external fundamental system (EFS). He graciously responded to an email question asking about the possible presence of an EFS. He said that not many *S. imperator* femurs were even available that would enable a check for an EFS. He said that he and his team only used scutes to estimate ages for their specimens.

Although they did not include an ontogenetic growth curve, they estimated that *S. imperator* would have taken 50–60 years to reach adulthood (Sereno et al., 2001, p. 1518):

> Thin sections of trunk osteoderms from a subadult individual (80% of maximum adult size) show about 40 annual growth rings or lines of arrested growth. This count suggests that a maximum adult size was achieved only after a duration of 50 to 60 years.

Note that Sereno et al. seem to have here assumed that 20% or so of the total growth time would be needed for *S. imperator* to attain the last 20% of adult body length. But this is very likely *not* the case. We can use Figure 8, despite its somewhat tentative nature, to see why.

As noted earlier, the adult *Deinosuchus* body length estimate L_∞ in Figure 8 is 9.449 meters. 80% of this final length is 7.559 meters. Inspection of Figure 8 and insertion of the fitted parameter values into Eq. (1) reveal that a length of 7.559 meters is attained at an age of 39 years. A nearly full-grown body length that is 99% of L_∞ is 9.354 meters. Also from Figure 8 and Eq. (1) it can be shown that a length of 9.354 meters is not attained until an age of 110 years. Thus the time required for *Deinosuchus* to attain nearly the entire fraction of its remaining 20% of adult body length is 110 – 39 = 71 years, *not* 10 or 20 years! Because of the shape of the von Bertalanffy growth curve, one cannot safely assume that the time for either *Deinosuchus* or *S. imperator* to attain the last 20% of its adult body length is simply 20% of the total growth time. Doing so could *greatly* underestimate the true ages at skeletal maturity t_{mature}.

Sereno et al. (2001, p. 1518) commented:

> Because extant crocodilians do not actively grow or typically survive this long in the wild (16, 23), *S. imperator* appears to have achieved its enormous body size by extending the duration of rapid growth as has been shown to be the case in the giant crocodylian *Deinosuchus* (20), rather than accelerating the rate of bone deposition. [footnotes in original]

In summary, evolutionary paleontologists estimate that *Deinosuchus* took about 50 years, and *S. imperator* took at least 50–60 years, to reach adulthood. However, these are likely underestimates, in light of the evidence for crocodilian determinate growth and the trajectory implied by the smoothed *Deinosuchus* curve in Figure 8.

Moreover, these giant crocodilians perished in the Flood. Hence, there is no reason that creationists should naively assume that 50–60 years represents the true longevity potential of these animals. Rather, these are just their ages at time of death. Because of the positive correlations between total longevity and body mass and between total longevity and time to adulthood discussed earlier, the large body sizes and extended growth intervals of these crocodilians are indirect evidences of great longevity.

Comparison with Extant Crocodilians

Both *Deinosuchus* and *S. imperator* had noticeable anatomical differences from

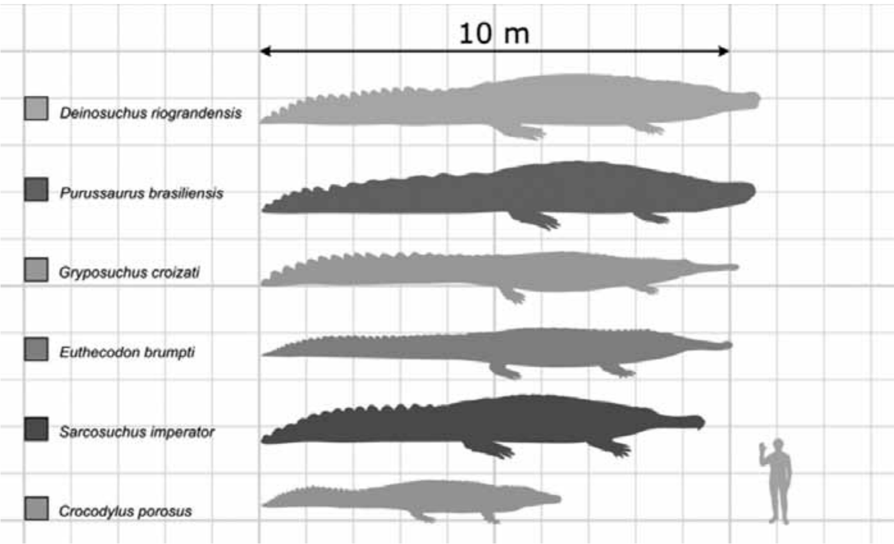

Figure 9. Length comparisons of five fossil and one extant crocodilian. Image credit: Smokeybjb. CC BY-SA 3.0. https://creativecommons.org/licenses/by-sa/3.0/.

extant crocodilians. Hence, they may not have belonged to the same Genesis kind or kinds as extant crocodilians. Indeed, creationists are still attempting to determine the number of original created crocodilian kinds (Hennigan, 2014; Cserháti, 2023).

However, their growth curves can perhaps tell us something about the ontogenies and longevities of other giant fossil crocodilians compared to extant ones. The estimated lengths of five giant fossil crocodilians, as well as the extant saltwater crocodile, are shown in Figure 9.

Purussaurus is a genus of giant caimans (Aureliano et al. 2015; Paiva et al., 2022) whose fossils have been found in Miocene deposits in Peru and Brazil. The largest specimen, *P. brasiliensis*, is thought to rival *D. riograndensis* in size and is estimated to have had the strongest bite force of any animal that ever lived.

Gryposuchus croizati is an extinct giant gavialid or gharial (Riff and Aguilera, 2008; Cidade et al., 2017). The fossils of both have been found in Miocene deposits in South America. Another giant fossil gharial (not depicted in Figure 10) is the *Rhamposuchus*, whose fossils are found in Pliocene deposits in India and Pakistan.

Euthecodon was very similar to a gharial in appearance; indeed the first remains from Ethiopia described by Joleaud (1920) were initially thought to belong to a false gharial. Its fossils are found in Miocene deposits in Africa, particularly Tunisia (Pickford, 2000; Agrasar, 2003). Evolutionists claim that the resemblance to living gharials is only superficial, and that the long snout evolved independently multiple times due to convergent evolution! The largest specimen, *E. brumpti*, was also a giant crocodilian.

Regardless of whether evolutionary scientists regard extant gharials or caimans as related to the giant gharials or caimans of the past, such ancestor-descendant relationships are very likely within a creationist framework. Indeed, even non-creationist authors have noticed that evolutionists tend to inflate the number of genera or species by failing to consider the possibility that differences in body sizes might have an environmental, rather than a genetic cause. Despite his strongly anti-Christian bias, author Vine Deloria, Jr. (1997, p. 156) astutely noted

> The problem with orthodox interpretation of the relationship of the megafauna to creatures of our present size is that most scientists have looked for *genetic* change, as the quotation by Loren Eiseley above demonstrates. They have therefore constructed a large bestiary of megafauna, and dinosaurs perhaps, which have no ancestors and no descendants. Instead of grouping animals by similarity of form and considering that they may represent a single species varying its size in accordance with the manner in which they were organically stimulated to grow, they have created all kinds of species.

Yes, it is true that in *today's* world growth trajectories and final adult body sizes for terrestrial vertebrates are strongly determined by genetics, with environmental effects playing a relatively minor role (Wilkinson et al., 2016). But evolutionists are failing to take into account the effects of truly radical environmental changes at the time of the Flood, and possibly afterward. Creationists should not be afraid to make reasonable comparisons between different-sized creatures with very similar morphologies, even if evolutionists have assigned them to different genera. In a creationist framework, *Gryposuchus croizati*, and *Rhamposuchus* likely belong to the same Genesis kind as extant gharials, and this may be true for *Euthecodon brumpti*, as well. Likewise, *Purussaurus brasiliensis* may belong to the same Genesis kind as extant caimans.

To the best of my knowledge, we don't currently have ontogenetic growth data for giant fossil gharials or caimans. However, in light of their giant crocodilian body forms, it is reasonable to assume that they had ontogenetic growth patterns similar to *D. riograndensis* and *S. imperator.* In that case, they too, would have been experiencing delayed maturation, which could be indirect evidence of greater longevity compared to their likely descendants, the extant gharials and caimans.

Implications for the Location of the Flood/ Post-Flood Boundary

Deinosuchus riograndensis and *Sarcosuchus imperator* fossils are found in Cretaceous strata, which, by definition, are stratigraphically located below the K-Pg (or K-T) boundary. Virtually all creationists would accept these fossils as dating from the Genesis Flood. Hence, *Deinosuchus* and *S. imperator* fossils represent creatures that were living in the pre-Flood world. These crocodilians grew very large and apparently took a long time to reach skeletal maturity.

Extant crocodilians may not necessarily belong to the same Genesis 'kind' or 'kinds' as *S. imperator* and *Deinosuchus*. However, other giant fossil crocodilians, with body sizes comparable to those of *Deinosuchus* and *S. imperator* (Figure 9), *are* very similar to some extant crocodilians. Extant gharials could be descended from *Gryposuchus croizati, Rhamposuchus,* and possibly *Euthecodon brumpti.* Likewise, extant caimans may be descended from *Purussaurus brasiliensis.* Hence, these fossil crocodilians could be larger, longer-lived representations of these extant crocodilian kinds. In that case, they too constitute additional evidence of extreme animal longevity in the pre-Flood animal world.

It should be noted that the fossils of these other giant crocodilians, such as *P. brasiliensis*, *Rhamposuchus*, *G. croizati*, and *E. brumpti*, are found in Pliocene and Miocene strata, which are stratigraphically above the K-Pg boundary. I concur with Baumgardner (Oard, 2002), Oard (Oard, 2013), Clarey, Werner, and Tomkins (2022), and Clarey and Werner (2023) that evidence for a 'high' Flood/post-Flood boundary, generally at or above the Mid-Pleistocene (Holt, 1996) is *overwhelming*. In that case, these other fossil crocodilians *also* date from the Flood. If greater longevity was the norm in the pre-Flood animal kingdom, and if larger body masses do indeed generally correlate with greater longevity, it would make sense that these other fossil crocodilians, living in the same pre-Flood world as *Deinosuchus* and *S. imperator*, would have comparable giant body sizes, despite being found in different strata. Thus, the similar body sizes of giant fossil crocodilians, found in strata both above and below the K-Pg boundary, may suggest that they all grew under similar environmental conditions, conditions which changed drastically at the Flood. Since the Cretaceous giant fossil crocodilians are from the Flood, it seems reasonable that the Miocene and Pliocene giant fossil crocodilians would date from the Flood, as well.

Final Comments

This paper adds to a growing body of direct and indirect fossil evidence for greater animal longevity in the pre-Flood and immediate post-Flood worlds. Preliminary lines of evidence were presented in Hebert (2023b), and subsequent papers have elaborated on these arguments. Growth curves of fossil *Crassostrea* oysters provide direct evidence of greater longevity compared to extant *Crassostrea* oysters (Hebert, Overman, and Sherwin, 2024). These same growth curves show evidence of delayed maturation and larger body sizes, which have been shown to be associated with greater longevity in living creatures. Moreover, fossil bivalves from Antarctica also show evidence for very long lifespans (Hebert, 2023b), a topic I hope to discuss in more depth in a future paper. Likewise, numerous fossil sharks show evidence of giantism and delayed maturation (Hebert, 2024a). As discussed in Hebert (2023b), some fossil birds show evidence of delayed maturation, although this needs to be explored in more depth before a strong claim can be made. Also, an apparently worldwide diminution in mammal body sizes at the end of the Pleistocene could be indirect evidence of decreasing longevity at the end of the post-Flood Ice Age (Hebert, 2023a, Hebert, 2024b). Also, mainstream paleontologists have recently found evidence for "surprisingly long" (Baisas 2024) lifespans in the small Jurassic mammals *Morganucodon* and *Kuehneotherium* (Newham et al., 2020). Subsequent research has revealed long lifespans (for their body sizes) for five additional small Jurassic mammals, as well as evidence of delayed maturation in four such mammals (Panciroli et al., 2024, Newham et al., 2024, Hebert, 2024c). I strongly encourage other creation researchers to "be on the lookout" for additional possible fossil evidence of greater longevity in the pre-Flood world.

References

Agrasar, E. L. 2003. New fossil crocodilians from the Middle/Upper Miocene of Tunisia. *Annales de Paléontologie* 89(2): 103–110.

Aureliano, T., A. M. Ghilardi, E. Guilherme, J. P. Souza-Filho, M. Cavalcanti, and D. Riff. 2015. Morphometry, bite-force, and paleobiology of the Late Miocene Caiman *Purussaurus brasiliensis. PLoS ONE* 10(3): e0124188.

Baisas, L. Baby teeth reveal surprisingly long lifespans of small Jurassic mammals. *Popular Science*. https://www.popsci.com/science/jurassic-mammal-teeth/ (accessed September 17, 2024).

Beasley, G. 1990. Pre-flood giantism: a key to the interpretation of fossil hominids and hominoids. *Journal of Creation* 4(1):5–55.

Booker, P. 2005. A new candidate for Leviathan? *Journal of Creation* 19(2): 14–16.

Brassey, C. A. and J. D. Gardiner. 2015. An advanced shape-fitting algorithm applied to quadruped mammals: improving volumetric mass estimates. *Royal Society Open Science* 2(150302): 1–14.

Broom, B. This monster of an alligator once roamed Mississippi. *Mississippi Clarion Ledger*. https://www.clarionledger.com/story/magnolia/2018/07/09/mississippi-hunting-ancient-gator-species-too-big-catch/759097002 (accessed November 1, 2023).

Calder, W. A. III. 1984. *Size, Function, and Life History*. Cambridge, Massachusetts: Harvard University Press.

Chabreck, R. H. and T. Joanen. 1979. Growth rates of American alligators in Louisiana. *Herpetologica* 35(1): 51–57.

Cidade, G. M., A. Solórzano, A. D. Rincón, D. Riff, and A. S. Hsiou. 2017. A new *Mourasuchus* (Alligatoroidea, Caimaninae) from the late Miocene of Venezuela, the phylogeny of Caimaninae and considerations of the feeding habits of *Mourasuchus*. *PeerJ* 5:e3056.

Clarey, T. L. and D. J. Werner. 2023. A progressive global flood model confirmed by rock data across five continents. *Proceedings of the 9th International Conference on Creationism*: Vol. 9, Article 23.

Clarey, T.L., D.J. Werner, and J.P. Tomkins. 2022. Globally extensive Cenozoic coals indicate high post-Flood boundary. *Journal of Creation* 36(1): 13–15.

Connor, S. 1999. Solved: Mystery of crocodile that feasted on dinosaurs. *The Independent*. https://www.independent.co.uk/news/solved-mystery-of-crocodile-that-feasted-on-dinosaurs-1081362.html (accessed November 1, 2023)

Coppedge, D. F. Life is devolving from a past world of giants. *Creation Evolution Headlines*. https://crev.info/2023/03/life-is-devolving/ (accessed January 8, 2024).

Cossette, A. P., A. D. Grass, and T. DeGuzman. 2022. The contribution of ontogenetic growth trajectories on the divergent evolution of the crocodylian skull table. *The Anatomical Record* 305(10): 2904–2925.

Cossette, A. P. and C. A. Brochu. 2020. A systematic review of the giant alligatoroid *Deinosuchus* from the Campanian of North America and its implications for the relationships at the root of Crocodylia. *Journal of Vertebrate Paleontology* 40(1).

Cserháti, M. 2023. Baraminic analysis of Crocodylia based on mitochondrial DNA similarity. *Answers Research Journal* 16: 259–263.

Day, T., and P.D. Taylor. 1997. von Bertalanffy's growth equation should not be used to model age and size at maturity. *The American Naturalist* 149(2): 381–393.

Deloria, V., Jr. 1997. *Red Earth, White Lies: Native Americans and the Myth of Scientific Fact*. Golden, CO: Fulcrum Publishing.

Diaz, J. 'Terror Crocodile' the Size of a Bus Fed on Dinosaurs, Study Says. *The New York Times*. https://www.nytimes.com/2020/08/13/science/large-crocodile-deinosuchus.html (accessed January 10, 2024).

Dobzhansky, T. 1973. Nothing in biology makes sense except in the light of evolution. *The American Biology Teacher* 35(3): 125–129.

Erickson, G. M. and G. A. Brochu. 1999. How the 'terror crocodile' grew so big. *Nature* 398(6724): 205–206.

Erickson, G. M., K. C. Rogers, and S. A. Yerby. 2001. Dinosaurian growth patterns and rapid avian growth rates. *Nature* 412(6845): 429–433.

Genade, T., M . Benedetti, E. Terzibasi, P. Roncaglia, D. R. Valenzano, A. Cattaneo, and A. Cellerino. 2005. Annual fishes of the genus *Nothobranchius* as a model system for aging research. *Aging Cell* 4(5): 223–233.

Guliuzza, R. J. and P. B. Gaskill. 2018. Continuous environmental tracking: An engineering framework to understand adaptation and diversification. *Proceedings of the International Conference on Creationism*: Vol. 8, Article 11. https://digitalcommons.cedarville.edu/icc_proceedings/vol8/iss1/11/ (accessed January 25, 2024).

Hebert, J. 2023a. Rarity of long-lived post-Flood human fossils? *Journal of Creation* 37(3): 23.

Hebert, J. 2024a. Giantism in fossil sharks: Evidence for extreme longevity? *Creation Research Society Quarterly* 60(4): 267–283.

Hebert, J. 2024b. Late Pleistocene body size reduction: evidence of a post-Flood decline in longevity? *Journal of Creation* 38(1): 60–66.

Hebert, J. 2024c. Methuselah-Like Longevity in Pre-Flood Mammals. *Creation Science Update*. https://www.icr.org/article/methuselah-like-longevity-pre-flood/ (accessed October 22, 2024).

Hebert, L., III. 2023b. Allometric and metabolic scaling: Arguments for design… and clues to explaining pre-Flood longevity? *Proceedings of the International Conference on Creationism*: Vol. 9, Article 18. https://digitalcommons.cedarville.edu/icc_proceedings/vol9/iss1/18/ (accessed January 25, 2024).

Hebert, J., R. Overman, and F. J. Sherwin. 2024. Fossil *Crassostrea* oysters show evidence of extreme longevity. *Creation Research Society Quarterly* 60(3): 171–190.

Hennigan, T. 2008. A fearsome reptile. *Creation* 30(3): 20–22.

Hennigan, T. 2014. An initial estimate toward identifying and numbering the Ark turtle and crocodile kinds. *Answers Research Journal* 7: 1–10.

Holland, W. J. 1909. *Deinosuchus hatcheri*, a new genus and species of crocodile from the Judith River Beds of Montana. *Annals of the Carnegie Museum* 6: 281–294.

Holt, R. D. 1996. Evidence of a Late Cainozoic Flood/post-Flood boundary. *Journal of Creation* 10(1):128–167.

Hutton, J. M. 1986. Age determination of living Nile crocodiles from the cortical stratification of bone. *Copeia* 1986(2): 332–341.

Jambura, P. L. and J. Kriwet. 2020. Articulated remains of the extinct shark *Ptychodus* (Elasmobranchii, Ptychodontidae) from the upper Cretaceous of Spain provide insights into gigantism, growth rate and life history of ptychodontid sharks. *PLoS ONE* 15(4): 1–16.

Joleaud, M. L. 1920. Sur la presence d'un Gavialide du genre *Tomistoma* dans le Pliocène d'eau douce de l'Ethiopie. *Comptes Rendus de l'Académie des Sciences* 170: 816–818.

Jones, D. S., M. A. Arthur, and D. J. Allard. 1989. Sclerochronological records of temperature and growth from shells of *Mercenaria mercenaria* from Narragansett Bay, Rhode Island. *Marine Biology* 102(2): 225–234.

Lee, W.-S., P. Monaghan, and N. B. Metcalfe. 2013, Experimental demonstration of the growth rate-lifespan trade-off. *Proceedings of the Royal Society B* 280(1752): 1–8.

Lehman, T. M. and H. N. Woodward. 2008. Modeling growth rates for sauropod dinosaurs. *Paleobiology* 34(2): 264–281.

Lindstedt, S. and W. A. Calder, III. 1981. Body size, physiological time, and longevity of homeothermic animals. *The Quarterly Review of Biology* 56(1): 1–16.

Line, P. 2013. Explaining robust humans. *Journal of Creation* 27(3): 64–71.

Markwardt, C. B. 2009. Non-Linear Least Squares Fitting in IDL with MPFIT. In D. Bohlender, P. Dowler, and D. Durand (editors), *Proceedings of Astronomical Data Analysis Software and Systems XVIII* (Quebec, CA), pp. 251–254. San Francisco: Astronomical Society of the Pacific Series, Volume 411.

Morris, H. M. 1993. *The Genesis Record: A Scientific and Devotional Commentary on the Book of Beginnings* (23rd printing). Grand Rapids, Michigan: Baker Book House.

Moss, D. K., L. C. Ivany, and D. S. Jones. 2021. Fossil bivalves and the sclerochronological reawakening. *Paleobiology* 47(4): 551–573.

Myhrvold, N. P. 2013. Revisiting the estimation of dinosaur growth rates. *PLoS ONE* 8(12): 1–24.

Natanson, L. J., N. E. Kohler, D. Ardizzone, G. M. Cailliet, S. P. Wintner, and H. F. Mollet. 2006. Validated age and growth estimates for the shortfin mako, *Isurus oxyrinchus*, in the North Atlantic Ocean. *Environmental Biology of Fishes* 77(3): 367–383.

Nelson, V. 2017. *Monumental Monsters*. Red Deer, Alberta, Canada: Untold Secrets of Planet Earth Publishing Company, Inc.

Newham, E., I. J. Corfe, P. Brewer, J. A. Bright, V. Fernandez, N. J. Gostling, S. Hoffmann et al. 2024. The origins of mammal growth patterns during the Jurassic mammalian radiation. *Science Advances* 10(32): eado4555.

Newham, E., P. G. Gill, P. Brewer, M. J. Benton, V. Fernandez, N. J. Gostling, D. Haberthür et al. 2020. Reptile-like physiology in Early Jurassic stem-mammals. *Nature Communications* 11(1): 5121.

Oard, M.J. 2002. Dealing carefully with the data. *Journal of Creation* 16(1): 68–72.

Oard, M.J. 2013. Geology indicates the terrestrial Flood/post-Flood boundary is mostly in the Late Cenozoic. *Journal of Creation* 27(1): 119–127.

O'Brien, H. D. L. M. Lynch, K. A. Vliet, J. Brueggen, G. M. Erickson, and P. M. Gignac. 2019. Crocodylian head width allometry and phylogenetic prediction of body size in extinct crocodyliforms. *Integrative Organismal Biology* 1(1), obz006.

Padian, K., J. R. Horner, and A. de Ricqlés. 2004. Growth in small dinosaurs and pterosaurs: The evolution of Archosaurian growth strategies. *Journal of Vertebrate Paleontology* 24(3): 555–571.

Paiva, A. L. S., P. L. Godoy, R. B. B. Souza, W. Klein, and A. S. Hsiou. 2022. Body size estimation of Caimaninae specimens from the Miocene of South America. *Journal of South American Earth Sciences* 118, 103970.

Panciroli, E., R. B. J. Benson, V. Fernandez, N. C. Fraser, M. Humphage, Z.-X. Luo, E. Newham, and S. Walsh. 2024. Jurassic fossil juvenile reveals prolonged life history in early mammals. *Nature* 632(8026): 815–822.

Patten, D. 1982. The longevity accounts in ancient history. *Creation Research Society Quarterly* 19(1): 40–52.

Paul, M.-J. 2010. Behemoth and leviathan in the book of Job. *Journal of Creation* 24(3): 94–100.

Pickford, M. 2000. Crocodiles from the Beglia Formation, Middle/Late Miocene boundary, Tunisia, and their significance for Saharan palaeoclimatology. *Annales de Paléontologie* 86(1): 59–67.

Riff, D. and O. A. Aguilera. 2008. The world's largest gharials *Gryposuchus*: description of *G. croizati* n. sp. (Crocodylia, Gavialidae) from the Upper Miocene Urumaco Formation, Venezuela. *Paläontologische Zeitschrift* 82: 178–195.

Rigby, S. 2021. *Sarcosuchus imperator*: The 'super croc' that could have hunted dinosaurs. *BBC Science Focus*. https://www.sciencefocus.com/nature/sarcosuchus-imperator (accessed January 11, 2024).

Sato, S. 1994. Analysis of the relationship between growth and sexual maturation in *Phacosoma japonicum* (Bivalvia: Veneridae). *Marine Biology* 118: 663–672.

Schilthuizen, M. 1999. A greater alligator. *Science.org*. https://www.science.org/content/article/greater-alligator (accessed January 25, 2024).

Schmidt-Nielsen, K. 1986. *Scaling: Why Is Animal Size So Important?* (3rd printing). Cambridge: Cambridge University Press.

Schwimmer, D. R. 2002. *King of the Crocodylians: The Paleobiology of Deinosuchus*. Bloomington and Indianapolis: Indiana University Press.

Sereno, P. C., H. C. E. Larsson, C. A Sidor, and B. Gado. 2001. The giant crocodyliform *Sarcosuchus* from the Cretaceous of Africa. *Science* 294 (5546):1516–1519.

Shimada, K., M. F. Bonnan, M. A. Becker, and M. L. Griffiths. 2021. Ontogenetic growth pattern of the extinct megatooth shark *Otodus megalodon*—implications for its reproductive biology, development, and life expectancy. *Historical Biology* 33(12): 3254–3259.

Sibley, A. 2023. A new 'marine crocodile' discovered on the Jurassic coast of England. *Journal of Creation* 37 (3): 9–10.

Taylor, C. C. 1958. Cod growth and temperature. *ICES Journal of Marine Science* 23(3): 366–370.

Taylor, P. S. 1987. *The Great Dinosaur Mystery and the Bible*. Master Books, El Cajon, California.

Thomas, B. and D. Biddle. 2023. Insight into Job's Theology from a new identification for Leviathan. *Creation Research Society Quarterly* 60(2): 72–83.

Viotto, E. V., J. L. Navarro, and C. I. Piña. 2020. Growth curves of wild and reintroduced broad-snouted Caimans (*Caiman latirostris*) and their management implications. *South American Journal of Herpetology* 16(1): 34–41.

von Bertalanffy, L. 1938. A quantitative theory of organic growth (inquiries on growth laws II). *Human Biology* 10:181–213.

West, G. B., J. H. Brown, and B. J. Enquist. 2001. A general model for ontogenetic growth. *Nature* 413(6856): 628–631.

Whitcomb, J. C. and H. M. Morris. 1991. *The Genesis Flood: The Biblical Record and Its Scientific Implications* (35th printing). Presbyterian & Reformed Publishing Company, Phillipsburg, New Jersey.

Wilkinson, P. M., T. R. Rainwater, A. R. Woodward, E. H. Leone, and C. Carter. 2016. Determinate growth and reproductive lifespan in the American Alligator (*Alligator mississippiensis*): Evidence from long-term recaptures. *Copeia* 104(4): 843–852.

Woetzel, D. *Chronicles of Dinosauria*. 2013. Illustrated by R. Dobbs. Master Books, Green Forest, Arkansas (USA).

Wood, T. The current status of baraminology. *Creation Research Society Quarterly* 43(3): 149–158.

Woodward, H. 2005. *Bone histology of the sauropod dinosaur Alamosaurus sanjuanensis from the Javelina Formation, Big Bend National Park, Texas* [masters thesis]. Lubbock, Texas: Texas Tech University.

Woodward, H. N., J. R. Horner, and J. A. Farlow. 2011. Osteohistological evidence for determinate growth in the American alligator. *Journal of Herpetology* 45(3): 339–342.

Creation Research Society Quarterly 2025 61:189–201

Original Polyploidy as a Contributor to Diversification

Harry Sanders*

Abstract

Plant life is incredibly diverse, with many plant families consisting of thousands or even tens of thousands of species. This extensive diversity must be explained within a creation model of origins. If, as is generally assumed, the taxonomic family is roughly the classification level of the created kinds, then many plant kinds are incredibly diverse. One way to account for this diversity may be created polyploidy. Created polyploidy would allow for an increased number of created alleles, thereby increasing the potential diversity of the original baramins. This increased diversity would enable created polyploids to diversify to the levels we see today within a creationist paradigm. A computer model of the differences in genetic diversity maintained by polyploid and diploid lineages was written in Python, a general-purpose, high-level, programming language. The model found that polyploids consistently maintained greater diversity than diploids. As such, created polyploidy should be considered as a potential explanation for genetic diversity. This article will propose a unique explanation for the origins of the diversity of many angiosperms as well as some gymnosperms where polyploidy is common.

Key Words: allopolyploidy, autopolyploidy, creation, genetic diversity, polyploidy

Introduction

Baraminology has largely been focused on animals, and with good reason. One of the common skeptical questions is "How do you fit millions of species on the Ark of Noah?" While species were not the taxonomic unit taken on the Ark, identifying kinds is crucial to answering the skeptic's question. Plants have largely, though not completely, been overlooked compared to vertebrate organisms. The question of the origin of plant diversity has largely also been overlooked. This article will overview plant polyploidy (i.e., the genetic condition of having more than two sets of replicated chromosomes) and examine the differences in genetic diversity among plants of various ploidy levels.

The Problem

Some plant groups have incredibly large numbers of species. For example, Asteraceae contains more than 32,000

---

* Harry Sanders, Moore's Hill, IN, hfsanders3@gmail.com

Accepted for publication May 2, 2024

species of plants and Orchidaceae has over 28,000 (WCSP, 2021). The grasses of Poaceae, representing 12,000 species, were tentatively placed in a holobaramin by Wood (2002). Data from a subsection of the Grammitidaceae ferns, which have over 700 species, was also used to claim they were a holobaramin (Wood, 2008). All these baramins are quite large. If a Flood year of 2348 BC is assumed, Poaceae had to form new species at the rate 2.75 species per year. Even if the Flood date is moved back to the oldest possible date under a young-Earth model, this rate of rapid speciation does not get much better. Note that this rate is almost certainly too high as it is likely more than a single grass seed survived the Flood. If more than one seed survived the Flood, as is probable, there may have been more than one founding species of grass post-Flood, hence lowering the number of species required to arise since the Flood. However, since the real rate cannot be known with certainty, 2.75 species per year serves as an upper boundary for what is required.

However, it is not just that new species form. Some of these proposed baramins are widely morphologically disparate. For example, Poaceae contains both woody and herbaceous grasses. Different members of the family have widely different life cycles, with both annuals and perennials present in the family. Further, both C3 and C4 photosynthesis occurs within the group, in one instance even in the same species! (Lundgren et al., 2016). If the actual baramin is as large as is claimed, a lot of diversity needs to be accounted for, and in a relatively short time compared to an evolutionary scenario.

To account for the staggering diversity of life, Jeanson and Lisle (2016) proposed the "created heterozygosity and natural processes" (CHNP) model which is the best model of diversification proposed so far. They showed that mutations are insufficient to account for genetic diversity across all life, but importantly for the purposes of this paper, especially for plants. However, while mutations are insufficient, is created diploid heterozygosity sufficient? This paper will propose extending the CHNP model to include created polyploids in plants to account for their greater diversity.

Survey of Current Thought in Polyploidy

Secular research in polyploidy has been ongoing for a long time. It is far beyond the scope of this paper to even attempt to cover over 100 years of research. Instead, it will provide a short overview of relevant secular polyploidy literature.

Many species are polyploid, limited largely to plants but including some animals and fungi as well. Evolutionists have proposed that up to 70% of angiosperms have polyploidy in their lineage at least once (Soltis and Soltis, 1999). However, the estimate assumes universal common ancestry, often based on duplicated genes (Blanc and Wolfe, 2004). Therefore, it is important when discussing polyploidy to distinguish between paleopolyploids and extant ones, distinctions evolutionists are not always careful to make. However, even discounting the proposed paleopolyploids, many species of extant plants are polyploid. A 2009 paper estimated that about 34.5% of plants were polyploid when compared to the lowest chromosome counts in the genus (Wood et al., 2009). In 2015, a separate paper estimated polyploids were roughly 24% of vascular plants (Barker et al., 2016). Returning to the Poaceae example, more than 60% of known species are considered polyploid (Levy and Feldman, 2002.) Since polyploid plants are common, it is important to account for them within the creation model.

It is important to note that polyploidy is a relative term. It is contextually dependent. The problem is that we do not know how many chromosomes the original kinds had. Generally, evolutionists select a chromosome base number for a taxonomic group and, from that number, evaluate the rest of the taxonomic group's ploidy status (Parris et al., 2010; Contreras et al., 2016). If the original base number is incorrect, the rest of the taxonomic group (usually a genus) may have improper ploidy classification. The only certain ploidy levels are those determined by observation of chromosome pairing during meiosis. Simply counting the number of chromosomes is not enough because it assumes a potentially inaccurate base number (Bennett, 2004.) It also ignores chromosomal pairings that might reveal a polyploid heritage when it has been lost due to diploidization. While specific species currently thought polyploid may or may not actually be polyploid, polyploidy itself is a real and common phenomenon as, within genera and other taxonomic groups, plants vary widely in chromosome number, often in multiples of the selected base number.

There are two main forms of polyploidy: allo and autopolyploidy. Allopolyploidy results from the cross of two different plant lineages. As a result, the offspring carry two divergent genomes (Wendel et al., 2008). The two genomes, referred to as subgenomes of the polyploid genome, are commonly thought to be differentially expressed, with a dominant genome often containing more genes and remaining dominant even if another whole genome duplication (WGD) occurs (Freeling et al., 2014). The genome shock associated with combining two disparate genomes often causes rapid genomic changes through multiple pathways to permit the two genomes to cohabitate, usually by allowing one genome to become dominant at the expense of the other (Edger et al., 2018). This consensus about genome dominance has recently been challenged, with the suggestion that differences between the genomes are tied to their progenitor genomes rather than post-polyploidy changes (Liu and Wang, 2022). Importantly, however, the rapid genomic changes associated with allopolyploidy are not in dispute, even by those challenging the genome dominance hypothesis.

Autopolyploids may comprise most polyploids (Barker et al., 2016). In autopolyploids, the parental genomes are homologs (due to shared ancestry) instead of having two separate parental genomes. As such, genome dominance may be unnecessary, as the genomes are already compatible. Thus, allopolyploids' rapid genomic changes likely do not occur in autopolyploids (Spoelhof et al., 2017).

Newly formed auto and allopolyploids both suffer from minority cytotype exclusion (MCE) during establishment. The higher the frequency of a particular cytotype in a population, the easier it will be to breed with a compatible mate, and therefore the more reproductively successful it would likely be (Levin, 1975). Because polyploids, according to the conventional model, begin at low population frequencies, founding a new lineage in the presence of their diploid progenitors is predicted to be difficult, something confirmed in experimental studies (Husband, 2000; Baack, 2005). Thus, the minority cytotype often occupies slightly different niches or entirely different habitats than their parental population (Felber-Girard et al., 1996; Baack, 2004; Scopece et al., 2016). Often there is little overlap between the cytotypes, because of differences in mode of life (Johnson et al., 2003), because hybridization either fails (Castro et al., 2012), or because triploids are less successful than their parents (Burton and Husband, 2000).

There are, however, ways around MCE. One is selfing. By pollinating itself, a neopolyploid can avoid MCE and reproduce, but at a potential long-term cost. Allopolyploids tend to self at a higher rate than diploids, but autopolyploids self at a lower rate (Husband et al., 2002). However, a large-scale meta-analysis found that there was no association between the ability to self and the number of polyploid taxa in a taxonomic group (Mable, 2004). More recent work has found that in at least some taxa, self-incompatibility breaks down over time in polyploid lineages (Horandl, 2008; Sutherland et al., 2018), and close association between polyploidy and self-compatibility has been found in certain groups (Barringer, 2007; Robertson et al., 2010; Gao et al., 2016). The question of polyploidy's association with selfing remains open, but the evidence seems to indicate that at least allopolyploid lineages may survive in part through selfing.

The problem with selfing is, it reduces reproductive success compared to outcrossing populations (Siopa et al., 2020). Over time, this can reduce a population's viability. Asexual reproduction is another way to deal with MCE, while avoiding the loss of reproductive success. Data suggests that polyploidy does not cause an increase in asexual behavior, but instead exploits existing asexuality to survive (Schwander et al., 2014). Where asexuality already exists, however, evidence suggests it might be important in promoting the survival of polyploid lineages (Kao, 2007). Asexuals, however, are subject to Muller's ratchet, which means that they are subject to mutational meltdown from a build-up of deleterious mutations (Muller, 1964), a phenomenon akin to genetic entropy (Sanford, 2014). While there is no escape from genetic entropy, asexual polyploids can slow the ratchet by periodically outcrossing (Hojsgaard and Horandl, 2015).

Genomic Changes Associated with Polyploidy

When polyploids arise, changes occur in the genome as a result. In an autopolyploid scenario, each allele is doubled, leading to an increased dosage of the allele. This may also be the case for some of the alleles under allopolyploidy as well. In some cases, this may not matter, but for many genes, an exact dosage balance is required for the gene products to work correctly. For example, many X-Y genes show dosage compensation (Muyle et al., 2017; Filatov et al., 2019). In hexaploid *Tritium*, deletion of an arm of one copy of the chromosome containing genes for glutenins and gliadins resulted in the other chromosomes increasing production of the protein to compensate (Galili et al., 1986). In an examination of almost 3100 transcripts in wheat, 60 changed because of allotetraploidy, with 80% being silenced (Kashkush et al., 2002). In *Leucanthemum*, two genes for subunits of a specialized protein are increasingly expressed with higher ploidy, but two other genes for photosystem II show no difference in expression intensity (Oberprieler et al., 2019). In maize, rRNA showed a rough 1:1 ratio of dosage effects, but not for every gene, and only 5 genes showed consistent dosage effects across the four ploidy levels studied (Guo et al., 1996). An examination of roughly 9,000 potato gene expressions found that few were linearly associated with changes in ploidy level (Stupar et al., 2007).

The contradictory nature of the evidence seems to indicate that dosage compensation varies from plant to plant and gene to gene. There is also a difference between allo- and autopolyploids. Around 1400 genes were dosage-compensated in a comparison of an *Arabidopsis* hybrid tetraploid with its diploid progenitors (making up slightly more than 5% of the studied genes) (Wang et al., 2006). A much smaller study in *Helianthus* autopolyploids showed no changes in gene expression due to polyploidy (Church and Spaulding, 2009). A larger study of autotetraploids versus diploids of over 21,000 genes showed differences in expression in just over 600 (<3%) (Tang et al., 2015). Polyploidy does seem to influence gene expression, but the effect seems limited to a small section of genes, and the exact number varies depending on the type of polyploidy involved.

Sometimes when dosage is increased, the resultant polyploid reacts by undergoing diploidization. Diploidization is the process of a polyploid losing redundant duplicate genes and becoming more diploid in nature. The product is termed a "paleopolyploid": a current diploid with a polyploid ancestor (Wolfe, 2001). Diploidization is believed to have made large-scale contributions to the evolution of angiosperms (Dodsworth et al., 2016) While this idea assumes deep time and multiple rounds of gene duplications in the history of life and the history of flowering plants (Conant et al., 2014), diploidization can begin to occur very quickly after the formation of a polyploid. For example, in a very recent (<100-years-old) polyploid species of *Tragopogon*, 11 of 13 analyzed loci had already lost at least one parental homeolog (Tate et al., 2009).

Transposable elements (TEs) can also be activated after a polyploid event. In tobacco allotetraploids, the polyploidization event significantly amplified retrotransposon activity (Grandbastien et al., 2010). Significant restructuring of the genome also often occurs, sometimes resulting in a reduction of discernible transposons (Ainouche et al., 2009). These deletions often take place quickly, within three generations in one study (Kashkush et al., 2010). However, other studies in different systems found no evidence for increased transposon activity (Belzile et al., 2009). In wheat allopolyploids, the additional transposons did not increase their rate of movement (Kashkush et al., 2002). Similar results were reported in cotton as well (Wendel et al., 2020). Thus, while transposon-mediated restructuring occurs, there is, as yet, no consistent pattern for when or why the restructuring will take place.

Importantly, TEs seem to preferentially insert themselves in areas of the genome that are gene-poor (i.e., near telomeres and centromeres) (Vicient and Casacuberta, 2017), though there are exceptions (Feschotte and Pritham, 2007). This fact hints at a possible structural or epigenetic effect for most TEs, rather than a directly genetic one. This is unsurprising given that TE movement is associated with significant methylation changes near the newly inserted TE (Ainouche et al. 2009; Kashkush and Yaakov, 2011). However, TEs are not usually mobile, being repressed by DNA methylation (Slotkin et al., 2016) using small noncoding RNA (sRNA) (Dubcovsky et al., 2010). Polyploidy can provide a release from the epigenetic control for TEs as discussed above, but it also can generate new epigenetic controls on other parts of the genome. Some TEs will generate short interfering RNA (siRNA) to control gene expression in either their own, or their counterpart subgenomes (Liu et al., 2021).

Interestingly, polyploid events are associated with homeologous exchanges (HE). These changes happen during meiosis, where chromosomes that are assumed to have a common ancestor but which do not normally pair or are from separate sub-genomes recombine (Pires and Gaeta, 2010). In cotton, the number of contigs (i.e., sets of *contig*uous or overlapping DNA segments) associated with HE is estimated to be roughly 2%, assuming a 1–2 mya origin of cotton (Wendel et al., 2009). Many synthetic polyploids show HE in at least a few cases (Mason and Wendel, 2020). The effect of HE is a net increase in genetic diversity in the resultant offspring (Liu et al., 2021). However, it can damage the genome, hindering normal meiosis and decreasing the fertility of the polyploid (Pires and Gaeta, 2010). This potential cost in fertility makes HE a double-edged sword for newly formed polyploids. MCE already restricts the number of possible mates, effectively reducing the likelihood of mating success. HE goes a step further, reducing fertility rates even if the newly formed polyploid can find a mate. The two compound each other, making it incredibly difficult for a newly formed polyploid to establish a population in the presence of its parents. However, if it does succeed, the increased diversity may give it an advantage in its new habitat.

Created Polyploids

If polyploids were created from the beginning, what might be expected as a result? How would such polyploids behave? If it is assumed that created polyploidy extends the CHNP model, then the created genomes would have been more like allopolyploids as this increases the amount of genetic diversity present. Mendelian rules of dominance and recessiveness would likely have been in place prior to the Fall of Genesis 3. However, genetic dominance (if it exists) in allopolyploids likely represents a post-Fall adaptation. In a perfect pre-Fall environment, existing plants would not have needed to subsume one genome to another as the two genomes would likely have been perfectly compatible within each plant. Thus, much of the genomic shock associated with allopolyploids in the present would have been absent in created polyploids, leading to their genomes functioning like autopolyploid genomes, but having the diversity of allopolyploid genomes.

However, perfect internal compatibility does not necessarily mean that each individual plant within a baramin had a genome completely compatible with every other individual plant in the baramin. Only in the Flood account are we told the number of surviving organisms and that is limited to the animal kinds that boarded the Ark (Genesis 6:19; 7:2). The creation account does not specify how many of each kind were created. From God's planting of the Garden of Eden (Gen. 2:8), it can be reasonably inferred that most plants were created with more than two organisms per baramin. The increased number of organisms per baramin increases the number of possible genomes available within the baramin, and therefore increases the amount of potential genetic diversity. Given the high potential diversity of a cross between two heterozygous tetraploids (136 possible genotypes per locus), adding additional distinct heterozygotes to the population only increases potential genetic diversity. Obviously much of this diversity was lost during the Flood, but much of it is still present today as evidenced by some of the incredibly large plant families and proposed baramins.

In a post-Fall, post-Flood environment, all organisms underwent a population bottleneck, and most would have also experienced a founder effect. Such effects may be deleterious to the genome of an organism as they tend to fix dominant (or at least increase the frequency of) deleterious mutations (Sunyaev et al., 2015). Founder events like this reduce the overall genetic diversity of the population (Shirk et al., 2014). However, polyploids are less susceptible to these effects as they have more alleles (Layman and Busch, 2018). While a founder event of equal proportion will likely remove the same number of alleles from both diploid and polyploid populations, polyploids have more alleles at the start of the process and, therefore, will retain more alleles.

Heterozygosity Changes in Model Populations

Computer modeling can demonstrate the extent of genetic diversity retained by polyploids compared to diploids. Using Python, three ploidy levels were modeled under both selfing and outcrossing systems. The code is available from the author on request. The simulation accounted for generation times, linkage, migration rate, recombination rate, environmental effects, selection strength, genetic drift, and deleterious mutations. Population sizes were assumed to be stable, and 100 generations were used for each simulation. Each model was simulated 10,000 times, and the data was exported in an Excel file. The data was then used to perform a Mann-Whitney U test, a non-parametric statistical test among two groups or samples, comparing the ploidy levels to each other in terms of median resultant heterozygosity within the selfing and outcrossing systems. Here heterozygosity means the proportion of heterozygous individuals in the simulated population for a given loci. The Mann-Whitney U test results were confirmed using histograms to determine whether the median heterozygosity was different or the distribution of heterozygosity between the two populations was different.

In the first simulation, initial heterozygosity was set to 0.5. All other parameters for each simulation can be seen in supplementary Table I. Table I shows the final heterozygosity of all simulations. Figure 1 shows the trajectory of the heterozygosity across 100 generations. A second simulation was run with slightly different parameters (found in Supplementary Table I). Figure 2 shows the trajectory of heterozygosity over 100 generations. Table II shows the results of the statistical tests for the first and second simulations. In all cases, the results are statistically significant with a p-value below 0.05. Histograms for each simulation showed comparable distributions (Supplementary Figures 1–16) except for the diploid-hexaploid comparisons. Therefore the diploid-tetraploid and tetraploid-hexaploid comparisons are interpreted as having significantly different means. The diploid-hexaploid comparisons are left uninterpreted as the diploid-tetraploid-hexaploid distributions show roughly step-wise comparable distributions, but the diploid-hexaploid distributions are not comparable.

In keeping with the CHNP model, heterozygosity was set to its maximum, 1, meaning full heterozygosity for two simulations. All other parameters can be found in supplementary Table I. Figure 3 shows the trajectory of heterozygosity across 100 generations. Interestingly, the selfed tetraploid and hexaploid maintain higher average heterozygosity than the outcrossing diploid. A second simulation for a heterozygosity of 1 with some adjusted parameters was performed as shown in Figure 4. In each case, the results were statistically significant as shown in Table III. In this instance, all histograms showed visually comparable distributions (Supplementary Figures 17–32), indicating a statistically significant difference in median between the populations.

This model makes it clear that higher ploidy maintains genetic diversity significantly better than diploids. Of course, this model is simplistic and does not account for things like genetic bottlenecks and founder effects. Both will decrease the heterozygosity either over time or during a founding event. Nor does it account for the effects of diploidization, which would drastically reduce heterozygosity. Nevertheless, initial results indicate

Table I. Average heterozygosity in multiple simulations.

Ploidy	Simulation	Breeding Method	Average Heterozygosity
Diploid	1	selfing	0.33
Tetraploid	1	selfing	0.36
Hexaploid	1	selfing	0.37
Diploid	1	outcrossing	0.351
Tetraploid	1	outcrossing	0.372
Hexaploid	1	outcrossing	0.379
Diploid	2	selfing	0.166
Tetraploid	2	selfing	0.198
Hexaploid	2	selfing	0.21
Diploid	2	outcrossing	0.224
Tetraploid	2	outcrossing	0.232
Hexaploid	2	outcrossing	0.233
Diploid	3	selfing	0.372
Tetraploid	3	selfing	0.433
Hexaploid	3	selfing	0.458
Diploid	3	outcrossing	0.413
Tetraploid	3	outcrossing	0.458
Hexaploid	3	outcrossing	0.479
Diploid	4	selfing	0.130
Tetraploid	4	selfing	0.162
Hexaploid	4	selfing	0.176
Diploid	4	outcrossing	0.191
Tetraploid	4	outcrossing	0.201
Hexaploid	4	outcrossing	0.203

that polyploid baramins would have maintained higher genetic diversity over time.

Since, within some baramins, some plants were created polyploid in this model, MCE is unlikely to be an issue and was excluded from the model. Instead, the newly formed diploids might suffer from MCE, but this would likely begin to be an issue after the Fall introduced genomic degradation. However, particularly after the Flood, niche differentiation would have allowed for a proliferation of new diploid and polyploid populations to arise quickly as seeds with different cytotypes landed in different habitats and reproduced into populations.

Post-Flood Recovery

Because the Flood completely reshaped the Earth's surface and wiped out all existing communities, the post-Flood landscape would have initially been completely bare, with many open spaces for plants to colonize. MCE would still have existed within populations, but it would have been much easier for a newly formed diploid to colonize an area that its polyploid ancestors were not utilizing. Indeed, today, many polyploid species are niche-differentiated, with cytotypes inhabiting different habitats and only occasionally overlapping (Baack, 2004; Castro et al., 2012; Kirchheimer et al., 2016; Castro et al., 2020). The Flood thus may have provided a release from MCE, allowing rapid establishments of different cytotypes in different habitats, leading to vast varieties of species and cytotypes in polyploid baramins that would further differentiate under selection and drift. This scenario would create incredibly speciose baramins in a very short period.

An additional benefit would be if selfing was possible within the baramin. Self-pollination may be a post-Fall adaptation, or it may have been built into the original creation, as the negative effects are only possible in a fallen world. In either case, self-fertilization almost certainly existed by the time of the Flood, some 1,656 years after Creation according to Genesis 5, either due to a breakdown of self-incompatibility or created design. Breaking down self-incompatibility is relatively simple, requiring the inactivation of a single locus, the *S*-locus, in many plants (Iezzoni et al., 2006; Kelly et al., 2017; Chai et al., 2022). In the nearly 1700 years prior to the Flood, it seems very unlikely that this locus suffered no mutations or that in at least a few species, the mutations did not proliferate due to its reproductive advantage. The ability to self in this way would have been a great benefit for any plant species able to do so in the post-Flood world. The nearest member of the same baramin might have been hundreds of miles away. The ability to self-fertilize, or alternatively, perform apomixis or other forms of asexual reproduction could have been a key driver of ecosystem recovery.

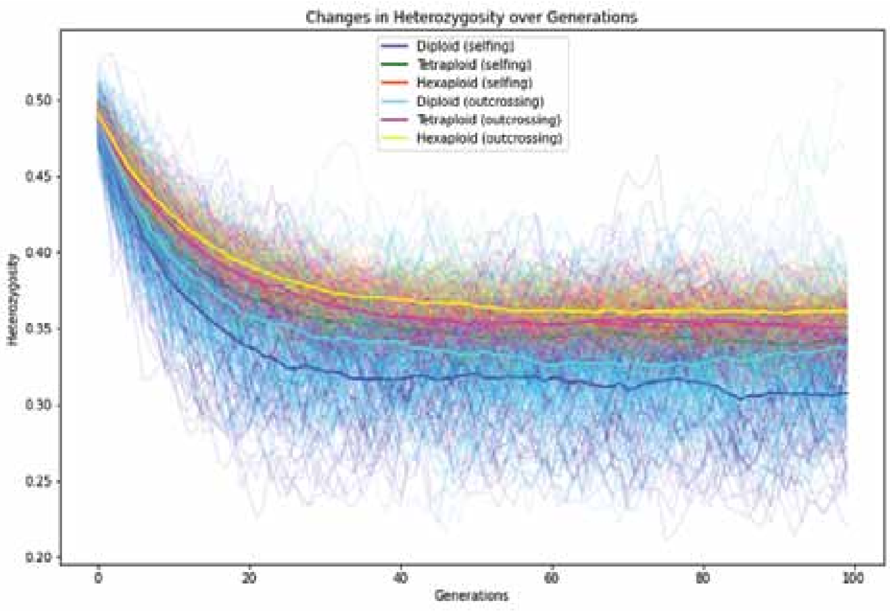

Figure 1. Trajectory of heterozygosity over 100 generations when starting with 0.5 heterozygosity.

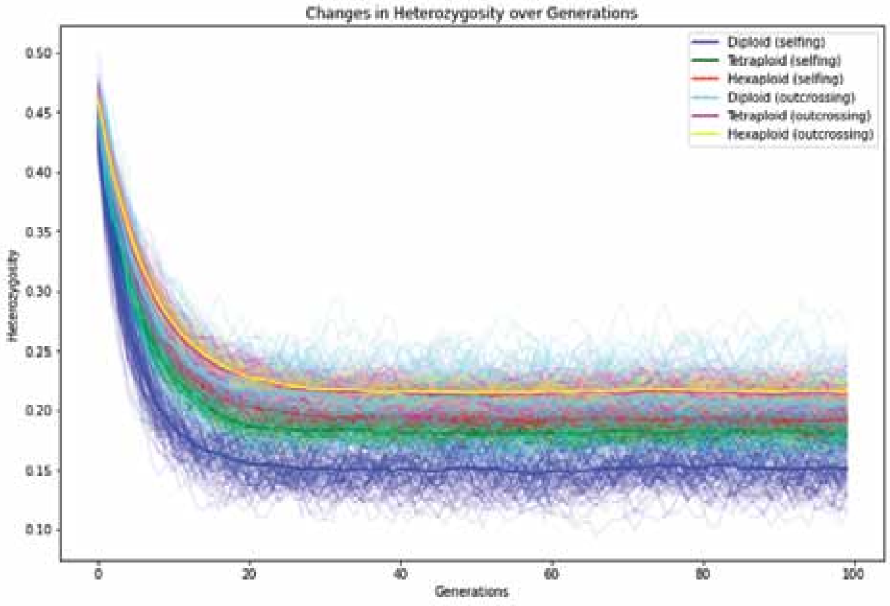

Figure 2. Trajectory of heterozygosity over 100 generations when starting with 0.5 heterozygosity and different starting parameters.

If polyploids were created as all or part of some pre-Fall baramins, we would expect that, if those baramins now contain multiple ploidy levels, some form of non-traditional sexual reproduction would be associated with that baramin. This could include vegetative reproduction, apomixis, selfing, or any other form of reproduction requiring only one plant. In some groups as noted above, selfing has been associated with polyploidy (Husband et al., 2002; Barringer, 2007; Robertson et al., 2010; Gao et al., 2016). In at least a few instances, apomixis is associated with polyploidy as well (Dickinson et al., 2007; Lo et al., 2009). In one genus of Rosaceae, diploids produced only 2% apomictic seeds while tetraploids produced 97% (Burgess et al., 2014)! In a species of Ranunculeae, 65% of the tetraploid populations were at least facultative apomicts (Horandl et al., 2016). An analysis of 940 Czech angiosperms found a similar correlation between increased vegetative reproduction and polyploidy (Herben et al., 2017). It is likely than many of these forms of reproduction, even potentially all of them, were present in the original created polyploids and were exploited in the post-Flood world to allow plants to rapidly fill niches.

Predictions of Created Polyploidy

If polyploidy was built into baramins from the beginning, what might we expect in the present? Baramins with created polyploidy would likely have multiple ploidy levels within them due to the potential for further polyploidization and diploidization (Chen et al., 2007). Due to genome degradation, it is likely that the present baramin has significantly differentiated in cytotypes. Another prediction would be a significant number of the species within the baramin would employ asexual reproduction or selfing at least part of the time. Neither of these predictions is particularly Earth-shattering and are in line with current research in polyploidy.

A corollary to the prediction that polyploids will be associated with

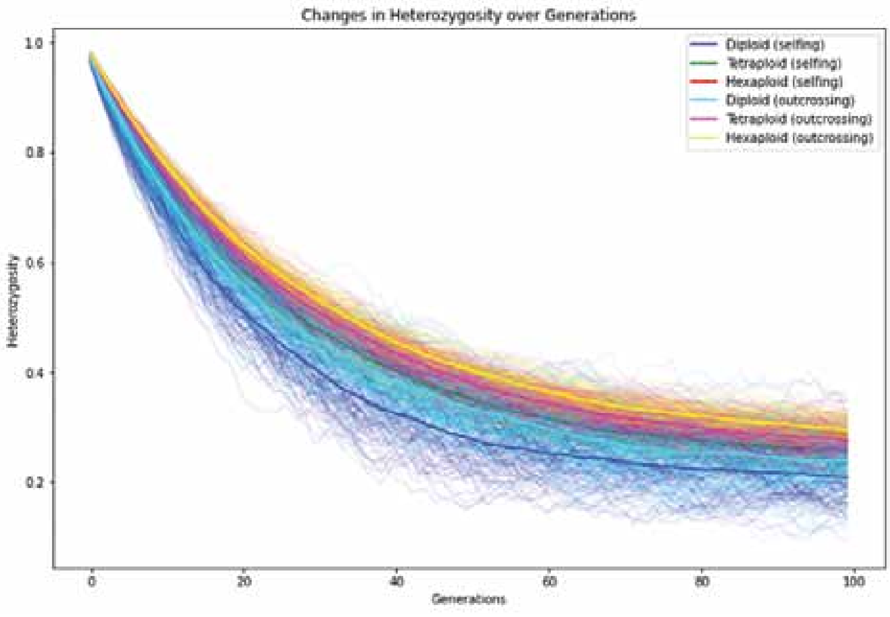

Figure 3. Trajectory of heterozygosity over 100 generations when starting with 1.0 heterozygosity.

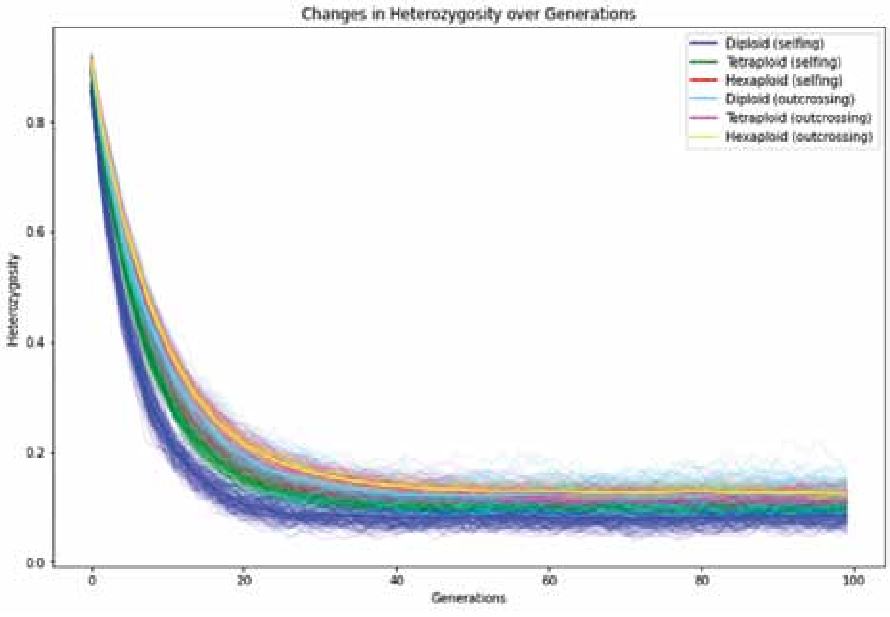

Figure 4. Trajectory of heterozygosity over 100 generations when starting with 1.0 heterozygosity and different starting parameters.

asexuals and selfing, is that polyploids are likely to be monoecious (having both gender organs on the same plant) because this would enable selfing. There is at least some evidence for this idea. The annual *Mercurialis annua* is a polyploid complex in which the diploids are dioecious (having separate male and female individuals), but the polyploids are either androdiocious (having males and hermaphrodites coexist) or completely monoecious (Pannell et al., 2004). However, in *Bryonia*, there is no association between polyploidy and sexual system (Volz and Renner, 2008) and the consensus is that dioecy is associated with polyploidy, not monoecy (Ashman et al., 2013). Dioecy is present in roughly six percent of total angiosperm species (Renner, 2014), which, given the vast number of angiosperm species presumed to have a polyploid origin (Levy and Feldman, 2002), makes a link between polyploids and dioecy seem to be a stretch. More research is needed in this area.

If polyploids were created and then diploidized later, we would expect that the polyploid members of the baramin in the present would generally have higher genetic diversity than their diploid relatives, provided they share the same mode of reproduction. By default, a change from tetraploidy to diploidy costs the plant 2 alleles of 4 at a given loci. Thus, if CHNP is true and the created polyploids were full heterozygotes, a drop in ploidy to diploid could cost the plant half (or more if it originated higher than a tetraploid) of its genetic diversity. However, if diploidy is the created state and polyploidy arises afterwards via autopolyploidy, the diploids should have higher genetic diversity. Allopolyploidy arising in a baramin not created polyploid may or may not have greater diversity than the paternal diploid species. If one species produces sexually, and the other asexually, diversity will usually be lower for the asexual species.

Because of the difficulty of determining the allele frequencies in polyploids, studies of genetic diversity are rarely done. That said, there have been a few investigations into the topic. Polyploidy has been proposed as the

Table II. Results of simulations with starting heterozygosity of 0.5.

Simulation Number	Breeding System	Comparison	p-value
1	Selfing	Diploid-Tetraploid	0 [1]
1	Selfing	Tetraploid-Hexaploid	$1.697\ e^{-206}$
1	Selfing	Diploid-Hexaploid	0
1	Outcross	Diploid-Tetraploid	0
1	Outcross	Tetraploid-Hexaploid	$5.181\ e^{-104}$
1	Outcross	Diploid-Hexaploid	0
2	Selfing	Diploid-Tetraploid	0
2	Selfing	Tetraploid-Hexaploid	0
2	Selfing	Diploid-Hexaploid	0
2	Outcross	Diploid-Tetraploid	$7.915\ e^{-103}$
2	Outcross	Tetraploid-Hexaploid	$1.273\ e^{-13}$
2	Outcross	Diploid-Hexaploid	0

[1] P values of zero are statistically impossible. They represent values too small for the software to record. In this instance it is likely due to the large (10,000 simulation) dataset. They have not been rounded.

Table III. Results of simulations with starting heterozygosity of 1.

Simulation Number	Breeding System	Comparison	p-value
3	Selfing	Diploid-Tetraploid	$3.541\ e^{-238}$
3	Selfing	Tetraploid-Hexaploid	$4.371\ e^{-57}$
3	Selfing	Diploid-Hexaploid	0 [2]
3	Outcross	Diploid-Tetraploid	$2.823\ e^{-118}$
3	Outcross	Tetraploid-Hexaploid	$1.094\ e^{-237}$
3	Outcross	Diploid-Hexaploid	$1.361\ e^{-33}$
4	Selfing	Diploid-Tetraploid	0
4	Selfing	Tetraploid-Hexaploid	$1.278\ e^{-291}$
4	Selfing	Diploid-Hexaploid	0
4	Outcross	Diploid-Tetraploid	$3.51\ e^{-52}$
4	Outcross	Tetraploid-Hexaploid	$8.39\ e^{-12}$
4	Outcross	Diploid-Hexaploid	$2.46\ e^{-90}$

[2] P values of zero are statistically impossible. They represent values too small for the software to record. In this instance it is likely due to the large (10,000 simulation) dataset. They have not been rounded.

explanation for the higher genetic diversity in the tetraploid of a diploid-tetraploid species complex (Ortiz-Dorda et al., 2005). Genetic diversity is believed to be maintained better in polyploids than in diploids (Soltis and Soltis, 2000). In a species of *Oxalis*, sexual tetraploids had higher mean genetic diversity than sexual diploids, but asexual pentaploids had lower genetic diversity than sexual tetraploids (Ferrero et al., 2015). Genetic diversity increased with increasing ploidy level in a study of Bermudagrasses (Yan et al., 2019). Obviously much more work is needed here, particularly baramin-wide analysis of genetic diversity, but early results look promising and align with the computer model presented above.

In the post-Flood world, the entire Earth would have been available for plants to colonize. Species able to reproduce quickly, and with a generalized genome that enabled them to adapt quickly, would be preferred in such an open environment. Polyploid plants fit both bills with their penchant for asexuality and their increased diversity. In a sense, the post-Flood dispersal was the ultimate invasion of foreign species, with little competition. Polyploidy has been associated with invasive species (Te Beest et al., 2012; Wani et al., 2018) through improved nutrient uptake (Qiang et al., 2019) and the potential for increased growth rate (Hahn et al., 2012). In a post-Flood environment, these traits would have likely made polyploidy a dominant factor in the landscape. Therefore, we might expect an association between polyploidy and invasiveness in at least the baramins with created polyploidy.

In addition to their invasive capabilities, there is an association between polyploid plants and perennialism across most angiosperms (Van Drunen and Husband, 2019). This association is not necessarily a prediction of the model, but it is not incongruous with created polyploidy. It is possible that created polyploids had the genes required for both an annual and perennial lifestyle, and post-Fall diploidization and diversification resulted in a prevalence of polyploid perennials and diploid annuals. Due to this gene loss, it is conceivable that there will be differences in flowering times, lengths, and frequencies between related annuals and polyploids. Indeed, in several perennials, tetraploids flower before diploids (Petit et al., 1997; Nuismer and Cunningham, 2005; Scopece et al., 2016). Since flowering time is epigenetically regulated in some polyploids (Pires et al., 2011; Jiang et al., 2022), and epigenetics is controlled in part by TEs (Ainouche et al., 2009), there is a potentially fruitful field of research here that could find an association between activity of transposable elements, flowering time, and ploidy level.

While this model argues for created polyploids, it does not argue that neopolyploids cannot be formed. Many of the same expectations for created polyploids will also be true of neopolyploids. There will, however, be a few differences. Neopolyploids formed by autopolyploidy will likely have lower genetic diversity than their parents while those formed by allopolyploidy likely will have higher genetic diversity than their paternal species. It is conceivable that neo-allopolyploids may have lower genetic diversity than one or both of their parents, however, depending on the paternal species.

Further, neopolyploids will be divergent in some way from their diploid progenitors. Likely this will be in habitat preference due to gene dosage and TE activation. In *Isoetes*, the six polyploid species all are found at lower altitudes than the four diploid species (Wang et al., 2004). Different ploidy levels of primrose exhibit habitat segregation based on several climactic traits (Theodoridis et al., 2013). These and other similar changes are likely for recently formed polyploids.

Conclusions

It is admittedly difficult to test the model as outlined above given the comparative inattention that baraminology has paid to plants and the unreliability of current baraminological methods (Sanders and Cserhati, 2022). However, in time, as baraminology improves and plant baramins are delineated successfully, this model will likely be easier to test. Importantly, using polyploidy as an explanation for the diversity of plant life helps not only to explain why some postulated baramins might be so large, but also helps to account for the vast diversity of created plants without appealing to "millions of years" of mutations. As such, creation biologists should consider created polyploidy as a potential answer to this question in plants.

References

Ainouche, M., C. Parisod, A. Salmon, T. Zerjal, M. Tenaillon, and M.A. Grandbastien. 2009. Rapid structural and epigenetic reorganization near transposable elements in hybrid and allopolyploid genomes in *Spartina*. *New Phytologist* 184:1003–1015.

Ashman, T.L., A. Kwok, and B.S. Husband. 2013. Revisiting the dioecy-polyploidy association: Alternative pathways and research opportunities. *Cytogenetic and Genome Research* 140:241–255.

Baack, E.J. 2004. Cytotype segregation on regional and microgeographic scales in snow buttercups (*Ranunculus adoneus*: Ranunculaceae). *American Journal of Botany* 91(11):1783–1788.

Baack, E.J. 2005. Ecological factors influencing tetraploid establishment in snow buttercups (*Ranunculus adoneus*, Ranunculaceae): Minority cytotype exclusion and barriers to triploid formation. *American Journal of Botany* 92(11):1827–1835.

Barker, M.S., N. Arrigo, A.E. Baniaga, Z. Li, and D.A. Levin. 2016. On the relative abundance of autopolyploids and allopolyploids. *New Phytologist* 210:391–398.

Barringer, B.C. 2007. Polyploidy and self-fertilization in flowering plants. *American Journal of Botany* 94(9):1527–1533.

Belzile, F., J. Beaulieu, and M. Jean. 2009. The allotetraploid *Arabidopsis thaliana-Arabidopsis lyrate* subsp. Petraea as an alternative model system for the study of polyploidy in plants. *Molecular Genetics and Genomics* 281:421–435.

Bennett, M.D. 2004. Perspectives on polyploidy in plants—Ancient and neo. *Biological Journal of the Linnean Society* 82:411–423.

Blanc, G., and K.H. Wolfe. 2004. Widespread paleopolyploidy in model plant species inferred from age distributions of duplicate genes. *Plant Cell* 16(7):1667–1678.

Burgess, M.B., K.C. Cushman, E.T. Doucette, N. Talent, C.T. Frye, and C.S. Campbell. 2014. Effects of apomixis and polyploidy on diversification and geographic distribution in *Amelanchier* (Rosaceae). *American Journal of Botany* 101(8):1375–1387.

Burton, T.L., and B.C. Husband. 2000. Fitness differences among diploids, tetraploids, and their triploid progeny in *Chamerion angustifolium*: Mechanisms of inviability and implications for polyploid evolution. *Evolution* 54(4):1182–1191.

Castro, M., J. Loureiro, B.C. Husband, and S. Castro. 2020. The role of multiple reproductive barriers: strong post-pollination interactions govern cytotype isolation in a tetraploid-octoploid contact zone. *Annals of Botany* 126(6):991–1003.

Castro, S., J. Loureiro, T. Prochazka, and Z. Munzbergova. 2012. Cytotype distribution at a diploid-hexaploid contact zone in *Aster amellus* (Asteraceae). *Annals of Botany* 110(5):1047–1055.

Chai, L., M.H. Ahmad, M.J. Rao, J. Hu, Q. Xu, C. Liu, Z. Cao, R.M. Larkin, X. Deng, and M. Bosch. 2022. Systems and breakdown of self-incompatibility. *Critical Reviews in Plant Sciences* 41(3):1–31.

Chen, J., L. Chen, Q. Lou, Y. Zhuang, X. Zhang, and J.N. Wolukau. 2007. Cytological diploidization and rapid genome changes of the newly synthesized allotetraploids *Cucumis x hytivus*.

Planta 225:603–614.

Church, S.A., and E.J. Spaulding. 2009. Gene expression in a wild autopolyploid sunflower series. *Journal of Heredity* 100(4):491–495.

Conant, G.C., J.A. Birchler, and J.C. Pires. Dosage, duplication and diploidization: Clarifying the interplay of multiple models for duplicate gene evolution over time. *Current Opinion in Plant Biology* 19:91–98.

Contreras, R.N., J.J. Rothleutner, and M.W. Friddle. 2016. Ploidy levels, relative genome sizes, and base pair composition in *Cotoneaster*. *Journal of the American Society of Horticulture* 141:457–466.

Dickinson, T.A., E. Lo, and N. Talent. 2007. Polyploidy, reproductive biology, and Rosaceae: Understanding evolution and making classification. *Plant Systematics and Evolution* 266:59–78.

Dodsworth, S., M.W. Chase, and A.R. Leitch. 2016. Is post-polyploidization diploidization the key to the evolutionary success of angiosperms? *Botanical Journal of the Linnean Society* 180(1):1–5.

Dubcovsky, J.D. Cantu, L.S. Vanzetti, A. Sumner, M. Dubcosky, M. Matvienko, A. Disteldeld, and R.W. Michelmore. 2010. Small RNAs, DNA methylation, and transposable elements in wheat. *BMC Genomics* 11:408.

Edger, P.P., K.A. Bird, R. VanBuren, and J.R. Puzey. 2018. The causes and consequences of subgenome dominance in hybrids and recent polyploids. *New Phytologist* 220:87–93.

Felber-Garard, M., F. Felber, and A. Buttler. 1996. Habitat differentiation in a narrow hybrid zone between diploid and tetraploid *Anthoxanthum alpinum*. *New Phytologist* 133:531–540.

Ferrero, V., S.C.H. Barrett, S. Castro, P. Caldeirinha, L. Navarro, J. Loureiro, and S. Rodrigues-Echeverria. Invasion genetics of the Bermuda buttercup (*Oxalis pes-caprae*): complex intercontinental patterns of genetic diversity, polyploidy, and heterostyly characterize both native and introduced populations. *Molecular Ecology* 24:2143–2155.

Feschotte, C., and E.J. Pritham. 2007. DNA transposons and the evolution of eukaryotic genomes. *Annual Reviews Genetics* 41:331–368.

Filatov, D.A., M. Krasovec, Y. Kazama, K. Ishii, and T. Abe. 2019. Immediate dosage compensation is triggered by the deletion of Y-linked genes in *Silene latifolia*. *Current Biology* 29(13):2214–2221.

Freeling, M., M.R. Woodhouse, F. Cheng, J.C. Pires, D. Lisch, and X. Wang. 2014. Origin, inheritance, and gene regulatory consequences of genome dominance in polyploids. *Proceedings of the National Academy of Sciences USA* 111(14):5283–5288.

Galili, G., A.A. Levy, and M. Feldman. 1986. Gene-dosage compensation of endosperm proteins in hexaploidy wheat *Triticum aestivum*. *Proceedings of the National Academy of Sciences USA* 83:6524–6528.

Gao, C., G. Zhou, C. Ma, W. Zhai, T. Zhang, Z. Liu, Y. Yang, M. Wu, Y. Yue, Z. Duan, Y. Li, B. Li, J. Shen, J. Tu, and T. Fu. 2016. *Helitron*-like transposons contributing to the mating system transition from out-crossing to self-fertilizing in polyploid *Brassica napus* L. *Scientific Reports* 6:33785.

Grandbastien, M.A., M. Petit, C. Guidat, J. Daniel, E. Denis, E. Montoriol, Q.T. Bui, K.Y. Lim, A. Kovarick, A.R. Leitch, and C. Mhiri. 2010. Mobilization of retrotransposons in synthetic allotetraploid tobacco. *New Phytologist* 186:135–147.

Guo, M., D. Davis, and J.A. Birchler. 1996. Dosage effects on gene expression in a maize ploidy series. *Genetics* 142:1349–1355.

Hahn, M.A., Y.M. Buckley, and H. Muller-Scharer. 2012. Increased population growth rate in invasive polyploid *Centaurea stoebe* in a common garden. *Ecology Letters* 15(9):947–954.

Herben, T., J. Suda, and J. Klimesova. 2017. Polyploid species rely on vegetative reproduction more than diploids: a re-examination of the old hypothesis. *Annals of Botany* 120(2):341–349.

Hojsgaard, D., and E. Horandl. 2015. A little bit of sex matters for genome evolution in asexual plants. *Frontiers in Plant Science* 6:82.

Horandl, E. 2008. Evolutionary implications of self-compatibility and reproductive fitness in the apomictic *Ranunculus auricomus* polyploid complex (Ranunculaea). *International Journal of Plant Science* 169(9):1219–1228.

Horandl, E., C.C.F. Schinkel, B. Kirchheimer, A.S. Dellinger, S. Klatt, M. Winkler, and S. Dullinger. 2016. Correlations of polyploidy and apomixis with elevation and associated environmental gradients in an alpine plant. *AoB Plants* 8:plw064.

Husband, B.C. 2000. Constraints on polyploid evolution: A test of the minority cytotype exclusion principle. *Proceedings of the Royal Society of London, B* 267(1440):217–223.

Husband, B.C., B. Ozimec, S.L. Martin, and L. Pollock. 2002. Mating consequences of polyploid evolution in flowering plants: current trends and insights from synthetic polyploids. *International Journal of Plant Science* 169(1):195–206.

Iezzoni, A.F., N.R. Hauck, H. Yamane, and R. Tao. 2006. Accumulation of nonfunctional *S*-haplotypes results in the breakdown of gametophytic self-incompatibility in tetraploid *Prunus*. *Genetics* 172:1191–1198.

Jeanson, N.T., and J. Lisle. 2016. On the origin of eukaryotic species' genotypic and phenotypic diversity. *Answers Research Journal* 9:81–122.

Jiang, H., C. Jingping, G. Zhang, L. Xu, and C. Liu. 2022. Altered H3K27 trimethylation contributes to flowering time variations in polyploid *Arabidopsis thaliana* ecotypes. *Journal of Experimental Botany* 73:1402–1414.

Johnson, M.T.J., B.C. Husband, and T.L. Burton. 2003. Habitat differentiation between diploid and tetraploid *Galax urceolata* (Diapensiaceae). *International Journal of Plant Science* 164:703–710.

Kao, R.H. 2007. Asexuality and the coexistence of cytotypes. *New Phytologist* 175:764–772.

Kashkush, K., M. Feldman, and A.A. Levy. 2002. Gene loss, silencing, and activation in a newly synthesized wheat allotetraploid. *Genetics* 160:1651–1659.

Kashkush, K., Z. Kraitshtein, B. Yaakov, and V. Khasdan. 2010. Genetic and epigenetic dynamics of a retrotransposon after allopolyploidization of wheat. *Genetics* 186(3):801–812.

Kashkush, K., and B. Yaakov. 2011. Methylation, transcription, and rearrangements of transposable elements in synthetic allopolyploids. *International Journal of Plant Genomics* 2011:569826.

Kelly, J.K., B. Koseva, D.J. Crawford, K.E. Brown and M.E. Mort. 2017. The genetic breakdown of sporophytic self-incompatibility in *Tolpis coronopifolia* (Asteraceae). *New Phytologist* 216:1256–1267.

Kirchheimer, B., C.C.F. Schinkel, A.S Dellinger, S. Klatt, D. Moser, M. Winkler, J. Lenoir, M. Caccianiga, A. Guisan, D. Nieto-Lugilde, J.C. Svenning, W. Thuiller, P. Vittoz, W. Willner, N.E. Zimmermann, E. Horandl, and S. Dullinger. 2016. A matter of scale: Apparent niche differentiation of diploid and tetraploid plants may depend on extent and grain of analysis. *Journal of Biogeography* 43(4):716–726.

Layman, N.C., and J.W. Busch. 2018. Bottlenecks and inbreeding depression in autotetraploids. *International Journal of Organic Evolution* 72(10):2025–2037.

Levin, D.A. 1975. Minority cytotype exclusion in local plant populations. *Taxon* 24(1):35–43.

Levy, A.A., and M. Feldman. 2002. The impact of polyploidy on grass genome evolution. *Plant Physiology* 130:1587–1593.

Lo, E.Y.Y., S. Stefanovic, and T.A. Dickinson. 2009. Population genetic structure of diploid sexual and polyploid apomictic hawthorns (*Crataegus*; Rosaceae) in the Pacific Northwest. *Molecular Ecology* 18:1145–1160.

Liu, B., Y. Wu, F. Lin, Y. Zhou, S. Sun, B. Wang, Z. Zhang, G. Li., X. Lin, X. Wang, Y. Sun, Q. Dong, C. Xu, L. Gong, J.F. Wendel, and Z. Zhang. 2020. Genomic mosaicism due to homoeologous exchange generates extensive phenotypic diversity in nascent allopolyploids. *National Science Review* 8(5):nwaa277.

Liu, C., and Y.-G. Wang. 2022. Does one subgenome become dominant in the formation and evolution of a polyploid? *Annals of Botany* 131(1):11–16.

Liu, S., A.R. Fenrie, R.A. Gill, F. Scossa, G.J. King, A.A. Golicz, C. Tong, and R.J. Snowdon. 2021. On the role of transposable elements in the regulation of gene expression and subgenomic interactions in crop genomes. *Critical Reviews in Plant Sciences* 40(2):157–189.

Lundgren, M.R., P.A. Christin, E.G. Escobar, B.S. Ripley, G. Besnard, C.M. Long, P.W. Hattersley, R.P. Ellis, R.C. Leegood, and C.P. Osborne. 2016. Evolutionary implications of C_3–C_4 intermediates in the grass *Alloteropsis semialata*. *Plant, Cell & Environment* 39:1874–1885.

Mable, B.K. 2004. Polyploidy and self-compatibility: Is there an association? *New Phytologist* 162:803–811.

Mason, A.S., and J.F. Wendel. 2020. Homoeologous exchanges, segmental allopolyploidy, and polyploid genome evolution. *Frontiers in Genetics* 11:1014.

Muller, H.J. 1964. The relation of recombination to mutational advance. *Mutation Research* 1:2–9.

Muyle, A.R. Shearn, and G.A.B. Marais. 2017. The evolution of sex chromosomes and dosage compensation in plants. *Genome Biology and Evolution* 9(3):627–645.

Nuismer, S.L., and B.M. Cunningham. 2005. Selection for phenotypic divergence between diploid and autotetraploid *Heuchera grossulariifolia*. *Evolution* 59(9):1928–1935.

Oberprieler, C., M. Talianova, and J. Griesenbeck. 2019. Effects of polyploidy on the coordination of gene expression between organellar and nuclear genomes in *Leucanthemum* Mill. (Compositae, Anthemidae). *Ecology and Evolution* 9:9100–9110.

Ortiz-Dorda, J., C. Martinez-Mora, E. Correal, B. Simon, and J.L. Cenis. 2005. Genetic structure of *Atriplex halimus* populations in the Mediterranean basin. *Annals of Botany* 95(5):827–834.

Pannell, J.R., D.J. Obbard, and R.J.A. Buggs. 2004. Polyploidy and the sexual system: What can we learn from *Mercurialis annua*? *Biological Journal of the Linnean Society* 82:547–560.

Parris, J.K., T.G. Ranney, H.T. Knap, and W.V. Baird. 2010. Ploidy levels, relative genome sizes, and base pair composition in *Magnolia*. *Journal of the American Society of Horticulture* 135:533–547.

Petit, C., P. Lesbros, X. Ge, and J.D. Thompson. 1997. Variation in flowering phenology and selfing rate across a contact zone between diploid and tetraploid *Arrhenatherum elatius* (Poaceae). *Heredity* 79:31–40.

Pires, J.C., and R.T. Gaeta. 2009. Homoeologous recombination in the allopolyploids: The polyploid ratchet. *New Phytologist* 186:18–28.

Pires, J.C., D. Mayfield, and Z.J. Chen. 2011. Epigenetic regulation of flowering time in polyploids. *Current Opinion in Plant Biology* 14:174–178.

Qiang, S., S. Wu, J. Cheng, X. Xu, Y. Zhang, Y. Zhao, and H. Li. 2019. Polyploidy in invasive *Solidago canadensis* increased plant nitrogen uptake, and abundance and activity of microbes and nematodes in soil. *Soil Biology and Biochemistry* 138:107594.

Renner, S.S. 2014. The relative and absolute frequencies of angiosperm sexual systems: Dioecy, monoecy, gynodioecy, and an updated online database. *American Journal of Botany* 101(10):1588–1596.

Robertson, K., E.E. Goldberg, and B. Igic. 2010. Comparative evidence for the correlated evolution of polyploidy and self-compatibility in Solanaceae. *Evolution* 65(1):139–155.

Sanders, H.F., and M.F. Cserhati. 2022. Statistics, baraminology, and interpretations: A critical evaluation of BDIST. *Creation Research Society Quarterly* (in press).

Sanford, J.C. 2014. *Genetic Entropy*. FMS Publications, Canadaigua, NY.

Schwander, T., M. Neiman, and T.F. Sharbel. 2014. Genetic causes of transitions from sexual reproduction to asexuality in plants and animals. *Journal of Evolutionary Biology* 27:1346–1359.

Scopece, G., L. Pegoraro, D. Cafasso, R. Rinaldi and S. Cozzolino. 2016. Habitat preference and flowering-time variation contribute to reproductive isolation between diploid and autotetraploid *Anacamptis pyramidalis*. *Journal of Evolutionary Biology* 29:2070–2082.

Shirk, R.Y., J.L. Hambrick, C. Zhang, and S. Qiang. 2013. Patterns of genetic diversity reveal multiple introductions and recurrent founder effects during range expansion in invasive populations of *Geranium carolinianum* (Geraniaceae). *Heredity* 112:497–507.

Siopa, C., M.C. Dias, M. Castro, J. Loureiro, and S. Castro. 2020. Is selfing a reproductive assurance promoting polyploid establishment? Reduced fitness, leaky self-incompatibility, and lower inbreeding depression in neotetraploids. *American Journal of Botany* 107(3):526–538.

Slotkin, R.K., K. Panda, L. Ji, D. A. Neuman, J. Daron, and RJ. Schmitz. 2016. Full-length autonomous transposable elements are preferentially targeted by expression-dependent forms of RNA-directed DNA methylation. *Genome Biology* 17(1):170.

Soltis, D.E., and P.S. Soltis. 1999. Polyploidy: Recurrent formation and genome evolution. *TREE* 14(9):348–352.

Soltis, P.S., and D.E. Soltis. 2000. The role of genetic and genomic attributes in the success of polyploids. *Proceedings of the National Academy of Sciences USA* 97(13):7051–7057.

Spoelhof, J.P., P.S. Soltis, and D.E. Soltis. 2017. Pure polyploidy: Closing the gaps in autopolyploid research. *Journal of Systematics and Evolution* 55(4):340–352.

Stupar, R.M., P.B. Bhaskar, B.S. Yandell, W.A. Rensink, A.L. Hart, S. Ouyang, R.E. Veilleux, J.S. Busse, R.J. Erhardt, C.R. Buell, and J. Jang. 2007. Phenotypic and transcriptomic changes associated with potato autopolyploidization. *Genetics* 176(4):2055–2067.

Sunyaev, S.R., D.J. Balick, R.Do, C.A. Cassa, and D. Reich. 2015. Dominance of deleterious alleles controls the response to a population bottleneck. *PLoS Genetics* 11(8):e1005436.

Sutherland, B.L., B.M. Quarles, and L.F. Galloway. 2018. Intercontinental dispersal and whole-genome duplication contribute to loss of self-incompatibility in a polyploid complex. *American Journal of Botany* 105(2):249–256.

Tate, J.A., P. Joshi, K.A. Soltis, P.S. Soltis, and D.E. Soltis. 2009. On the road to diploidization? Homeolog loss in independently formed populations of the allopolyploid *Tragopogon miscellus* (Asteraceae). *BMC Plant Biology* 9:80.

Te Beest, M., J.J. Le Roux, D.M. Richardson, A.K. Brysting, J. Suda, M. Kubesova, and P. Pysek. 2012. The more the better? The role of polyploidy in facilitating plant invasions. *Annals of Botany* 109(1):19–45.

Theodoridis, S., C. Randin, O. Broennimann, T. Patsiou, and E. Conti. 2013. Divergent and narrower climactic niches characterize polyploid species of European primroses in *Primula* sect *Aleuritia*. *Journal of Biogeography* 40(7):1278–1289.

Van Drunen, W.E., and B.C. Husband. 2019. Evolutionary associations between polyploidy, clonal reproduction, and perenniality in the angiosperms. *New Phytologist* 224:1266–1277.

Vicient, C.M., and J.M. Casacuberta. 2017. Impact of transposable elements on polyploid plant genomes. *Annals of Botany* 120(2):195–207.

Volz, S.M., and S.S. Renner. 2008. Hybridization, polyploidy, and evolutionary transitions between monoecy and dioecy in *Bryonia* (Cucurbitaceae). *American Journal of Botany* 95(10):1297–1306.

Wang, Q.F., X. Liu, and W.R. Gituru. 2004. Distribution of basic diploid and polyploid species of *Isoetes* in East Asia. *Journal of Biogeography* 31:1239–1250.

Wang, J., L. Tian, H.S. Lee, N.E. Wei, H. Jiang, B. Watson, A. Madlung, T.C. Osborn, R.W. Doerge, L. Comai, and Z.J. Chen. 2006. Genomewide nonadditive gene regulation in *Arabidopsis* allotetraploids. *Genetics* 172(1):507–517.

Wani, G.A., M.A. Shah, Z.A. Reshi, and M.A. Dar. 2018. Polyploidy determines the stage of invasion: clues from Kashmir Himalayan aquatic flora. *Acta Physiologiae Plantarum* 40:58.

Wendel, J., L. Flagel, J. Udall, and D. Nettleton. 2008. Duplicate gene expression in allopolyploid Gossypium reveals two temporally distinct phases of expression evolution. *BMC Biology* 6:16.

Wendel, J.F., A. Salmon, L. Flagel, B. Ying, and J.A. Udall. 2009. Homoeologous nonreciprocal recombination in polyploid cotton. *New Phytologist* 186:123–134.

Wendel, J.F., G. Hu, C.E. Grover, and J.S. Hawkins. 2010. The history and disposition of transposable elements in polyploid *Gossypium*. *Genome* 53:599–607.

Whitton, J., C.J. Sears, E.J. Baack, and S.P. Otto. 2008. The dynamic nature of apomixis in the angiosperms. *International Journal of Plant Science* 169(1):169–182.

Wolfe, K.H. 2001. Yesterday's polyploids and the mystery of diploidization. *Nature Reviews Genetics* 2:333–341

Wood, T.C. 2002. A baraminology tutorial with examples from the grasses (Poaceae). *Journal of Creation* 16(1):15–25.

Wood, T.C. 2008. *Animal and Plant Baramins*. Wipf and Stock, Eugene, OR.

Wood, T.E., Takebayashia, N., Barker, M.S., Mayrose, I., Greenspoon, P.B., and L. Riesenberg. 2009. The frequency of polyploid speciation in vascular plants. *Proceedings of the National Academy of Sciences USA* 106:13875–13879.

World Checklist of Selected Plant Families. 2021. Facilitated by the Royal Botanic Gardens, Kew, UK.

Yan, X., J. Zhang, M. Wang, Z. Guo, Y. Guan, J. Liu, and Y. Guo. 2019. Genetic diversity and population structure of Bermudagrass [*Cynodon dactylon* (L.) Pers.] along longitudinal gradients and the relationship with polyploid level. *Diversity* 11:9.

Creation Research Society Quarterly 2025 61:202–212

Numerical Evaluation of Post-Flood Formation of Transverse Drainages (Water Gaps)

Nathan W. Mogk*

Abstract

Transverse drainages (water & wind gaps) have been proposed as a criterion for determining the Flood/post-Flood boundary, but what are the limits of the conventional formation mechanisms? In this study I establish an index for comparing transverse drainages of differing depth scales. An index value near zero implies that the stream passes through the lowest divide, and is associated with plausible lake spillover or tectonic and erosional changes to the hydraulic system. An index value near one implies that the transverse drainage is hydraulically close to the same configuration as when it was carved. This index is used to select the Shoshone-Rattlesnake and Wheeler Ridge transverse drainages for modeling their formation by antecedence. Linear and logarithmic uplift models are used. The maximal depth of an antecedent or superimposed transverse drainage is determined to be around 200 ft. without enhanced erosion. Enhanced uplift rate at the end of the Flood is found to necessitate higher erosion rates, and sets a minimum catastrophe size required to generate a gap. For the Shoshone-Rattlesnake transverse drainage, the necessary erosion strongly implies a late-Flood origin, whereas for Wheeler Ridge, the required erosion is of the same order of magnitude as modeled, and could plausibly be generated in post-Flood time by antecedence.

Key Words: antecedence, Shoshone, transverse drainages, water gaps, Wheeler Ridge

Introduction

Transverse drainages (also known as water and wind gaps) are landforms that are as enigmatic as they are ubiquitous (Lee, 2019). The primary characteristic of transverse drainages is that the axis of a valley (in the case of wind gaps) or stream (in the case of water gaps) crosses the trend of a structural barrier. It was this feature of crossing pre-existing barriers which thwarted alternative uniformitarian models of the Missoula Flood at the beginning of the last century, and this same feature

---

* Nathan W. Mogk, Tucson, AZ, nm8911@gmail.com

Accepted for publication June 5, 2024

ensures research on the origin of the Grand Canyon is perpetually vigorous. There has been a resurgence in recent decades in research relating to the formation of transverse drainages by overspill of a bedrock ridge (Meek, 2019). In the past, transverse drainages were primarily explained by *antecedence*, whereby a preexisting river cuts through rising terrain, and very occasionally *superimposition*, when the river eroding through soft sediment sets its course and drapes itself across buried resistant topography (also referred to as superposition), and piracy by drainage-head erosion, regardless of the presence or absence of any applicable evidence. The cause for this was largely paradigmatic (i.e., overspill mechanisms were considered philosophically unacceptable). However, this has been changing partly due to the abundant evidence for spillover (Hilgendorf et al., 2020).

Douglass et al. (2009) summarize the four conventionally invoked mechanisms for transverse drainage formation as well as many variants and in-between cases. They then develop a suite of criteria that can be used to help distinguish the various types. The distinguishing criterion of first importance is the relative timing between ridge uplift and stream establishment. Antecedence and superimposition require that the stream predates the uplift of the bedrock high that will eventually become the crossed range. Overspill and piracy, on the other hand, have the ridge forming before being breached. It is also noted that because superimposition implies erosion of not only the transverse drainage gorge but also a large volume of covermass over the whole area, it is expected to take significantly longer to develop a transverse drainage by this mechanism than antecedence. The authors also note that drainage-head erosion will also take a significant amount of time and that it is only applicable in special circumstances. Instead, the authors point to other variants of piracy that are more likely to occur.

Figure 1. View of Shoshone Canyon looking West. Photo courtesy of Michael Oard.

Beyond the mechanisms discussed in the conventional literature, Oard (2013) has laid out numerous lines of evidence that most large-scale transverse drainages were carved during the latter half of the Genesis Flood. While obviously sharing many characteristics in common with the overspill mechanism, there are enough differences that make Flood runoff its own unique formation mechanism. Lake overspill is expected to develop at the topographic low point of the bounding basin. Flood runoff is not limited to pre-existing low points, and in some cases can be expected to form transverse drainages near the top of the ridge. Flood runoff can also produce multiple gaps simultaneously in the same range. Both of these distinguishing characteristics of Flood runoff are features shared with antecedence and superimposition in the criteria of Douglass et al. (2009).

Though the Flood is a sufficient mechanism for carving any transverse drainage, the other mechanisms remain as potential explanations, and should be considered as alternatives when interpreting the origin of any particular transverse drainage, particularly overspill and antecedence. Transverse drainages need to be analyzed individually for applicable evidences for all of the available mechanisms. Additional theoretical work to evaluate the full spectrum of formation mechanisms within the framework of Flood Geology needs to be produced. This study aims to constrain the maximal scale of transverse drainage that is possible by antecedence (and by extension, superimposition) to constrain its applicability in the post-Flood era. The applicability of post-Flood lake spillover is also briefly addressed through measurements of water gap configurations.

Transverse Drainages Examined in This Study

The Shoshone-Rattlesnake transverse drainage, commonly called Shoshone Canyon near Cody, Wyoming, cuts over 3000 ft. across the trend of Rattlesnake Mountain, which is an uplift block of Laramide age (Figure 1). The uplift is comprised of numerous well-indurated formations from the Cambrian Flathead Sandstone to the upper Cretaceous Frontier Sandstone with a granitic core. The interven-

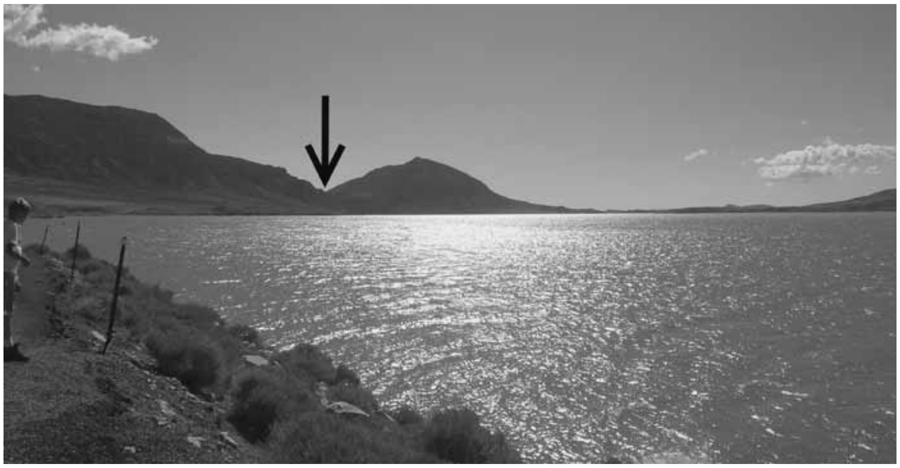

Figure 2. View of the Rattlesnake Mountains with Shoshone Canyon looking southeast. The alternate divide between the upstream and downstream basins is at lake level in the center-right. Photo courtesy of Michael Oard.

ing formations run the gamut from mudstone, shale, and sandstone to limestone and dolomite. The canyon has been cut without regard to the inherent strength of the underlying rocks (Johnson, 1934). Despite the great depth of the gorge through which the Shoshone River runs, there is essentially no divide separating the reaches above and below the canyon because the mountain range ends only three miles to the south. When the dam for Buffalo Bill Reservoir was built inside the gorge, a secondary dam also had to be built along the southern end of the reservoir (Figure 2) to prevent it from spilling around the edge of the range (Oard, 2018).

The Wheeler Ridge transverse drainage addressed in this study is a recently defeated wind gap through Wheeler Ridge through which the California Aqueduct flows south of Bakersfield, California (Figure 3). A water gap with a stream flowing through it is defeated when tectonic uplift forces the stream to abandon the water gap and flow through a lower-elevation alternate route, leaving a wind gap behind. Wheeler Ridge also has a smaller, presently active water gap, and a creek flowing around the

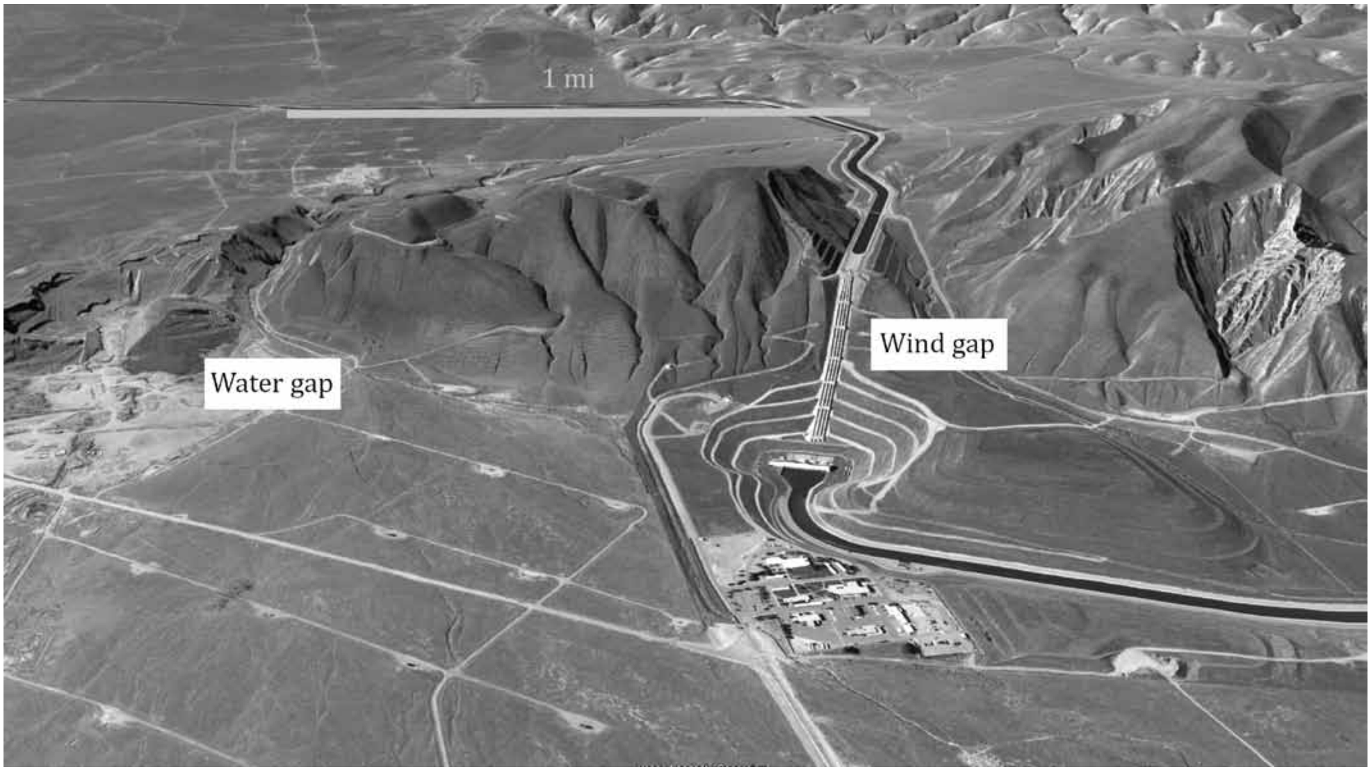

Figure 3. Oblique view of Wheeler Ridge looking south. Image credit: Google, Landsat/Copernicus.

eastern nose of the ridge which may cause the abandonment of the current water gap. Wheeler Ridge is an actively deforming fault-bend fold developed from a series of blind thrusts that are migrating laterally eastward (Mueller and Talling, 1997). Wheeler Ridge is located on the "Big Bend" segment of the San Andreas fault where it trends more east-west, whereas the large-scale trend of the overall fault is southeast-northwest. Shortening associated with Pacific plate movement is accommodated on minor thrust fault systems like the Pleito-Wheeler Ridge thrust fault system, while the main San Andreas fault remains largely strike-slip. Wheeler Ridge is composed of Pliocene to Pleistocene gravel, sand, and clay of the Tulare Formation which is locally up to 1960 ft. thick. The Tulare Formation is unconsolidated, and is sourced from the San Emigdio Mountains to the south. Distinct terrace levels with eastward decreasing dissection by gullies indicate that the fold is progressively migrating eastwards (Keller et al., 1998).

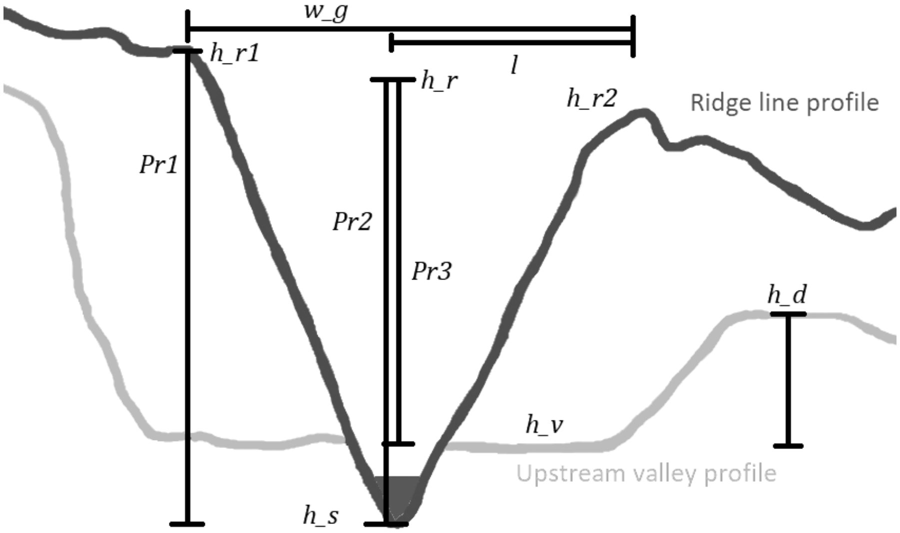

Figure 4. Schematic transverse drainage showing features and points of measurement.

Both of the examined transverse drainages are conventionally considered to have been carved by antecedence.

Erosion Rate Model

Given the central role of erosion rate in the formation of transverse drainages, it is important to establish an erosional model that will apply to the post-Flood conditions evaluated in this study. Several authors have made models of erosion rate based on the stream power equation (Rosenbloom and Anderson, 1994; Stock and Montgomery, 1999; Snyder et al., 2000), with calibration points selected based on the age dating of events in the distant past. The model implemented as part of this study, however, was that of Whipple et al. (2000) which provides an empirically derived erosion model based on measurements of the Upper Ukak River in the Valley of Ten Thousand Smokes, Alaska. The 1912 eruption of Novarupta buried the old Upper Ukak river pathway in ash, forcing the establishment of a new channel where there had previously been none. The new channel eroded into bedrock with some loose ash covering. Vegetation was largely disrupted by ash covering in the area as well. These conditions are well analogous to those expected in the aftermath of the Flood. Whipple et al. (2000) measured thalweg depth (i.e., the deepest portion of the stream crossing the ridge) from this known starting condition in 1997 covering 85 years of erosion, and their erosion rates were derived by fitting a model directly to the observations without any timing or old-age boundary assumptions.

Methods

Transverse drainage index and measurements

To facilitate direct comparison of transverse drainages in different geological contexts, I define a standard set of measurements and metrics that are broadly applicable to all transverse drainage scales. The typical features of a transverse drainage are shown in Figure 4. Transverse drainages comprise at minimum a ridge line with an eroded gorge transverse to the trend of the ridge. On the upstream side, there is typically a broad valley with a generally defined base level. The stream may be incised below the elevation of the valley in an inner gorge.

First, we define the ridge line path to be composed of line segments which connect adjacent local high points along the ridge line while being generally aligned with the overall ridge line trend. Then, let h_{r1}, h_{r2} be the elevation of the high points immediately adjacent to the transverse drainage on either side of the stream with $h_{r1} \geq h_{r2}$. Additionally, let h_s be the elevation of the stream as it crosses the ridge line path, and l be the map projected distance from h_{r2} to the stream along the ridge line path. Finally, let the gap width, w_g, be the map projected distance between h_{r1} and h_{r2}. The elevation of the upstream valley above the inner gorge shall be denoted h_v, and the elevation of the alternate divide between the upstream and downstream valleys shall be denoted h_d.

Given the above measurements, we may determine the interpolated height of the ridge line at the location of the transverse drainage as

$$h_r = h_{r2} + \frac{l}{w_g}(h_{r1} - h_{r2}).$$

We may also define three prominence measures for transverse drainages, $\mathrm{Pr}_1 \geq \mathrm{Pr}_2 \geq \mathrm{Pr}_3$. The first prominence metric is the difference in elevation between the highest adjacent ridge point and the stream elevation. The second is the difference between the interpolated ridge line height and the stream elevation. The third is the difference between the interpolated ridge line height and the upstream valley elevation. According to the terminology established above, these can be written as:

$$\begin{aligned} \mathrm{Pr}_1 &= h_{r1} - h_{s,} \\ \mathrm{Pr}_2 &= h_r - h_{s,} \\ \mathrm{Pr}_3 &= h_r - h_v. \end{aligned}$$

The above measurements allow direct comparison between different transverse drainages based on their overall size—very useful in its own right. We can also use these measurements to categorize and compare transverse drainages independently of absolute size by comparing the height of the transverse drainage achieved compared to the height of the alternate divide. This dimensionless index is defined as

$$k = 1 - \frac{\max\{h_d - h_v, 0\}}{\mathrm{Pr}_3}.$$

The transverse drainage k index provides a measure of the significance of the transverse drainage in its overall hydraulic system context. When the transverse drainage cuts through the ridge line at the lowest overall upstream basin outlet elevation (meaning there are no other likely lower elevation passes for a stream to pass through), the index is 0. However, when the alternate divide is at the same elevation or lower than the bottom of the upstream valley, the index is 1. Examples of both of these extremes are shown in Figure 5. The index is a measure of the incongruence of the transverse drainage to the "natural" or pre-existing drainage pathways, and can be used to gain insight into the most probable geological history and formation mechanisms (described below).

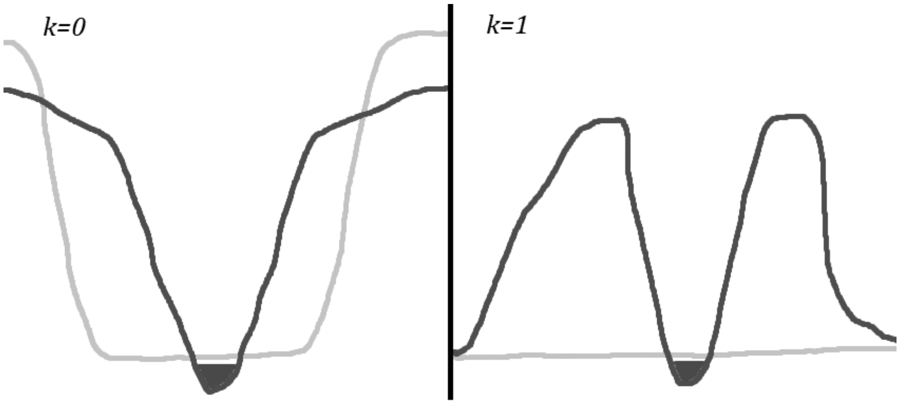

Figure 5. Schematic examples of an index 0 transverse drainage (left) and an index 1 transverse drainage (right).

Logarithmic uplift model

I will use two simplified models of mountain uplift to compare with erosion for the formation of transverse drainages. The first is a linear model where all of the uplift occurs at a constant rate from the time of the end of the Flood to reach the current modern height at present. In both models, the ridge is at the same height as the river with the river crossing the incipient ridge immediately at the end of the Flood, then reaching its modern height at the present. The linear uplift model, of course, implies continuing rapid uplift, which generally is not the case for most mountain ridges at the rates implied. The modern uplift rate does not impact the model results. Tectonic events are well-known to occur in discontinuous jumps followed by periods of quiescence. If these jumps occur, then the behavior of the real system may diverge from these models. Generally, a system with discontinuous jumps will decrease its ability to form transverse drainages by antecedence. For the sake of these models, we will assume tectonic events are frequent and do not deviate far from the long-term trend.

The second model is logarithmic, which shifts the majority of uplift into the past, and most closely adheres to the intent behind the descriptive phrase, "exponentially decreasing tectonic activity" in the post-Flood era (Austin et al., 1996). With $t = 0$ being the end of the Flood with time progressing forward to the present day, the ridge uplift is given by:

$$y(t) = a\ln(bt + 1).$$

The parameter b is free, and controls both the slope of the uplift at present (which likewise must be greater than 0) and the amount of uplift accomplished near the beginning of the time interval. For this paper, b is arbitrarily set so that 50% of the total uplift is accomplished by 500 years. The parameter a is solved by specifying the initial value conditions $y(0) = 0$, and $y(T) = h_r$ with T being the present day. The result is:

$$a = \frac{h_r}{\ln(bT + 1)}.$$

The "working time," t', represents the amount of time before the incipient transverse drainage thalweg rises to the height of the alternate divide, taking into account both the uplift rate and erosion rate over time as well as the total time available from the beginning of the time interval. As soon as water begins to flow through the alternate divide, then the transverse drainage will be abandoned and form a wind gap. If the ridge elevation rises, but does not cause the stream to divert through the alternate divide, then the stream would be expected to pond on the upstream side. For the transverse drainage carving to be successful, the stream must erode the entire elevation of the ridge in less time than the working time. The governing equation is

$$h_d = y(t') - ct',$$

where c is the modeled erosion (cutting) rate. For the logarithmic uplift model, the working time solution is:

$$t' = \frac{-ab\mathrm{W}_0\left(\frac{-ce^{(h_d - c/b)}}{abe^a}\right) - c}{bc},$$

where W_0 is Lambert's W function, principal branch (also known as the product log function).

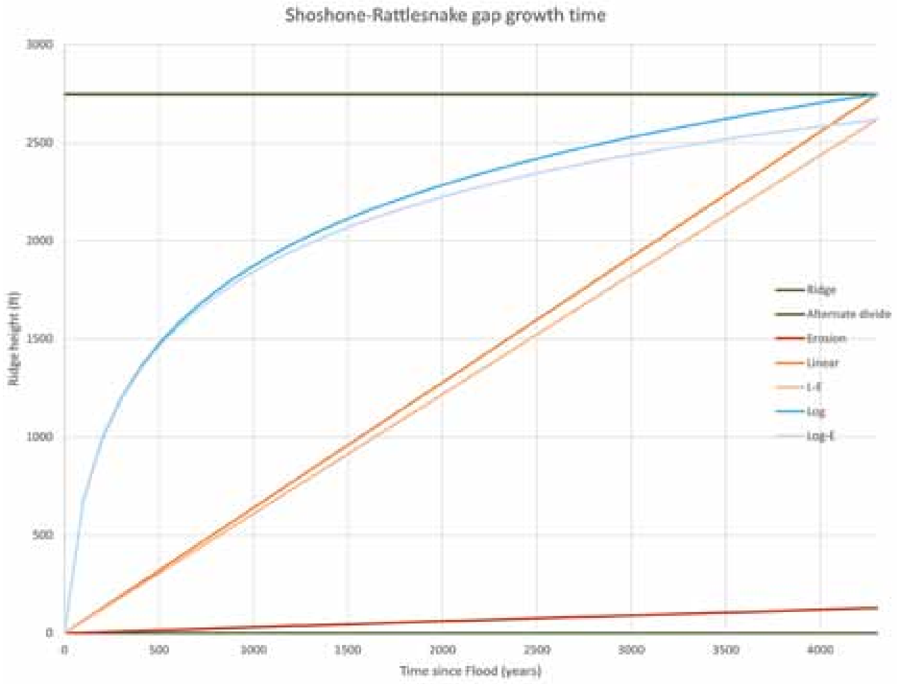

Figure 6. Uplift and erosion model of the Shoshone-Rattlesnake transverse drainage with baseline erosion rate.

Description of system model

For this study, measurements of the Shoshone-Rattlesnake water gap and Wheeler Ridge wind gap were taken using Google Earth Pro to determine the k index, and prominence measures Pr_2 and Pr_3. The overall time at the end of the Flood was taken to be 4300 years before present. Both transverse drainages were chosen because their k indexes were 1. For each transverse drainage, three erosion rates were determined according to the strong, weak, and totals models of Whipple et al. (2000). The first examination was to compare the expected incision from the available total time and modeled erosion rates in comparison to the overall transverse drainage height (Pr_2 from ridge to stream). Then the time required to erode the inner gorge is calculated and subtracted from T to provide a maximal constraint to working time. The working time is then calculated for both tectonic models to provide a maximal transverse drainage depth that is achievable. Finally, erosion rates are adjusted until the transverse drainage can be eroded within the given constraints. For each transverse drainage, the erosion and uplift rates are analyzed graphically.

Discussion

Transverse drainages are amongst the youngest landforms since they cut mountains, which themselves are universally geologically young (Ollier and Pain, 2000). Nevertheless, the hydraulic system of any transverse drainage can have been altered since the time that it was first eroded. Two possibilities for this include uplift/subsidence or erosion of the region of the alternate divide. Because it depends on the ratios of the transverse drainage depth and the height of the alternate divide, the index also provides a measure of how likely it was in the past for the transverse drainage ridge and the alternate divide to have traded roles.

Table I. Measured parameters and calculated erosion rates for the two transverse drainages.

Parameter	Shoshone-Rattlesnake	Wheeler Ridge
Pr_2 (ft)	2949	481
Pr_3 (ft)	2747	463
Index	1	1
Alternate divide (ft)	0	0
Gorge depth (ft)	202	18
Slope (ft/mi)	73.4	244
Width (ft)	114	490
Erosion rate – resistant (ft/yr)	$3.00 \cdot 10^{-2}$	$2.71 \cdot 10^{-2}$
Erosion rate – weak (ft/yr)	$3.53 \cdot 10^{-2}$	$3.02 \cdot 10^{-2}$
Erosion rate – total (ft/yr)	$5.09 \cdot 10^{-2}$	$4.59 \cdot 10^{-2}$

When the index is near zero, the ridge and alternate divide are close to the same elevation and either could have been the lowest point depending on the tectonic and erosive history of the system. Conversely, when the index is high, then the elevation of the ridge and alternate divide are significantly different, and it is unlikely that the ridge was ever lower than the alternate divide absent a compelling geological case. For this reason, transverse drainages with indexes near 1 (as the two selected ones do) justify applying this particular formation model.

It is also worth noting the relationship between the index and transverse drainages formed by lake overspill. A lake will always overtop its lowest barrier, so in this case, the ridge and alternate divide are the same point and the same elevation. This will cause its index to be 0. Further modification of the overall system may occur, changing the index value, but any transverse drainage plausibly carved by lake overspill should have a low index value. This constraint does not apply to Flood overspill formation. Neither of the transverse drainages considered here has evidence of impounded lakes on their upstream sides, and neither has a geometry that is favorable for impounding a lake or deep sediment. The index of the Grand Canyon is also 1, as the upstream valley elevation (represented by Cape Solitude) is higher than multiple alternate divides.

Table I shows the measured values and modeled erosion rates for both the Shoshone-Rattlesnake water gap and Wheeler Ridge wind gap. A value for each of the modeled erosion trends given in Whipple et al. (2000) is calculated for both transverse drainages, though in the case of the Shoshone-Rattlesnake the rock is resistant, and in the case of Wheeler Ridge, the rock is weak. In all three cases, the modeled erosion rates are remarkably similar between the two transverse drainages. The erosion rates according to the total erosion model are among the highest seen in an informal survey of around a dozen North American transverse drainages (not otherwise here reported on) and so provide a case for the maximal scale of transverse drainages formed by antecedence in the post-Flood period at around 220 ft. This was calculated by assuming continuous erosion at the rate of the fit Shoshone-Rattlesnake total erosion rate over 4300 years. In neither case can erosion successfully cut the observed depth, though in the case of the Wheeler Ridge wind gap, the maximal depth is the same order of magnitude as the total gap depth. So, for any transverse drainage greater than 220 ft. deep from ridge line to gorge to form in the post-Flood period by antecedence (or superimposition), significantly enhanced erosion is required.

Figure 6 shows the modeled uplift and erosion history of the Shoshone-Rattlesnake gap with the resistant rock erosion rate from the Whipple et al. (2000) model. The height of the ridge line and the height of the alternate divide are shown as horizontal green lines with the alternate divide below at zero height. Since both of these gaps have indexes of 1, the alternate divide line is sitting on top of the horizontal (time) axis. The red erosion trend shows the total amount of downcutting that has occurred since the beginning of the simulation. The saturated blue curve shows the logarithmic uplift model for the ridge line height. The saturated orange line is the linear uplift model. The less saturated curves of both colors are the uplift with the erosion subtracted, representing the height of the stream thalweg at any given time. The point at which the less saturated curves cross the alternate divide height defines the working time for that uplift model. In this case, the working time is zero for both. For the carving of the transverse drainage by antecedence to be successful, the erosion line must reach the ridge line height before the uplift minus erosion line reaches the alternate divide height. With the modeled erosion rate, the stream would make very little progress overall in the erosion of the gorge. In both the linear and logarithmic uplift cases, it would not even get the chance, as any uplift at all would send the stream around the ridge through the alternate divide. Because the alternate divide is at 0 ft., the only possible scenario for successful transverse drainage generation is for the erosion to completely out-pace the uplift.

Figure 7 shows the same system but with the erosion rate enhanced sufficiently to carve the gap with the linear uplift model. This requires boosting the erosion rate by a factor of 22.9. The red erosion line now comfortably reaches the ridge line height. This intersection occurs slightly before the present time. The difference represents the time required to erode the inner gorge at the modeled erosion rate. Any lower erosion rate would have insufficient time to erode both the gap and the inner gorge by the present day. As the erosion line is rotated upwards (counter-clockwise from the origin), the uplift minus erosion lines are rotated downwards. Now that the erosion rate outstrips the linear uplift rate, the linear uplift minus erosion line is entirely negative and does not cross the alternate divide height at any time. This negative height is slightly unphysical, as the base level of the system is at zero height, and the stream would tend to maintain that level as long as it could sufficiently erode any uplift that was occurring. That aspect of the system is out of the scope of the model. All that is required is to show that the uplift rate never overwhelms the gorge erosion rate. In this case, the logarithmic minus erosion line curves downwards, but it still crosses the alternate divide height.

Figure 8 shows the same system with the erosion rate boosted from the baseline sufficiently to cause a successful transverse drainage cutting with the logarithmic uplift model. The erosion required for this is 410 times that which the slope and channel width would otherwise indicate. At this rate, the entire height of the gap would be carved

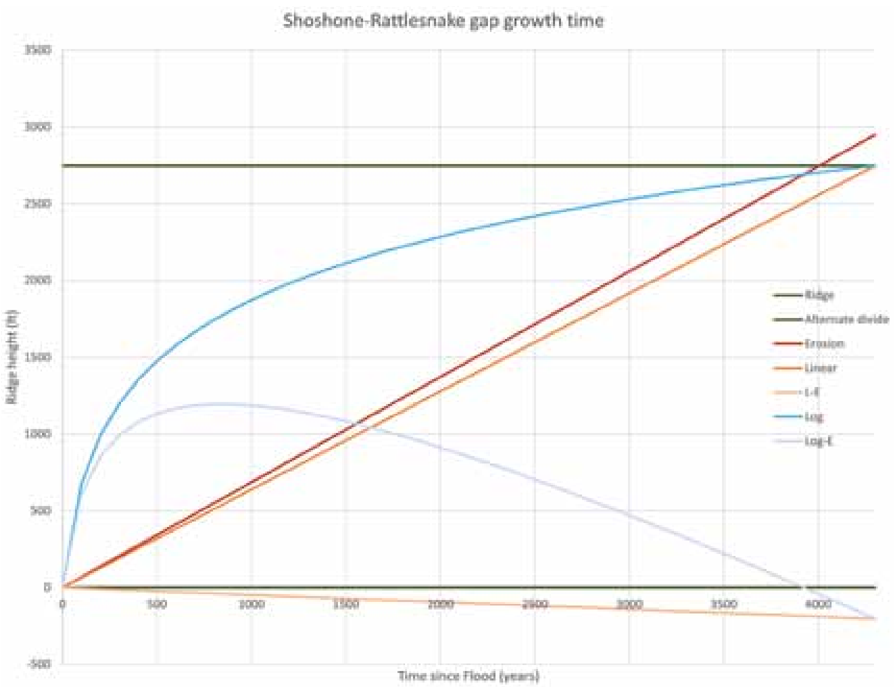

Figure 7. Uplift and erosion model of the Shoshone-Rattlesnake transverse drainage with erosion rate enhanced by a factor of 22.9.

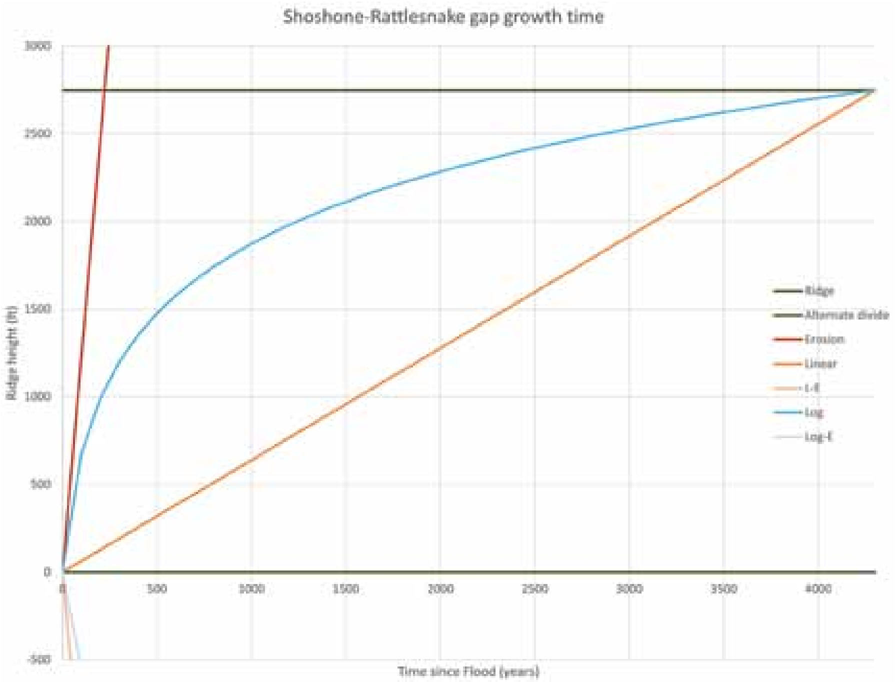

Figure 8. Uplift and erosion model of the Shoshone-Rattlesnake transverse drainage with erosion rate enhanced by a factor of 410.

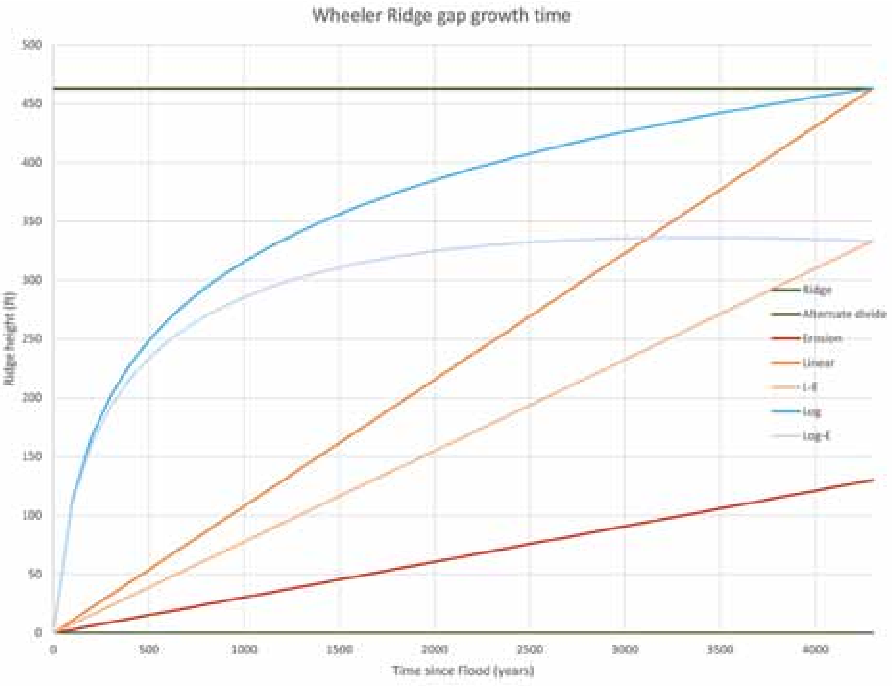

Figure 9. Uplift and erosion model of the Wheeler Ridge wind gap with baseline erosion rate.

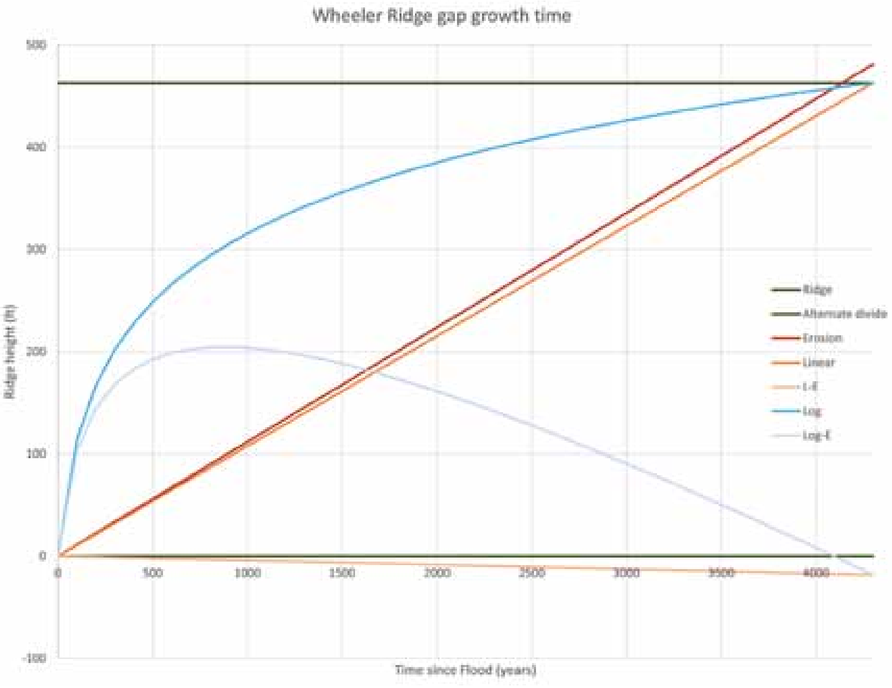

Figure 10. Uplift and erosion model of the Wheeler Ridge wind gap with erosion rate boosted 3.6 times.

in just over 200 years. Even with this remarkably high average erosion rate, discontinuous jumps of uplift, which are concentrated during the same early time frame would be likely to disrupt gap carving, since there is no barrier of any height preventing the stream from reorganizing around the ridge line.

It is also exceedingly difficult to devise a cause for the extreme erosion rate of over 12 ft. per year on average. The erosion rates from Whipple et al. (2000) are already measured on a denuded terrain with unconsolidated ash cover. This rate would necessitate repeated large-magnitude catastrophes. These would manifest as discontinuous outbursts over time. In the intervening time, uplift along the ridge is likely to have occurred, which would divert future outbursts smaller than a certain scale around the ridge. A more plausible scenario is for a single catastrophe large enough to carve the entirety of the water gap in a single episode. The minimum magnitude of such a catastrophe (water surface elevation of at least 7800 ft. ASL) is large enough to imply flooding on a continental scale. It should be clear then that the required catastrophe is identical to the Global Flood. Even the relatively more modest erosion rate associated with the linear uplift model would be difficult to justify given the geological context of the Shoshone-Rattlesnake transverse drainage.

The Wheeler Ridge wind gap, given its smaller magnitude, weaker rock composition, and formation dynamics offers another situation for an otherwise similar transverse drainage. Figure 9 shows the dynamics of the Wheeler Ridge wind gap with the baseline weak rock erosion rate from Whipple et al. (2000). Similarly, to the Shoshone-Rattlesnake gap above, this rate is insufficient to successfully carve the gap by antecedence in the time since the Genesis Flood. Figure 10 is the same system with sufficient erosion rate to carve the transverse drainage with the linear uplift model. In this case, the boost to the average erosion rate is a modest 3.6 times the modeled rate. Unlike the Shoshone-Rattlesnake case, this erosion rate is potentially justifiable by enhanced erosion in the post-Flood period, though I don't identify any specific mechanisms based on local evidence to arrive at a concrete expected erosion rate in this study.

Figure 11 shows the Wheeler Ridge wind gap system with sufficient erosion rate to overcome uplift associated with the logarithmic model. The boost, at 68.6 times is greater than that required for the linear uplift at the Shoshone-Rattlesnake transverse drainage, but not at the astronomically high erosion rate required by the equivalent logarithmic model. Nevertheless, it is likely outside the realm of easy justification. However, given Wheeler Ridge's relationship to the actively deforming San Andreas fault system, the linear uplift model for Wheeler Ridge is likely defensible, and so the lower required erosion rate can be justified.

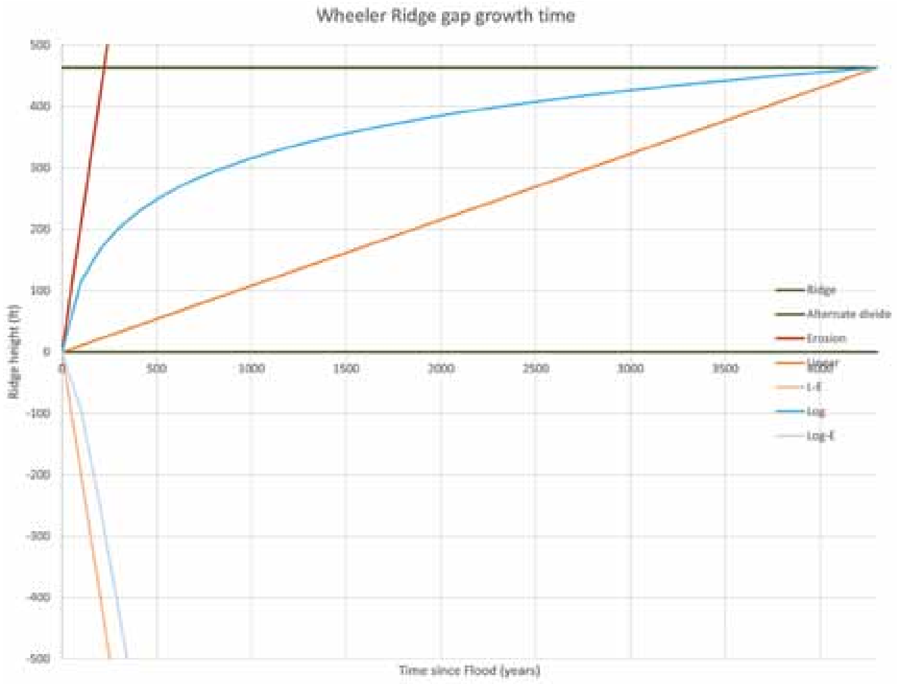

Figure 11. Uplift and erosion model of the Wheeler Ridge wind gap with erosion rate boosted 68.6 times.

The methodologies demonstrated above in addition to the criteria laid out in Douglass et al. (2009) are useful for distinguishing among the various formation mechanisms for transverse drainages and have been proved useful for distinguishing Flood-carved vs. post-Flood water gaps. In general, if the required erosion rate is more than an order of magnitude larger than the maximal measured erosion rates, then the generation of such transverse drainages can confidently be placed during the waning stage of the Flood. This applies to any transverse drainages 2200 ft. or deeper. For transverse drainages less than 220 ft. deep, a post-Flood origin is eminently reasonable. The in-between cases are potentially ambiguous, and the tools laid out in this paper can aid in deciding or identifying the necessary pathways for achieving transverse drainage generation. For these in-between cases, an elevated long-term erosion rate should be supported by local evidence and modeling of the conditions. Possible mechanisms for enhanced erosion can include mass wasting from unconsolidated or denuded ridges, or frequent upstream flooding events. The specific mechanisms invoked in each case should be shown to produce the required scale of erosion.

Declining catastrophic tectonism and erosion in the early post-Flood period, while generally accepted as a means of generating mesoscale and smaller landforms and features, tends to work against transverse drainage formation by catastrophes smaller than a minimum threshold.

Conclusion

Modeling uplift and erosion can aid in the identification of formation mechanisms for individual transverse drainages in addition to the other criteria that have been developed. Post-Flood erosion can only account for relatively small transverse drainages in post-Flood time by antecedence or superimposition. Erosion rates within an order of magnitude of those that have been observed are potentially justifiable given the conditions in the immediate post-Flood period with possible post-Flood catastrophism. However, hypothetical erosion rates more than an order of magnitude higher should be justified by particular evidence of a more energetic catastrophic process. In the case of the Shoshone-Rattlesnake transverse drainage, neither repeated large catastrophes nor lake overspill can be supported by the evidence, and antecedence is implausible as a mechanism. The only remaining plausible mechanism is runoff from the Genesis Flood. This is true of many large-scale transverse drainages, justifying its applicability as a Receding Stage of the Flood criterion. Rapid tectonic change following the Flood increases the required catastrophism of the erosive mechanism, and so decreases the likelihood that a particular gap can be carved by antecedence. The Wheeler Ridge wind gap and other small-scale transverse drainages cut through unconsolidated sediment and presently active tectonics may be generated in the post-Flood era by antecedence if the required enhanced erosion rates can be supported by the local evidence. The transverse drainage index is useful to compare gaps of multiple scales and can help inform whether or not a gap has been created by overspill. The index should be measured and used in future transverse drainage studies.

Acknowledgment

This research was inspired by discussions held as part of the Flood Boundary Study Group, a Logos Research Associates initiative.

References

Austin, S.A., J.R. Baumgardner, D.R. Humphreys, A.A. Snelling, L. Vardiman, and K.P. Wise. 1996. *Catastrophic Plate Tectonics: A Global Flood Model for Earth History*. Geology Education Materials, Santee, CA.

Douglass, J., N. Meek, R.I. Dorn, and M.W. Schmeeckle. 2009. A criteria-based methodology for determining the mechanism of transverse drainage development, with application to the southwestern United States. *Geological Society of America Bulletin* 121(3–4):586–598.

Hilgendorf, Z., G. Wells, P.H. Larson, J. Millett, and M. Kohout. 2020. From basins to rivers: Understanding the revitalization and significance of top-down drainage integration mechanisms in drainage basin evolution. *Geomorphology* 352:107020.

Johnson, G.D. 1934. Geology of the mountain uplift transected by the Shoshone Canyon, Wyoming. *The Journal of Geology* 42(8):809–838.

Keller, E., R. Zepeda, T. Rockwell, T. Ku, and W. Dinklage. 1998. Active tectonics at Wheeler ridge, southern San Joaquin valley, California. *Geological Society of America Bulletin* 110(3):298–310.

Lee, J. 2019. A global database of large-scale transverse drainages. *Data in Brief* 23:103650.

Meek, N. 2019. Episodic forward prolongation of trunk channels in the western United States. *Geomorphology* 340:172–183.

Mueller, K., and P. Talling. 1997. Geomorphic evidence for tear faults accommodating lateral propagation of an active fault-bend fold, Wheeler Ridge, California. *Journal of Structural Geology* 19(3-4):397–411.

Oard, M.J. 2013. Earth's surface shaped by Genesis Flood runoff, Chapters 75–79. http://michael.oards.net/GenesisFloodRunoff.htm. (accessed May 13, 2024).

Oard, M.J. 2018. Genesis Flood drainage through southwest Montana—Part III: Water gaps. *Creation Research Society Quarterly* 55(2):81–97.

Ollier, C., and C. Pain. 2000. *The Origin of Mountains*. Routledge, London, UK.

Rosenbloom, N.A., and R.S. Anderson. 1994. Hillslope and channel evolution in a marine terraced landscape, Santa Cruz, California. *Journal of Geophysical Research: Solid Earth* 99(B7):14013–14029.

Snyder, N.P., K.X. Whipple, G.E. Tucker, and D.J. Merritts. 2000. Landscape response to tectonic forcing: Digital elevation model analysis of stream profiles in the Mendocino triple junction region, northern California. *Geological Society of America Bulletin* 112(8):1250–1263.

Stock, J.D., and D.R. Montgomery. 1999. Geologic constraints on bedrock river incision using the stream power law. *Journal of Geophysical Research: Solid Earth* 104(B3):4983–4993.

Whipple, K.X., N.P. Snyder, and K. Dollenmayer. 2000. Rates and processes of bedrock incision by the Upper Ukak River since the 1912 Novarupta ash flow in the Valley of Ten Thousand Smokes, Alaska. *Geology* 28(9):835–838.

Creation Research Society Quarterly 2025 61:213–220

Does the Mature Creation Concept Explain the Solar System's Creation?

Jerry Bergman

Abstract

The concept of the 'appearance of age' (or creation with an 'appearance of history') is a viable option for the Creation explanation of origins. This view posits that creation was brought into existence in a fully mature and functionally complete state. The example of Adam and Eve being formed as adult humans and the fruit trees in the Garden of Eden with seed-bearing fruit at their origin illustrates two widely accepted examples of the 'appearance of history,' or God's directly producing a mature creation. This example can be extended to the creation of the solar system and even the entire universe. The major problems with the evolutionary origin of our solar system were also briefly reviewed. It is concluded that 'appearance of age' is a viable explanation for the origin of the solar system and, by extension, of the universe.

Key Words: Appearance of age/history, Big Bang, creation of the moon and the planets, creation of the mniverse, the Garden of Eden, problems with the Nebular Hypothesis, the solar system

Introduction

One of the most controversial areas of the entire creation worldview is the short time during which the Creation occurred according to Genesis. In fact, the mature-creation view is very logical, supported by the evidence, and accepted by many early Bible scholars (Bradshaw, 1998). The creation of Adam could not have involved large amounts of time. The reason is that he must have been created as a fully functioning human to even be alive with blood traversing in his circulatory system. Humans become unconscious within only twenty seconds after the heart stops. Without the oxygen and sugars required to function, the brain is unable to deliver the electrical signals required to maintain breathing and organ function. After only three minutes, global cerebral ischemia—the lack of blood flow to the entire brain—causes brain injury that becomes progressively worse after each second.

To separately create a lung, heart, and the other 100 organs required for life is not a viable option. Without the protection of the body, and the sustenance provided by nutrient and oxygen circulation, these organs would rapidly deteriorate. Consequently, for all these reasons, Adam would have had to be created *ex nihilo* from dust with a fully functioning body and oxygenated blood traversing through his body. Furthermore, Adam and Eve arrived in this world with adult minds pre-wired with human thought processes, language, and a knowledge of the Creator. Their hair length also would have given apparent evidence of previous growth (DeYoung, 2010, p. 57). Likewise, the fruit trees in the garden would display maturity upon their *ex nihilo* creation. As Philo of Alexandria (c. 20 B.C.–A.D. 50) explained:

Accepted for publication July 11, 2024

> But in the first creation of the universe….God produced the whole race of trees out of the earth in full perfection, having their fruit not incomplete, but in a state of entire ripeness, to be ready for the immediate and undelayed use and enjoyment of the animals. (Yonge, 1993, p. 7)

If the newly created Adam was examined by a modern doctor, he would conclude that Adam was a very healthy young adult, even though he was actually only a few hours old. Adam thus, from the account in Genesis, had the 'appearance of age.' He was not a baby or child. Conversely, he would not have any of the negative signs of aging, such as the beginnings of plaque in his arteries and veins or normal minor age skin spots. Arterial plaque occurs when cholesterol builds up in the arteries' inner lining with age. Nor would he have the normal cellular deterioration that slowly builds up, usually manifesting itself when we are in our 40s.

Of the numerous Biblical examples of the appearance of age one would have to include the wine Christ created at the Cana wedding which tasted like mature expensive wine when it was only minutes old. John 2:10 says, "Everyone brings out the choice wine first and then the cheaper wine after the guests have had too much to drink; but you have saved the best till now." In other words, after drinking the good wine and expecting cheap wine later in the evening (after guests were properly inebriated), the wine Jesus produced was expensive wine normally served early in the evening. Another example is when Jesus fed 5,000 men besides women and children (Matthew 14:13–21), and later when He fed 4,000 men besides women and children (Matthew 15:32–39), with freshly made food that was only minutes old. The food tasted like it was grown, harvested, or recently acquired, and prepared as normal for food that would normally require many months for full maturation, yet that which was served was only minutes old.

Appearance of History and the Solar System

The same is true of the solar system. Logically, the planets and our sun-centered system must have been created as a functional unit, operational from the first day of their creation. Like Adam, they would appear to be mature, even though in this case the evolution model would give a date of many millions of years old.

One example is the Earth-Moon system. The moon's critical role is required both for Earth's stability and for life to exist on the Earth's surface. The origin of our moon has dumbfounded evolutionary cosmologists for over a century. One popular proposal was the *Capture Theory,* which postulated that the moon was once a small planet orbiting around the sun in close to the same orbit as the Earth (DeYoung, 2010a, p. 210).

Another theory of its origin is that it originated from some other part of our solar system, or even outside of it. The moon was somehow captured by the Earth's gravitational field and began orbiting the Earth instead of the sun as formerly. However, the rocks that creationist astronaut James Irwin brought back from his trip to the moon created problems for the Capture Theory. Analyzing them forced the conclusion that the moon rock composition was far too much like that of the Earth to have come from some other part of the solar system.

According to the *Giant Impact Theory,* at some point in Earth's very early history, the moon formed as a result of a massive collision between the Earth and a planet about the size of Mars called Theia. The debris from this impact collected in an orbit around Earth, eventually coalescing to form the moon. This theory would explain why moon rock composition is very similar to the Earth's, but according to the late astronomer Carl Sagan (1980, pp. 90–91), it encounters other problems such as the geophysical impossibility of a collision producing the Earth-Moon system that exists today.

This issue was involved in the Immanuel Velikovsky impact theory controversy. Velikovsky postulated that around the 15th century B.C., the planet Venus was ejected from Jupiter by a large, massive object that passed nearby, or collided with, the Earth (Velikovsky, 1950). The encounter changed Earth's orbit and axis tilt, causing innumerable catastrophes. However, these impact theories were so overwhelmingly rejected by the scientific community that they forced Macmillan to cease publishing the book within two months of its publication (Friedlander, 1995, p. 14). A detailed refutation of impact-theory claims by six leading astronomers and other scientists was published by astrophysicist and science communicator Donald Goldsmith (1977).

One problem with all impact theories is, where did the hypothetical Mars-sized (or some speculate the size was closer to twice the mass of Mars) planet come from that collided with the Earth? The theory assumes that, before the Earth and the moon existed, a proto-Earth and a body called Theia existed. No valid evidence exists for this impact theory except for its being superior to the competing scenarios because it can explain why the moon's rocks are very similar to the Earth's rocks. A few of the other origin-of-the-moon theories include the *Fission Theory* and the *Condensation Theory,* both of which also have major problems. The fission theory explains the moon's lack of a large core and the oxygen-isotope similarity, but calculations indicate that the Earth would require at least *four times its present angular momentum* for the theory to work. The *Condensation Theory* includes it but does not satisfactorily explain the angular momentum of the Earth-Moon system, nor why the moon has a relatively small iron core compared to the Earth's, comprising an estimated 25% of its radius compared to 50% for the Earth (Whitcomb and DeYoung, 1978; DeYoung, 2010).

Why Giant Impacts Would Destroy the Earth

The Earth's inner core is believed to be a hot, part-liquid, dense ball mostly made of iron, with a radius of about 1,220 kilometers (758 miles). The Earth's inner core temperature is about 5,200° Celsius (9,392° Fahrenheit), close to that of the outer surface layer of the sun, the solar photosphere.

The mantle, the solid bulk of Earth's interior, makes up a whopping 84 percent of Earth's total volume. The mantle rock is made up of mostly olivine/peridotite. It lies between Earth's dense, super-heated core and its thin outer layer. Olivine/peridotite rock has a Mohs hardness of 5.5–6 (at 1g and surface temperature) medium hardness on a 1-to-10 scale. A giant impact would crush the crust, thereby smashing into the brittle mantle, which is about 2,900 kilometers (1,802 miles) thick (Perna et al., 2013). The temperature of the mantle varies from 1,000°C (1,832°F) near its boundary with the crust (the Mohorovičić discontinuity), to 3,700°C (6,692°F) near its other boundary with the outer core (the Gutenberg discontinuity).

Compared to all other moons, our moon is enormous relative to the size of the Earth. Specifically, the moon is about 1/3 of the size of the Earth but its mass is about 1/80th of the Earth's! Nonetheless, crashing into the Earth, or being captured, would require colossal catastrophic events that would likely damage the Earth beyond repair, destroying it (Perna et al., 2019). Due to the improbability of all of the proposed events for the production of the Earth-Moon system, the question of where the moon came from is a mystery unexplained by naturalism (DeYoung, 2010a). However, given that a supernatural origin is a credible alternative to naturalism, an *ex nihilo* creation explains it.

Movement Required to Produce Stability

Our solar system's planets are all held in their orbit in a smooth-running system by our giant sun's gravity. To produce the required stable solar system that supports life, God would not have created a set of planets without momentum-producing movement. Just as a bike is stable when moving, but will fall over when still, likewise the planets are stable only when moving. This is a requirement both in order for life to exist on our planet, and a requirement for a solar system to exist.

The Earth not only rotates on its axis at 24,898 mph measured at the surface,[1] but it orbits around the sun at an average speed of 67,000 mph, or 18.5 miles a second. The center of mass of the solar system is moving at an average speed of 448,000 mph (720,000 km/h). At this rate it would take about 230 million years to travel all the way around the Milky Way Galaxy where our solar system is located. The Milky Way Galaxy itself is moving at a speed of 25 miles a second. Our galaxy is part of the *Local Group* of galaxies that, as a group, are moving at the astonishing rate of 375 miles a second toward the Virgo Supercluster. The Virgo Supercluster is an enormous collection of galaxies some 45 million light-years from Earth.

In short, the entire universe must exist as a functional unit in motion to support life, just as must the human body. Its movement produces the stability that we experience on Earth. And, just as Adam was created with the appearance of age, the same is true of the universe. Evolution would require that it has evolved to its functional maturity, thus, based on uniformitarian thinking, enormous ages for its development would be required, going back to its assumed naturalistic origin.

However, as with the recent creation of Adam, substantial evidence argues that the solar system is also young. New discoveries by the James Webb Space Telescope found a remarkable assemblage of, as of this writing, over 5,000 galaxies that did not appear *relatively young,* as evolutionists had expected, but rather these galaxies looked about as fully formed as the galaxies nearest Earth. This provides evidence that the entire universe was created at about the same time. Among them, one galaxy unveiled an array of extraordinary cosmic phenomena to the extent that scientists are baffled as to how it could possibly exist. At the edge of the universe, cosmologists expect to find young, underdeveloped galaxies because, when viewing a galaxy 100 million light years away, they believe that they are seeing what the galaxy looked like 100 million years ago. The problem is that much of what our telescopes are revealing has proven very difficult for scientists to understand from a naturalistic, deep-time interpretation.

The Origin of the Solar System

The origin of the moon was discussed in some detail because astronomers have been able to study it in great

---

[1] The circumference of the Earth is around 24,898 miles (40,070 kilometers) and hence, dividing the distance by time, it can be observed that the Earth is spinning at 1,037 mph.

detail, thus having some basis to postulate its origin. As the solar system is now being studied in more detail, we are also learning more about its construction, and thus can postulate its origin. It now appears that the same problems encountered in determining the moon's origin also exist in theorizing planetary origin as well. The most widely accepted model of planetary formation is the *Nebular Hypothesis* proposed by Pierre Simon Marquis de Laplace (1749–1827) in 1796 (Cameron, 1975; Numbers, 1977). This theory postulates that the solar system originated from vast clouds of gas and dust within interstellar space. The material that created the solar system and Earth was once allegedly a slowly rotating cloud, or nebula, of extremely hot gas. The gas cooled and the nebula began to shrink. As the nebula became smaller, it rotated more rapidly, supposedly evolving into an enormously wide flattened disk (Woolfson, 1993).

Thus, the Nebular Hypothesis postulates that about 4.6 billion years ago, the solar system was formed by the gravitational collapse of this giant molecular cloud spanning several light-years across. Evolutionists believe that the sun was also originally a giant cloud of ionized plasma that contracted due to cooling and the pull of gravity. This forced the ionized plasma to rotate faster, conserving angular momentum, just as an ice skater rotates faster when her extended arms are drawn onto her chest closer to her center of gravity and her rotational axis. This faster rotation would conceptually throw off a rim of ionized plasma blobs which, following cooling, could condense into planets. The Nebular Hypothesis postulates that all the planets were likewise formed by this same process.

In summary, the theory states that, through a combination of forces produced by the nebula's rotation, and gravitational force from the mass of the nebula, the nebula left behind rings of gas as it shrank. These rings condensed into planets and their satellites, while the central part of the nebula formed a sun.

Problems with the Nebular Hypothesis

Although now over 300 years old, the Nebular Hypothesis is still the most widely accepted explanation for our solar system for one reason: *no better naturalistic theory has been proposed*. Nonetheless, the Nebular Hypothesis suffers from many serious problems (Brush, 1990). The main problem with the Nebular Hypothesis is that it assumes the original cloud already existed and was spinning, ignoring the problem of where it came from, and how and why its rotation began.

Furthermore, when calculated on the basis of the known orbital momentum of the planets, the Nebular Hypothesis predicts that the sun must rotate about 50 times more rapidly than it actually does (Simon, 2023). This theory predicted that the sun would be spinning so fast that it would make one rotation every few hours. In fact, it spins only once in approximately every 25 Earth days (Simon and Zwart, 2009, p. L13). The sun is believed to originally have a short period—around a day—and then afterward slowly degraded through natural angular momentum loss. Young sun-like stars display very rapid rotation and evidence supports the conclusion that they are losing angular momentum, thus spinning down. But active, fast-rotating suns are dangerous for life on the planets that surround them. They would have superflares which would destroy life on planets nearby them. Our sun was created mature and stable. Non-mature stars send out plasma flows (winds) that follow along the magnetic field lines, north and south, which torque the star through magnetic braking, slowing its rotation over time.

One response to this problem is to attribute the slower rotation to magnetic braking that results from the solar wind material following the stiff magnetic field lines that extend well beyond the stellar surface (Alfven radius <50 radii). This coupling exerts a torque on the surface layers of the sun, thus slowing down its rotation (Meynet et al., 2010). However, in determining the efficacy of the braking model, "Various assumptions are made regarding both the magnitude of the magnetic field and of the efficiency of the angular momentum transport mechanisms in the stellar interior" (Meynet, 2011). The problems of the secular theories of the origin of the solar system are well described by one leading astrophysicist:

> A decades-long dispute over how much carbon, nitrogen, and oxygen lie within our closest star has implications for the entire universe As astronomers gaze into the depths of space, they do so with unease: They don't know precisely what the universe is made of. It's not just the true nature of dark matter that eludes them; so does the essence of the stars that speckle the sky and populate the many galaxies throughout the cosmos. Surprisingly, no one knows the stars' exact chemical composition: how many carbon, nitrogen, and oxygen atoms they have relative to hydrogen, the most common element.…Twenty years ago, astronomers expressed confidence in the numbers they had been working with. Now, not so much…Astonishingly, scientists don't know exactly what the sun is made of. As a result, they don't know what the other stars are made of, either. "The sun is a fundamental yardstick…When we determine the abundance of a certain element in a star or a galaxy or a gas cloud

> anywhere in the universe, we use the sun as a reference point." (Croswell, 2020)

Another problem is that the Nebular Hypothesis also predicts that the total gas that formed the solar system was only slightly more massive than the sun itself (Woolfson, 2000). Most of this gas was concentrated in the center which became the sun. The rest of the mass is assumed to have flattened into a proto-planetary disk. Within this swirling debris, rocky particles allegedly began to collide, forming larger and larger masses that soon attracted even more particles due to the force of gravity. These particles then supposedly contracted also due to gravity, creating planetesimals, which collided with one another to become the solid inner planets.

Meanwhile, the ionized plasma froze into giant balls that built the outer gas giants. In all, eight planets, 290 moons, asteroids, and the other celestial bodies in the solar system formed from this gas ball. However, the moon number per planet does not fit the pattern expected from this nebular notion, but rather it seems almost random: 1 moon for Earth, 2 for Mars, 95 for Jupiter, 146 for Saturn, only 30 for Uranus, 16 for Neptune, but 5 for the dwarf planet Pluto; and zero moons for both Mercury and Venus (Rabie, 2024).

Why the rocky planets formed closer to the sun, and the gas giants farther away is explained by another theory which involves the so-called solar wind, which is not a 'wind' (a movement of air) but is instead the steady flow of plasma that emanates from a star. When the sun first formed, this 'wind' was postulated to be far stronger than it is today—strong enough to blast lighter elements, such as hydrogen and helium, away from the inner orbits. When these expelled elements reached the outer orbits, the solar wind strength dropped off. The gravity of the outer gas giants quickly drew these elements in, bloating these planets into their current forms once thought to be solid cores of rock and ice covered with gas. The gas giants (Jupiter and Saturn) and icy giants (Uranus and Neptune) are fluid planets with atmospheres primarily made of hydrogen and helium. The part of their atmospheres accessible to remote sensing occupies only a small fraction of their radii, only 0.05% (Sanchez-Lavega, 2019).

This planetary-formation theory presumes that gas giants occur in a solar system's outer orbits. However, in 1995, astronomers discovered the distant planet 51 Pegasi b, a gas giant like Jupiter that orbited very close to its sun. This anomaly is explained by the belief that such planets form far away from the central star, and then move into a closer orbit. Such orbital migration, powered by a gravitational tug-of-war with other cosmic bodies, would also destroy the smaller, inner planets in its path.

For the gas giants, Jupiter and Saturn, the process is similar, with gravity causing gas and dust to accumulate and form massive planets. Nebular theories involve a process known as 'gravitational contraction,' causing parts of the cloud to clump together, which would allow for the sun and planets to form from it. Yet the asteroids between Mars and Jupiter were caused by rings that for some unexplainable reason *failed* to condense.

The problem with the 'gravitational contraction' theory is that all known physics indicates that gases tend to *expand* in a vacuum. The particles that form planets and asteroids are largely dust or frozen gases that do clump together and are not gas-like. Gravity is *by far* the weakest of the four fundamental forces, specifically 10^{40} times weaker than the electromagnetic force that holds atoms together (Clegg, 2012). Of note, electromagnetic forces are weak over great distances while gravitational forces exert significant attraction over great distances, enough to hold the proto-dwarf planet Pluto in orbit. Scottish physicist James Clerk Maxwell demonstrated that even a fluid in space would not condense but rather form a ring, such as those around Saturn, or a belt of planetoids, as in the asteroid belt.

In the Standard Model, only when a gas cloud is massive enough will it collapse, causing the temperature and pressure to rise to the point where nuclear fusion can occur, leading to the formation of a light-producing sun. Actually, no one has observed the complete formation process of a star, although stages of their development have been said to be observed. Furthermore, numerical codes do give strong evidence that star formation occurs. Evolutionists see stars and they also see gas clouds, then assume the former was formed from the latter by natural processes. The process of a cloud's gravity overcoming its internal pressure and causing a collapse to produce a burning star requires the core to reach a minimum temperature before the atoms inside fuse (Ranzan, 2016). The minimum temperature for hydrogen to fuse into helium is estimated at ten million degrees Kelvin. These facts create even more problems for the Nebular Hypothesis.

Other cosmologists have concluded that this theorized contraction will never happen naturally; normally the outward radiation pressure will always exceed the inward 'gravitational collapse' until the star's size exceeds a certain level, depending on the star's composition (Stephens, 2009). Evidence exists that compressional forces due to radiation pressure from *surrounding* stars and supernovae can cause coalescence. On the other hand, the formation of new stars requires the prior existence of other stars. For this reason, Population III star formation of the universe's very first stars is a problem.

In the early 20th century, some scientists rejected the Nebular Hypothesis for the *Planetesimal Hypothesis*, which proposed that planets formed from material drawn out of the sun. This naturalistic proposal has also been proved unsatisfactory (Fairchild, 1904; Moulton, 1928).

Other Problems with the Nebular Hypothesis

This planet-formation hypothesis, widely accepted for about a hundred years, has several other serious flaws. For example, it is now known that not all planets move in the same way as the Nebular Hypothesis predicted. At the time when Laplace proposed the theory, Neptune and the dwarf planet Pluto were unknown. All the planets in the solar system have rotations in the same direction, namely "counter-clockwise" as seen from above (the North Celestial Pole), except Venus and Uranus. Venus and Uranus both spin clockwise or backward, known as retrograde rotation (Sullivan, 2000)·

This difference cannot be explained by a hypothesis postulating that all of the planets formed from a gas cloud rotating in one direction. This problem is usually explained by collisions and/or that the planets have flipped due to planetary perturbations. Fortunately, the Earth is gyroscopically stable from the problem of variable inclinations due to its large moon. Its noticeable tilt, probably the result of the Genesis Flood, was ordained for several reasons, including to produce the seasons (Genesis 8:22).

Yet another problem is that differences in the planet-axis tilts do not conform to predictions of the Nebular Hypothesis. Earth's axis is tilted about 23–1/2 degrees, and Uranus' axis is so tilted, 82.23 degrees, that the planet is rotating on its "side." Mercury is tilted at an angle of 0.03 degrees; Venus, 2.64 degrees; Jupiter, 3.13; Mars, 25.19; Saturn, 26.73; Neptune, 28.32; and Pluto, 57.47 degrees (Hamblin, 1990).

If all planets formed from the same gas cloud, all of them should lie in the plane of their sun's equator. In our solar system, the orbital planes of several planets *are at different angles* to the sun's equatorial plane. Most planets in our solar system are within three degrees of the ecliptic, but Mercury's orbit is inclined to the ecliptic by 7 degrees, and even the dwarf planet Pluto is inclined by over 17 degrees. It is true that the planets as a set are *close* to orbiting in a plane. The problem with Pluto is its dwarf nature and, consequently, its greater likelihood of perturbations.

The naturalistic explanation for all of these differences is that some unknown rogue planet rammed into some of the planets, altering their tilt and rotational direction. However, in spite of decades of searching, no one has been able to find any evidence of these rogue planets, a finding that surely would merit a Nobel Prize. If rogue planets were to collide, then the existing planets' clear evidence of such an impact, such as meteorite perturbations on the rocky planets, would certainly exist.

Studies on the kinetic energy of the sun and the planets have empirically demonstrated that 98% of this energy is involved in the movement of the planets. According to the Nebular Hypothesis, most of the energy should still be in the sun because, as the ball of gas (actually plasma) contracted, the energy of motion would be tied up in the newly formed sun at the center. As the ball spun faster, it would fling rings of matter outward, resulting in some energy leaving the system. These rings would consist of only a small amount of mass compared to the central gas ball. Therefore, given our current understanding, it would likely have removed only comparatively small amounts of energy from the gas center, not the 98% as measured today.

A major objection to this imaginary scenario is the motivation used to originate the theory. It was not based on science, but rather was designed to support the philosophical worldview called methodological naturalism (Mortenson, 2004). Evidence for this stems from a conversation Laplace had with Napoleon Bonaparte. Napoleon inquired of Laplace after reading his musings, "Where does God fit into your system?" Laplace replied: "Sire, I have no need for that hypothesis" (Tyson, 2005). The Nebular Hypothesis is an attempt to explain the creation of the solar system without a creator. Secular astronomers are today bound by this axiom: there does not exist a Creator God.

Support for the Mature Creation of the Solar System

The idea of the "mature creation" of the solar system has many supporters. Rabbi David Gottlieb wrote that the objective scientific evidence for an old universe is strong, but *wrong*, and that the traditional Jewish calendar is close to correct, being based on the Seder Olam, which is off by at least 164 years (Gottlieb, 2023). Furthermore, John D. Morris, former president of the Institute for Creation Research, wrote in 1990 that the *appearance of age* is what God created that was "functionally complete right from the start—able to fulfill the purpose for which it was created" (Morris, 1990, p. 1).

Old-Earth creationist Vern Poythress writes the idea that God constructed a universe 6,000 years ago which is coherently mature. He also concluded that apparent age was originally built into all parts of nature, including the heavens, the solar system, and even the Earth (Poythress, 2006). Lastly, Don DeYoung effectively refuted the four major objections to the mature creation view. He noted that a mature creation does not include such present realities as disease and death that follow from the post-creation Fall (or Curse) as described in Genesis 3. Likewise, the mature creation description does *not* include the idea that fossils were created *ex nihilo* in Earth rocks. Rather, a mature, fully functioning universe, including starlight formed in transit, remains a credible option for the young-Earth creationist worldview (DeYoung, 2010).

Another explanation, in opposition to the mature creation theory proposed here, is the time dilation theory of many creationists with an interest in astronomy, including Drs. Repp, Humphreys, Hartnett, Samec, etc. Time dilation accepts the view that vast galaxies, gas-dust clouds, and other cosmological phenomena are real events rather than adopting the position that the universe only *appears* that it has dynamically changed in the past. These astronomers believe that astronomy is a science that can be studied to determine what has happened in the past following Creation despite the size and masses involved. The ideas of an original, mature creation currently are accepted by creationists but have a limited application in current astronomy.

Conclusion

This brief review of some of the evidence against the leading secular theories postulated to explain the origin of the solar system and universe has documented a few of the fatal problems with these theories. Removing these explanations from the position of viability leads to the conclusion of Genesis 1:1: "In the beginning God created the heavens and the Earth." This includes our solar system and the entire universe. The intricate solar system dynamics are required to be in place from the start.

Before this Genesis beginning, creationists teach that neither time, space, matter, nor energy existed. This partly agrees with the secular belief that, before the "Big Bang," neither time, space, matter, nor energy existed (Hawking, 2018). However, instead of God being the Creator, the "Big Bang" idea postulates that time, space, matter, and energy were created from a quantum fluctuation derived from eternal nothing. From this singularity event, Big Bang theory postulates that the entire universe as we know it has filled out and matured by cosmological and biological evolution over billions of years. The mature creation position postulates that time, space, matter, and energy were created ex nihilo producing the Day-One Universe, with the solar system being made on Day Four of Creation week.

References

Bradshaw, R.I. 1998. Creationism & the Early Church: Chapter 3, www.robibrad.denom. co.uk/Chapter3.htm.

Brush, S.G. 1990. Theories of the origin of the Solar System, 1956–1985. Review of Modern Physics 62(1):43–112.

Cameron, A. 1975. The origin and evolution of the Solar System. Scientific American 233(3):32–41.

Clegg, B. 2012. Gravity: How the Weakest Force in the Universe Shaped our Lives. St. Martin's Press, New York, NY.

Croswell, K. 2020. An elemental problem with the Sun. Scientific American, https://www.scientificamerican.com/article/an-elemental-problem-with-the-sun/.

DeYoung, D. 2010. Mature creation and seeing distant starlight. Journal of Creation 24(3):54–59.

DeYoung, D. 2010a. Our Created Moon: Earth's Fascinating Neighbor. Master Books, Green Forest, AR.

Fairchild, H. 1904. Geology under the planetesimal hypothesis of Earth-origin. GSA Bulletin 15(1):243–266.

Friedlander, M. 1995. At the Fringes of Science. Westview Press, Boulder, CO.

Goldsmith, D. (editor). 1977. Scientists Confront Velikovsky. Cornell University Press, Ithaca, NY.

Gottlieb, D. 2023. https://www.dovidgottlieb.com/comments/AGEOFTHEUNIVERSE.htm.

Hamblin, W. 1990. Exploring the Planets: An Introduction to Planetary Geology. Macmillan Publishing Company, New York, NY.

Hawking, S. 2018. Brief Answers to the Big Questions. Bantam Books, New York, NY.

Meynet, G., et al. 2010. Massive star models with magnetic braking. Astronomy & Astrophysics 525(L11), https://doi.org/10.1051/0004–6361/201016017.

Morris, J.D. 1990. Did God create with appearance of age? Acts & Facts 19(9), https://www.icr.org/article/did-god-create-with-appearance-age.

Mortenson, T. 2004. Philosophical naturalism and the age of the Earth: Are they related? The Master's Seminary Journal 15(1):71–92.

Moulton, F.R. 1928. The planetesimal hypothesis. Science 68(1771):549–559.

Numbers, R. 1977. Creation by Natural Law: Laplace's Nebular Hypothesis in American Thought. University of Washington Press, Seattle, WA.

Perna, D., M.A. Barucci, and M. Fulchignoni. 2013. The near-Earth objects and their potential threat to our planet. Astronomy and Astrophysics Review 21(65):10.1007/s00159–013–0065–4.

Poythress, V.S. 2006. Redeeming Science: A God-Centered Approach. Good News Publishers, Wheaton, IL.

Rabie, P. 2024. New moons discovered around Uranus and Neptune. The three new moons include the first to be discovered around Uranus in more than 20 years, https://gizmodo.com/new-moons-discovered-around-uranus-and-neptune-1851282795.

Ranzan, C. 2016. The nature of gravitational collapse. American Journal of Astronomy and Astrophysics 4(2):15–53, http://www.cellularuniverse.org/G8(ajaa)GravityCollapse-Ranzan.pdf.

Sagan, C. 1980. Cosmos. Random House, New York, NY.

Sanchez-Lavega, A., et al. 2019. Chapter 4: Gas Giants, pp. 72–103, https://ntrs.nasa.gov/api/citations/20190001263/downloads/20190001263.pdf.

Stephens, T. 2009. New study resolves mystery of how massive stars form. UC Santa Cruz News, https://news.ucsc.edu/2009/01/2673.html.

Sullivan, E. 2000. Retrograde Planets: Traversing the Inner Landscape. Samuel Weiser, York Beach, ME.

Tyson, N.D. 2005. The perimeter of ignorance. Natural History Magazine.

Velikovsky, I. 1950. Worlds in Collision. Macmillan, New York, NY.

Whitcomb, J.C., and D. DeYoung. 1978. The Moon: Its Creation, Form, and Significance. BMH Books, Winona Lake, IN.

Woolfson, M.M. 2000. The Origin and Evolution of the Solar System. Institute of Physics Publishing, Bristol, England.

Woolfson, M.M., et al. 1993. Solar System—its origin and evolution. Journal of the Royal Astronomy Society 34:1–20.

Woolfson, M.M. 2000. The Origin and Evolution of the Solar System. Institute of Physics Publishing, Bristol, England.

Yonge, C.D. 1993. The Works of Philo: Complete and Unabridged. Hendrickson Publishers, Peabody, MA.

YouTube. 2023. James Webb Telescope just detected an ancient energy at the edge of the universe, https://www.youtube.com/watch?v=mYwytJQSjkk.

Zwart, S.F.P. 2009. The lost siblings of the sun. Astrophysical Journal 696:L13-L16

Creation Research Society Quarterly 2025 61:221–238

The North American Midcontinent and the Genesis Flood

Part II: Rifting and the Flood

John K. Reed, Michael J. Oard, Peter Klevberg

Abstract

If rifting in the North American Midcontinent reflects early Flood processes, then defining the thickness and distribution of the total diluvial record requires mapping the base of these rifts. Using publicly available data, we created a 3D map of the base of the largest, the Midcontinent Rift. Combined with similar maps of the East Continent Basin, the Reelfoot Rift-Rough Creek Graben, and Rome Trough, we propose a basal diluvial boundary for the upper Midcontinent Region. The scale of the rifting is seen in the volume of fill; rift fill comprises well more than half of the total diluvial volume. Despite significant erosion, the rifts remain as stunning reminders of crustal disruption at the onset of the Flood, revealing significant geological activity—structural, erosional, volcanic, intrusive, and depositional—before the transgressive marine front of the Flood. Using these maps, quantitative estimates of all of the Flood and Ice Age rock records can be estimated, providing a solid basis for forensic interpretation.

Key Words: Early Flood, East Continent Basin, Midcontinent Rift, Precambrian, Reelfoot Rift, rifting, Rome Trough, Rough Creek Graben, sedimentary basin, Sudbury impact, volcanism

Introduction

The North American Midcontinent Region (Figure 1) is geologically well known but remains to be interpreted in terms of the Flood. Understanding that diluvial perspective requires good data; among the most basic are the thickness and distribution of key sedimentary volumes (Figure 2). We provide these for (1) Ice Age and recent sediments, (2) marine diluvial sediments, and (3) rift fill. These logically require four gridded surfaces: (1) DEM (Digital Elevation Model), (2) subglacial bedrock, (3) the base of marine post-rift diluvial sediments, and (4) the base of the region's rifts.

Reed et al. (2024) presented the results of mapping the first three boundaries and first two volumes, showing the volume and distribution of Ice Age and diluvial marine sediments by state (Figure 3) and by sedimentary basin (Reed et al., 2024). Large sedimentary basins are found over a broad cratonic region—the Michigan, Illinois, and

Accepted for publication May 14, 2024

Williston Basins—as well as parts of the Appalachian, Anadarko, and Denver Basins. Small basins, such as the Salina and Forest City Basins are also present. The Williston, Michigan, and Illinois Basins range in depth to over 13,000 ft. (3,962 m), 16,000 ft. (4,877 m), and 14,000 ft. (4,267 m) deep, respectively.

In addition to the basins, the study area exhibits five major rifts. In the south, the Reelfoot Rift, Rough Creek Graben, and Rome Trough have been mapped and described (Drahovzal et al., 1992; Dart, 1995; Drahovzal and Noger, 1995; Csontos et al., 2008; Dart and Swolfs, 2008; Hickman, 2011, 2013). They are much deeper than the basins; the Rough Creek Graben reaches more than 38,000 ft. (11,582 m) below sea level. These rifts contain few volcanics and most of their fill is marine sedimentary rock.

The other two rifts are larger, less-defined, and contain significant volcanic and non-marine sedimentary fills. The largest by far is the North American Midcontinent Rift. Its size reveals the magnitude of crustal disruption at the beginning of the Flood (Reed, 2000; Clarey, 2020). Though many studies continue to be published and significant data accumulated (i.e., Miller and Nicholson, 2013; Stein et al., 2015; Woelke and Hinze, 2015; Stein et al., 2016; Fairchild et al., 2017; Stein et al., 2018; Grauch et al., 2020; Hinze and Chandler, 2020), maps of the Midcontinent Rift are limited to its surface or bedrock (sub-glacial) two-dimensional extent, showing the distribution of volcanics and sediments at the erosional unconformity that forms its top.

In the Lake Superior Basin, thick sediments of the rift overlie thicker basalt flows and intrusive rocks. In its western arm, running from Minnesota and Wisconsin through Iowa and Nebraska and into Kansas, a central volcanic horst is flanked by sedimentary basins. Horst-top and flanking basins have been characterized (e.g., Anderson, 1990; Jirsa et al., 2012; Woelke and Hinze, 2015). The configuration of the eastern arm, running the length of Michigan, is poorly described; whether or not it shows the same flanking basins as the western arm is unknown.

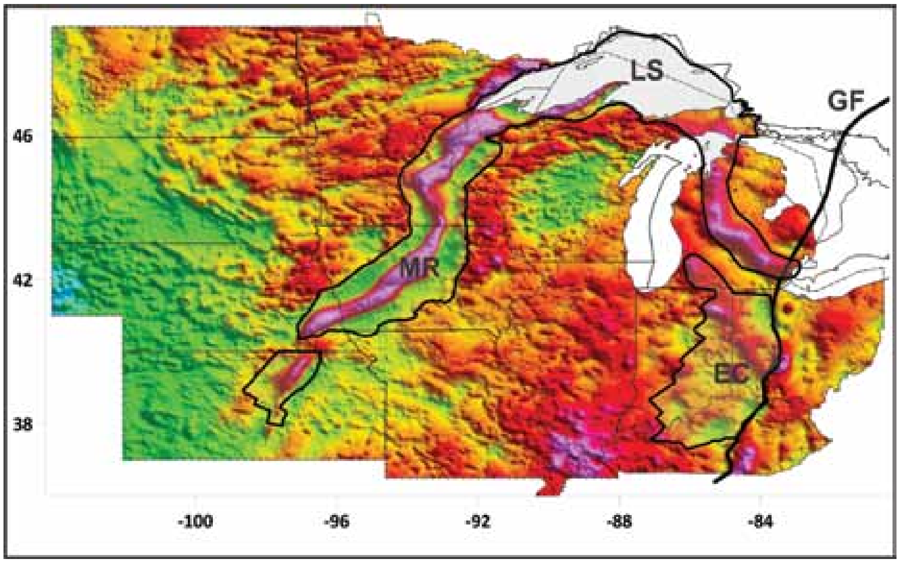

Figure 1. The study area of this paper is shown on the Bouguer Gravity Anomaly map (Kucks, 1999), including the Midcontinent Rift (MR), East Continent Basin (EC), and Grenville Front (GF). The largest, deepest part of the Midcontinent Rift is in the Lake Superior Basin (LS). Pink, purple, and red are positive gravity anomalies, while green colors are negative gravity anomalies. Notice in the MR that high gravity anomalies, representing horsts of uplifted denser rocks, are found in the center. They are surrounded by low gravity anomalies, representing sedimentary basins along the edge.

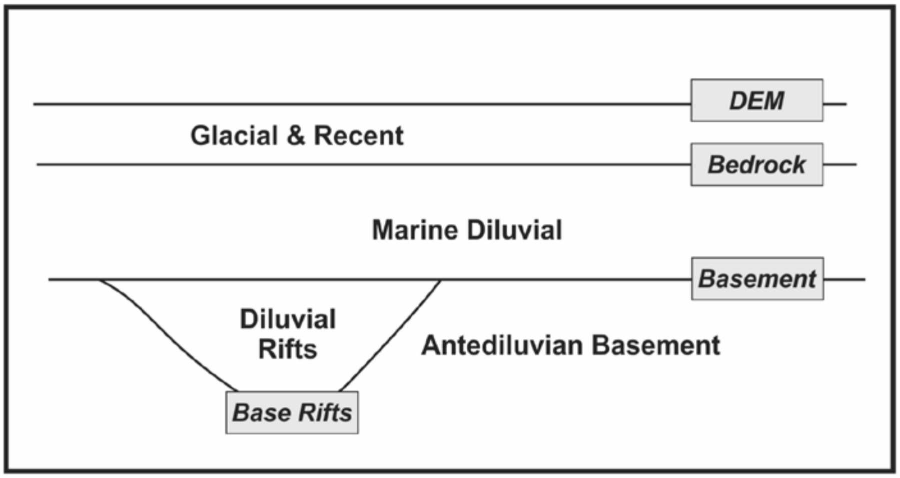

Figure 2. Determining volumes and their distribution requires mapping of four major surfaces. The first three were presented in Reed et al. (2024).

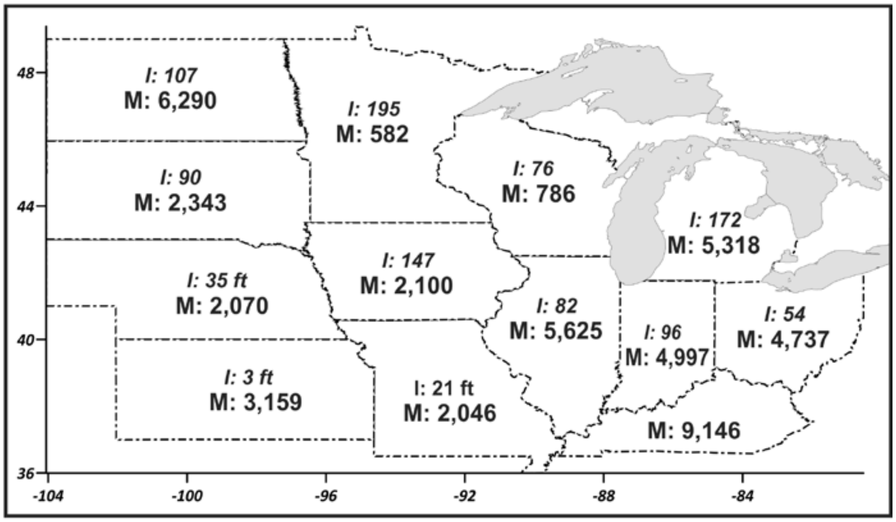

Figure 3. Average thicknesses in feet, by state, of Ice Age (I) and marine diluvial (M) sediments for the study area.

The East Continent Basin has been described (Drahovzal et al., 1992; Baranowski et al., 2009), although there is significant uncertainty about its depth and debate about its extent. Like the Midcontinent Rift, it contains Proterozoic basalt and terrestrial sediment of the Middle Run Formation. It extends across western Ohio into Indiana and Kentucky, where it either intersects or terminates at the Rough Creek Graben. Combined with the existing maps of the southern rifts, we propose that three-dimensional maps of the northern rifts, combined with the map of the unconformity underlying mostly marine sediments would show the actual basal diluvial boundary for the study area. Mapping the basal diluvial boundary allows calculation of the volume and distribution of Flood rocks, including both marine and non-marine portions.

Mapping the Midcontinent Rift and East Continent Basin

Mapping the rifts is difficult. They are covered by thousands of feet of sediment. There are few wells because there has been little economic incentive to drill. So they are known primarily from seismic data and maps of gravity (Kucks, 1999) and magnetic (Bankey et al., 2002) anomalies. Well penetrations help define their two-dimensional extents, as do outcrops around Lake Superior. Oil and gas prospecting in the southern rifts (Reelfoot, Rough Creek, Rome), combined with their shallower depths, has resulted in more wells and seismic lines, and a better definition of their 3D morphology (e.g., Hickman, 2013).

The Midcontinent Rift's present configuration suggests segmentation (Dickas and Mudrey, 1997), but estimates of significant erosion (Green et al., 1987; Hutchinson et al., 1990), based on dike swarms away from its margin, indicate a larger original extent. Green et al. (1987) estimated up to 2 million km^3 of basalt was originally emplaced. If significant erosion took place, some of the rift segments (e.g., Kansas and Iowa-Nebraska) might have been once joined. For convenience, we will address five geographic segments: (1) Kansas, (2) Iowa-Nebraska, (3) Minnesota, (4) the Lake Superior Basin, and (5) Michigan.

A greater understanding of the Midcontinent Rift and its place in the Flood requires a three-dimensional map. Reed (2000) drew a strike section but no map has been published. Despite limited data, it is well worth attempting to constrain its total volume and its relative volumes of volcanic and sedimentary rocks. This can be done as a whole, by state, and by basin. Our map is developed from publications and data from state geological surveys, publications from journals, and dissertations. Although there are only four deep test wells into the Midcontinent Rift—in Kansas, Iowa, Wisconsin, and Michigan—numerous shallow wells help constrain the two-dimensional boundaries of the rift. Publications of the state surveys were essential in working at any level of detail.

In Reed et al. (2024), we showed the surface of the erosional unconformity between Precambrian crystalline rock and Phanerozoic sediments. This surface (Figure 4) also shows where crystalline basement is exposed or immediately underlies glacial sediments—in other words, where marine diluvial strata are absent, primarily in Minnesota, Wisconsin, and Michigan. Smaller exposures of crystalline basement occur in the Black Hills of South Dakota and the St. Francois Mountains of Missouri. All of these were blanked during gridding. We also blanked areas of Proterozoic metaquartzites (the Sioux and Baraboo) since we have no data for mapping their base. We believe that these are likely early Flood deposits, but their total volume is very small relative to the study area.

The Midcontinent Rift

The first step in mapping the rift is an accurate outline of its lateral extents. In places around Lake Superior,

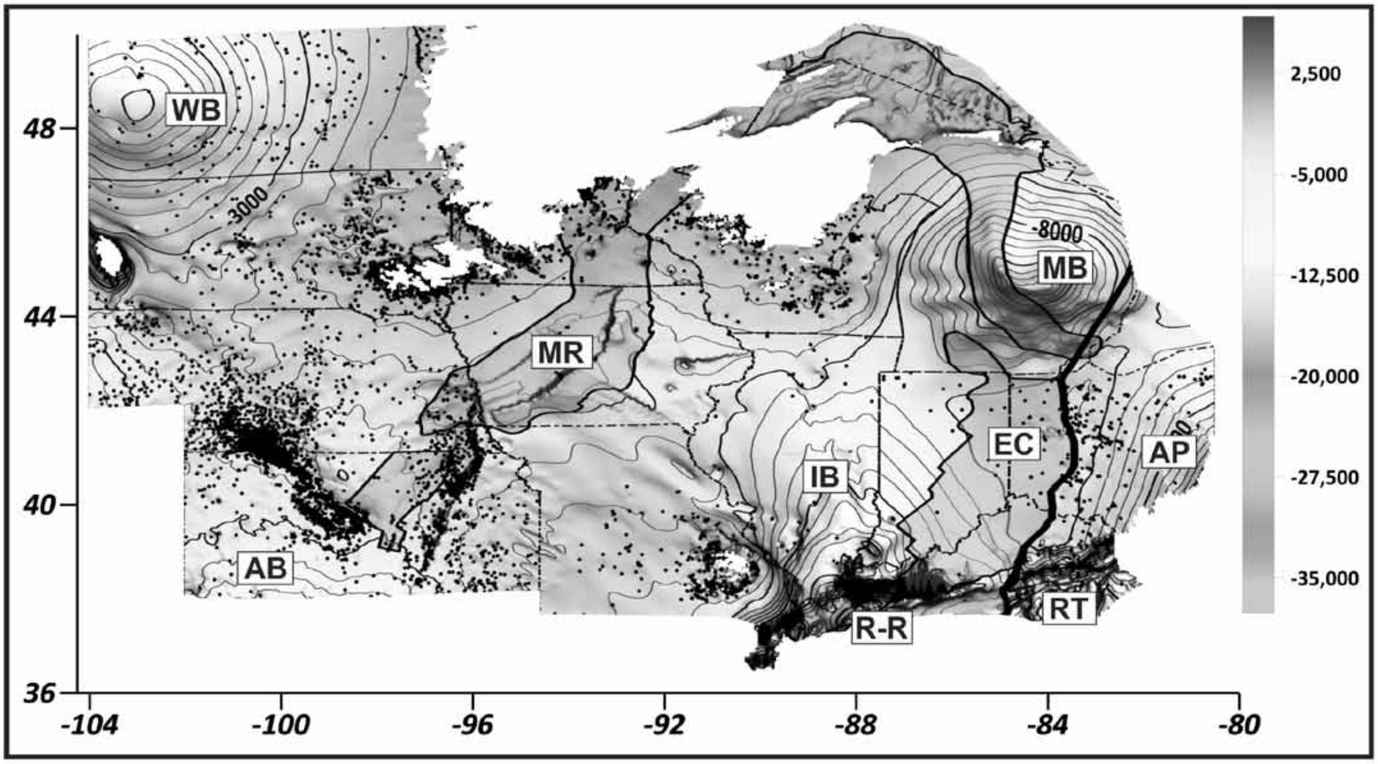

Figure 4. The base of marine diluvial rocks in the upper Midcontinent Region in feet A S L. The contour interval is 1000 feet. Blanked areas show exposed or subglacial Precambrian crystalline rock, the Sioux Ridge in southeastern South Dakota, the Black Hills in southwestern South Dakota, the Baraboo quartzites in Wisconsin, and the St. Francois Mountains in southeastern Missouri. Major sedimentary basins in the study area include the Anadarko (AB), Williston (WB), Illinois (IB), Michigan (MB), and Appalachian (AP) Basins. This surface also forms the top of the Proterozoic Midcontinent Rift (MR) and East Continent Basin (EC), shown outlined. The Reelfoot Rift-Rough Creek Graben (R-R) and Rome Trough (RT) form deep grabens along the southern boundary of the study area. Well control is shown by black dots.

this is constrained by outcrops and shallow wells. In other places, it is constrained by bedrock geological maps, seismic lines, and gravity and magnetic anomaly maps. For example, the Bouguer Gravity Anomaly map of the region (Figure 1) clearly shows the outline of the rift.

In Kansas, additional control is provided by well penetrations, interpretive maps (Cole, 1976; Bickford et al., 1979; Berendsen and Blair, 1996a, 1996b), and a COCORP seismic line across the northern part of the rift (Serpa et al., 1984; Berendsen et al., 1988; Woelk and Hinze, 1991; Berendsen, 1997; Woelk and Hinze, 2015). In Nebraska, control is provided by well penetrations, gravity and magnetic data, and interpretive maps (Burchett and Carlson, 1986), primarily those in Iowa (Anderson, 1995, 2006). Control in Iowa is provided by gravity and magnetic data, a few deep wells, and seismic data (Chandler et al., 1989; Anderson, 1990). The extent in Minnesota and Wisconsin is constrained by significant outcrop and well penetration data (Dickas and Mudrey, 1999) and in Minnesota by detailed County Atlas Maps and a statewide geologic maps (Jirsa et al., 2011). These include data from numerous outcrops and thousands of wells. Wisconsin's bedrock geological map (Mudrey et al., 1982) is relatively old, though the state survey is working on an update. In Michigan, control based on outcrops around Lake Superior, a bedrock geological map (Michigan Geological Survey Division, 1987), and by studies of the Lake Superior Basin provide control in the northern part of the state, but otherwise, control is limited to geophysical data, three COCORP seismic lines (Brown et al., 1982; Zhu and Brown, 1986), and sparse well control in the Michigan Basin.

We evaluated two boundaries for the rift because of current disagreements in Michigan and in Kansas. In Kansas, deep-well data were used in Bickford et al.'s (1979) map of Precambrian basement rocks in Kansas

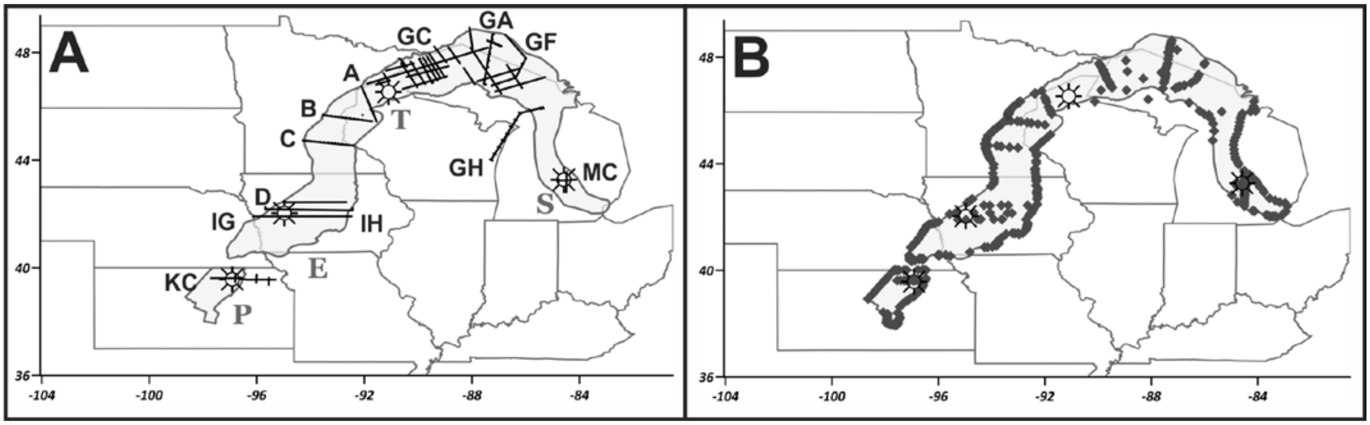

Figure 5. A = Data sources for mapping the base of the Midcontinent Rift. Wells include the Poersch #1 in Kansas (P), the Eischeid #1 in Iowa (E), the Terra-Patrick #1–7 in Wisconsin (T), and the Sparks McClure #1–8 in Michigan (S). Seismic lines include the COCORP lines in Kansas (KC) and Michigan (MC), the GLIMPCE lines in Lake Superior and Lake Michigan (GC, GA, GF, and GH), the Chandler et al. (1989) seismic line sections in Iowa and Minnesota (A, B, C, and D), Halliburton Lines in Iowa (IG and IH), and other seismic lines in Lake Superior (see text). Data points from the intersection of top Precambrian contours with the boundary of the rift resulted in the perimeter control points shown in B.

to show the extent of the rift. However, Berendsen and Blair (1996b) later drew a subcrop map of the Precambrian, showing different boundaries for the rift's volcanics and sediments, shaped by their interpretive fault patterns. But Woodruff et al. (2021) show a map more in line with Bickford et al. (1979).

In Michigan, there is an ongoing debate over whether or not the rift terminates at the Grenville Front. We created one boundary using Woodruff et al.'s (2021) Kansas boundary and terminating the rift at the Grenville Front in Michigan. Another boundary used Berendsen and Blair's (1996b) map in Kansas and extended the rift past the Grenville Front, following the gravity anomaly of Kucks (1999). We also drew the rift in Michigan slightly wider than some depictions (e.g., https://project.geo.msu.edu/geogmich/rift_zone.html) based on the COCORP lines in southern Michigan (Brown et al., 1982).

In addition to the 13 states, the study area extends slightly into Ontario, adjacent to Lake Superior. We set this boundary to improve gridding accuracy along the northern boundary of the rift. This total defined study area covered 2,295,682 km^2. Our Boundary 1 of the Midcontinent Rift enclosed 285,464 km^2, including 20,308 km^2 in the Kansas segment, or 12.43% of the study area. Our Boundary 2 enclosed 280,948 km^2, including 21,684 km^2 in Kansas, or 12.24% of the study area. These numbers are very close and, for simplicity, we use Boundary 2 in the rest of this paper.

Mapping the Base

Data defining the base of the Midcontinent Rift come from seismic reflection profiles. Although four wells along the rift margins play a role in understanding rift fill geology and calibrating seismic velocities, they do not penetrate the deep rift. These include the Texaco Noel Poersch #1 well in Kansas (Berendsen et al., 1988), the Amoco M.G. Eischeid #1 well in Iowa (Anderson, 1990), the Terra-Patrick #7–22 well in Wisconsin (Dickas et al., 1999), and the McClure Sparks et al. 1–8 well in Michigan (Sleep and Sloss, 1978). In addition to COCORP lines in Kansas and Michigan (Figure 5), seismic data are available through a Halliburton line in Iowa (Anderson, 1990), Petty-Ray geophysical lines described by Chandler et al. (1989) in Iowa and Minnesota, and several generations of seismic data around and under Lake Superior (Halls and West, 1971; Halls, 1982; Luetgert and Meyer, 1982; Hutchinson et al., 1986; Behrendt et al., 1988; Canon et al., 1989, 1991; Allen, 1997; McGinnis and Mudrey, 2003). Of primary interest are the 1986 lines from the Great Lakes International Multidisciplinary Program on Crustal Evolution (GLIMPCE) program (Agena et al., 1988). Depth control points from these sources used to map the Midcontinent Rift base are shown in Figure 5B.

Additional depth control was provided by the intersection of the rift margins and contours of the Precambrian surface (from the map used to create Figure 4), as shown in Figure 5B. These depths range from above sea level to -16,000 ft. (-4,877 m) in the Michigan Basin. Contouring was also constrained by the structural interpretation of features such as the White's

Ridge and Grand Marais Ridge (Allen et al., 1997).

The base of the rift (Figures 6 and 7) was mapped by contouring the control points using the rift morphology shown on the seismic lines. Though interpretive and general, it provides an initial picture of the rift relative to its surrounding crust. Once a map was constructed, the resulting contours and data points were gridded and a 3D surface was generated. Figure 6 includes the base of the East Continent Basin and other cratonic rifts. It therefore forms a true diluvial basal unconformity surface. The map of the Precambrian surface shown in Figure 4 (Reed et al., 2024) forms an upper rift surface and allows volumetric calculations of the Midcontinent Rift, as well as the East Continent Basin. Combined with the volumes of the southern rifts and the diluvial marine volume (Reed et al., 2024), we were able to calculate the total diluvial rock volume for the region.

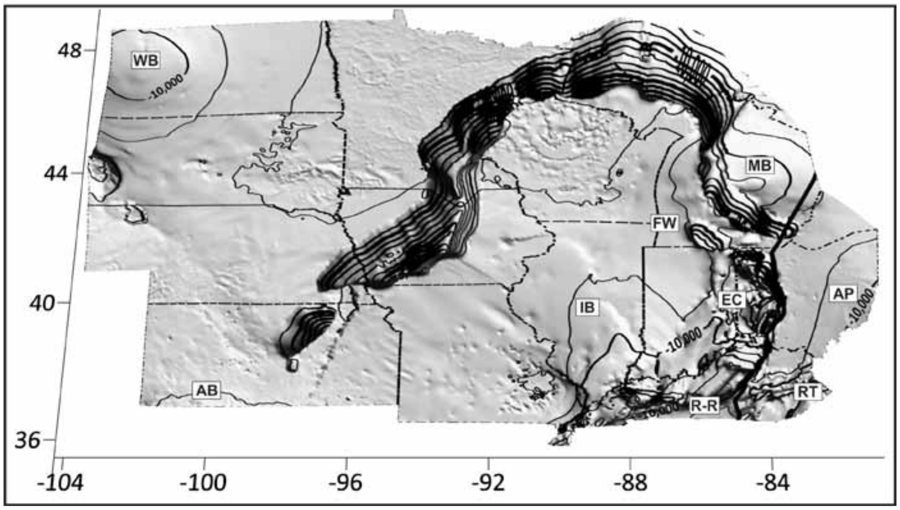

Figure 6. Configuration of the Upper Midcontinent Precambrian surface including the base of Midcontinent Rift and East Continent Basin (EC) in feet ASL. The contour Interval is 5,000 feet. The Williston (WB), Anadarko (AB), Illinois (IB), and Michigan (MB) basins are dwarfed by the Midcontinent Rift. The East Continent Basin (EC), Reelfoot Rift-Rough Creek Graben (R-R), Fort Wayne Rift (FW), and Rome Trough (RT) are likely all a result of continent-scale crustal deformation at the onset of the Flood. The Grenville Front (GF) forms the eastern boundary of the East Continent Basin.

Figure 6 reinforces the proposal of Dickas and Mudrey (1997) that the feature is segmented, though perhaps more in the sense of eruptive centers rather than continent-scale, strike-slip faulting. Local factors obviously affected the morphology, as seen in the impact of basement ridges under western Lake Superior that the rift bypassed (Allen et al., 1997).

The rift was once larger. Significant erosion occurred after the emplacement of rift fill. Green et al. (1987) and Hutchinson et al. (1990) suggested, based on the distance of possible feeder dikes from the rift, that up to half of its volume had been removed. Erosion is also visible in large horst top basins, which appear to be scours in the central horst along the western arm. The shallower depth of the Kansas segment as compared to the Lake Superior Basin and the Iowa segment, combined with the basement separation of the Kansas and Nebraska segments suggests that either rifting and volcanism were less in Kansas or that erosion was greater. The greater depth and size of the rift in the Lake Superior Basin and the Iowa segment indicate centers of deformation and volcanism.

The East Continent Basin

Basement data for the Midcontinent Rift, though sparse, exceeds that for the East Continent Basin. The East Continent Rift Basin (Figure 6) was described by Drahovzal et al. (1992), and their monograph included a boundary that extended into northern Tennessee and a basement surface map based on available seismic data. Since then, little additional information has been published. Baranowski et al. (2009) proposed that the East Continent Rift was distinct from the younger East Continent Basin, which they considered a later foreland basin of the Grenville thrust front, based on reprocessing of the Ohio COCORP Line 1. They proposed several Precambrian seismic stratigraphic units. However, their cross section little resembled the earlier basement map. Moecher et al. (2018) used seismic and well data to develop a new boundary that terminated the basin at the northern edge of the Reelfoot Rift-Rough Creek Graben-Rome Trough system, shown also in Clay et al. (2021).

The Drahovzal et al. (1992) basement map ended in northern Ohio. In the absence of data, we used the Moecher et al. (2018) outline of the East Continent Basin, continued the contours from the Drahovzal et al. (1992) map, and contoured to a conservative 20,000-ft. depth for the Fort Wayne Rift (Figure 6). Contouring north of the Reelfoot Rift-Rough Creek Graben and Rome Trough is also based on Drahovzal et al. (1992). The East Con-

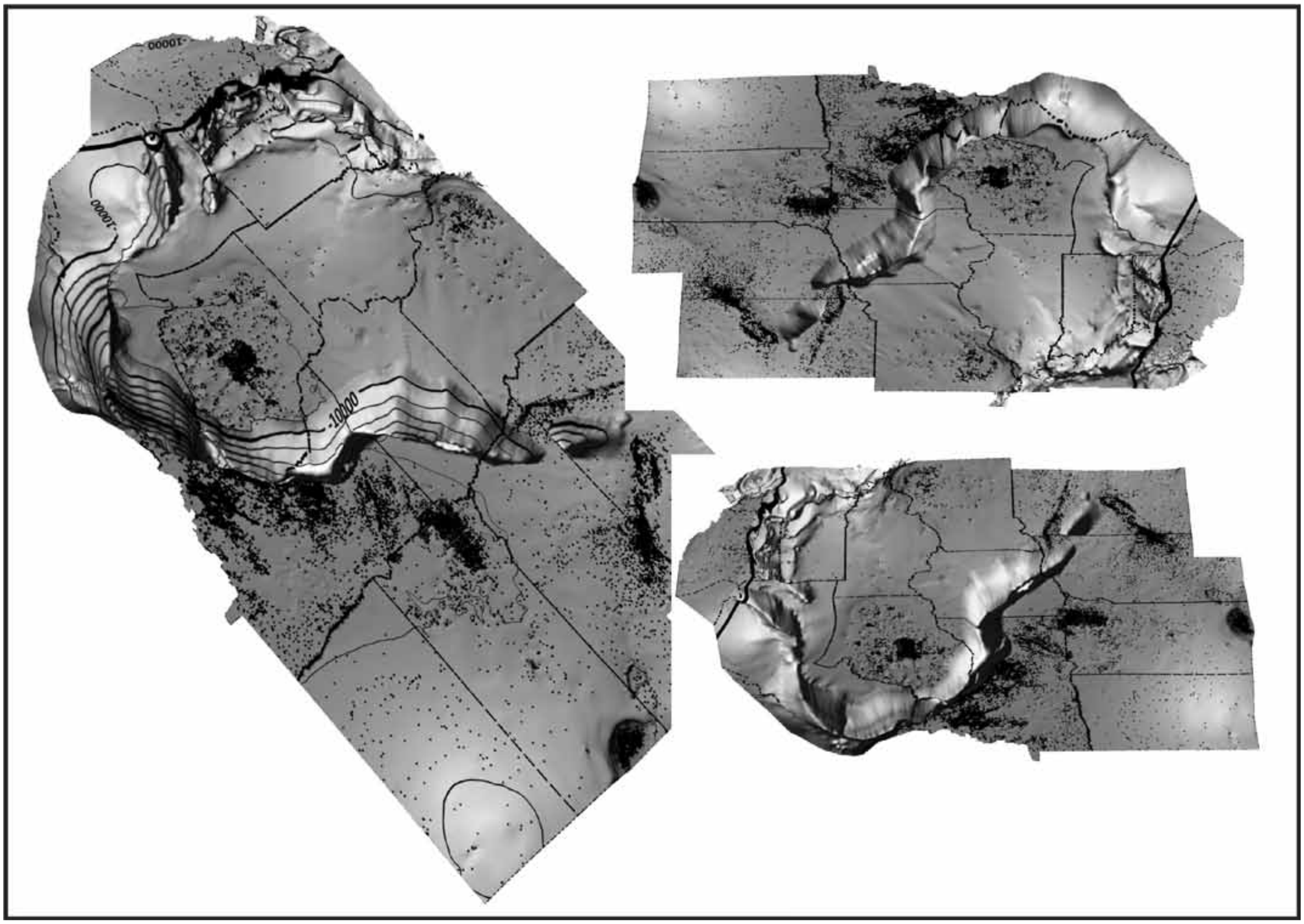

Figure 7. Different angles help visualize the configuration of the base of midcontinent rifting, which probably marks the onset of the Flood. The Grenville Front is shown by a black line in the eastern area and black dots show well control for the surrounding basement.

tinent Basin is a feature that requires significantly more data and effort to understand.

Results

These maps allow initial calculations of both marine diluvial and rift-fill volumes. The volume of the Midcontinent Rift is over 2.3 million km^3. This is greater than published estimates and nearly an order of magnitude more than the volume of the East Continent Basin of 238,435 km^3. Figures 6 and 9 illustrate that difference by simply comparing the cratonic basins (Illinois, Michigan, Williston, etc.) to the rifts. Although the East Continent Basin (and the southern rifts) exceed 10 km in depth and are certainly impressive compared to the cratonic basins, the Midcontinent Rift exceeds 30 km in depth in places and its areal extent dwarfs that of the other rifts.

The Midcontinent Rift and East Continent Basin together occupy a little over 17% of the study area, but account for over 53% of the *total* diluvial and Ice Age volume. For 83% of the study area, the basal diluvial surface is the Precambrian/Phanerozoic unconformity. For the rifts, it is the base of rift fill. If they are Flood features, these two rifts must have come very early because they formed, were filled, and were eroded prior to the arrival of the post-rift transgressive marine sediments (Figure 8).

Volume of the Midcontinent Rift

The total volume of the Midcontinent Rift has been estimated between 1,000,000–2,000,000 km^3 (Green, 1983;

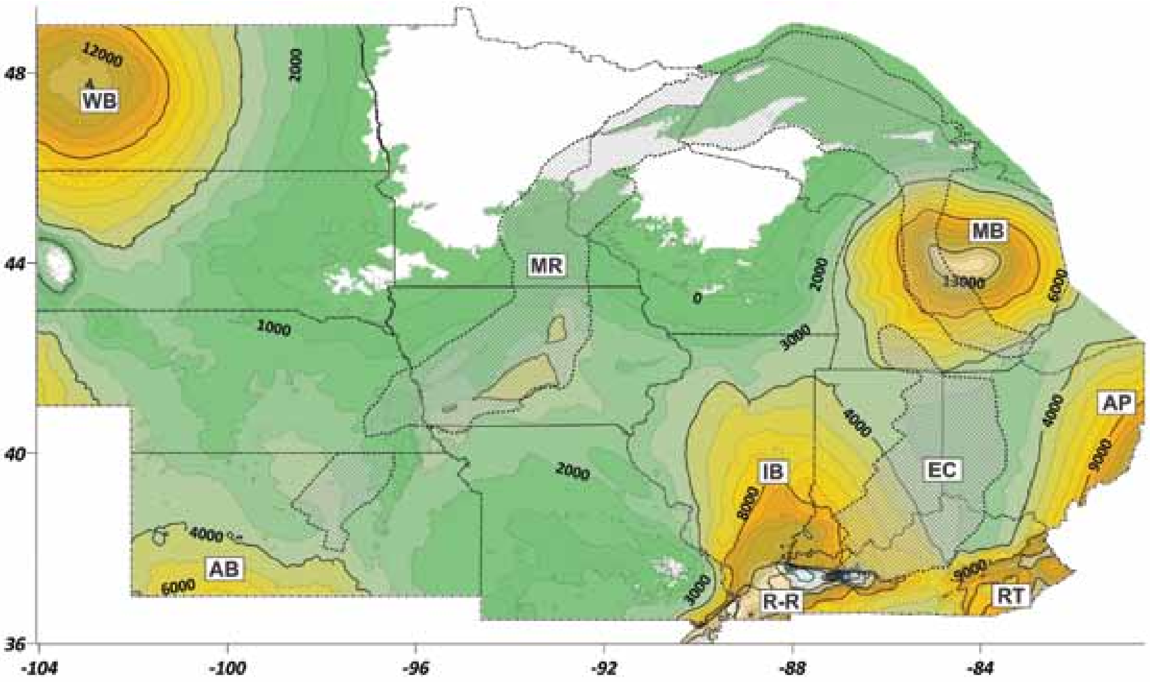

Figure 8 ***(above)*****. Isopach map of the Phanerozoic for the upper midcontinent region in feet. The contour interval is 1,000 feet. This does not include rift or basin fill in the Midcontinent Rift (MR) and East Continent Basin (EC). Note how the cratonic basins and southern rifts stand out as depocenters.**

Figure 9 ***(below)*****. Isopach map from the ground surface to the diluvial basement in the study area in feet. The contour interval = 5,000 ft. The Midcontinent Rift (MR) dwarfs the later cratonic basins and other rifts; the Williston (WB), Illinois (IB), Michigan (MB), and Appalachian Basins (AP), as well as the other rifts; the East Continent Basin (EC) and the Reelfoot/Rough Creek/Rome (RR) Rifts.**

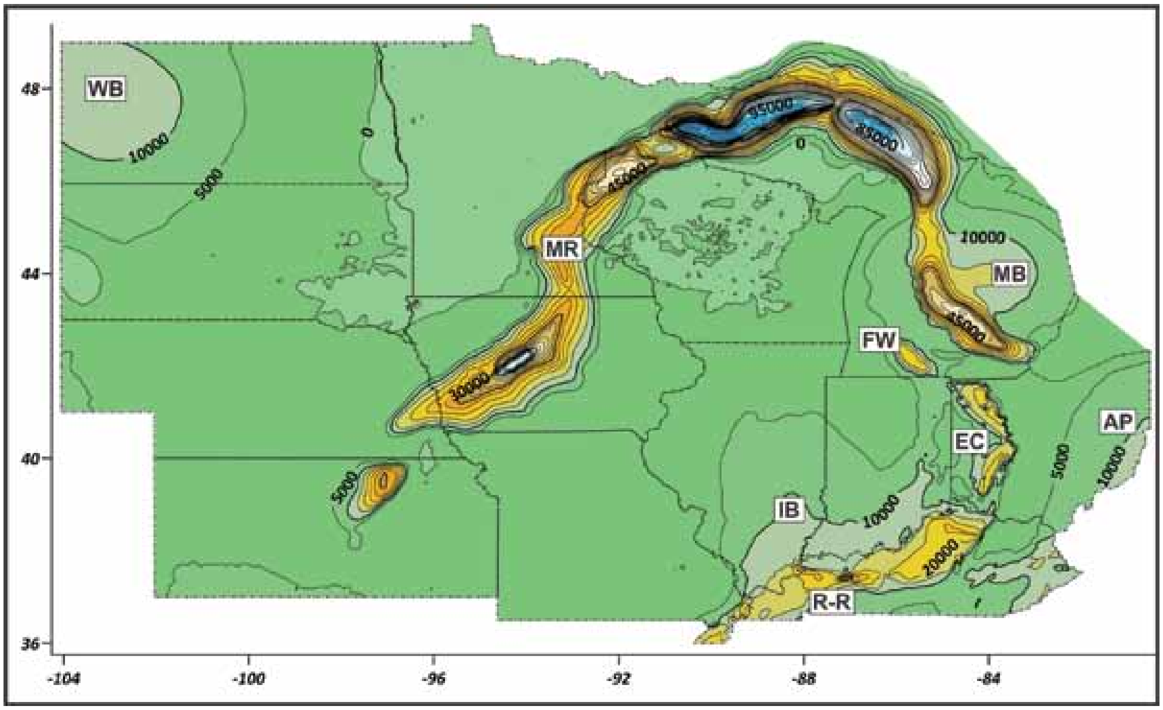

Table I. Volume and average thickness of Midcontinent Rift by state. There is a slight discrepancy between the totals shown here and those from calculating the total rift boundary.

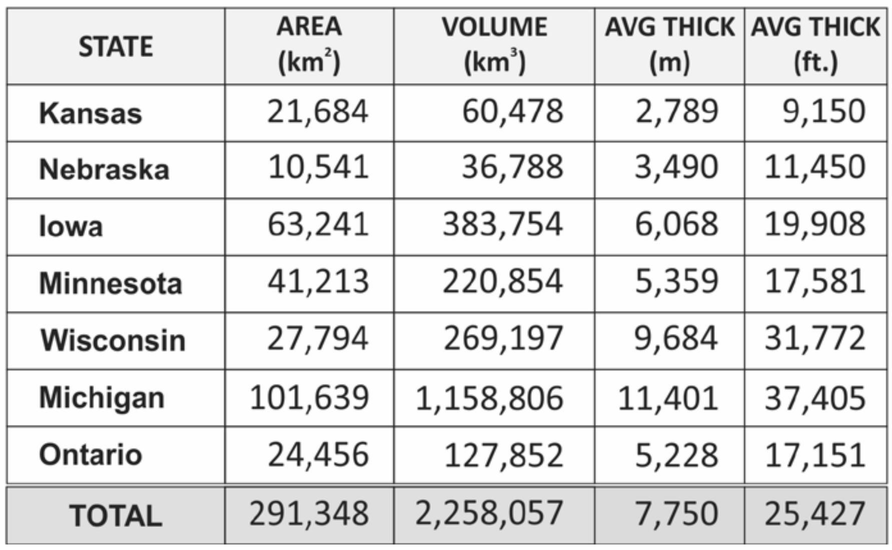

STATE	AREA (km^2)	VOLUME (km^3)	AVG THICK (m)	AVG THICK (ft.)
Kansas	21,684	60,478	2,789	9,150
Nebraska	10,541	36,788	3,490	11,450
Iowa	63,241	383,754	6,068	19,908
Minnesota	41,213	220,854	5,359	17,581
Wisconsin	27,794	269,197	9,684	31,772
Michigan	101,639	1,158,806	11,401	37,405
Ontario	24,456	127,852	5,228	17,151
TOTAL	291,348	2,258,057	7,750	25,427

Hutchinson et al., 1990; Ojakangas et al., 1997). Stein et al. (2015) calculated 2,100,000 km^3. Our calculated volume is slightly larger, 2,311,378 km^3, but supported by maps of the base and the top of the rift. This volume came from subtracting the gridded surface of the base of the rift (Figure 6) from the basal marine diluvial surface (Figure 4), which is the erosional unconformity underlying widespread marine diluvial sedimentation.

The 13-state study area covers 2,295,682 km^2. The Midcontinent Rift occupies a surface expression of 295,965 km^2, or 12.9% of the total study area. The rift's total volume of 2,311,378 km^3 yields an average thickness of 25,631 ft. (7,812 m), with maximum depths exceeding 100,000 ft. (30,480 m)—*or 19 miles*—in the Lake Superior Basin! Thus, an area that occupies less than 13% of the study area holds 48% of the study area's total volume (4,837,013 km^3) of diluvial and Ice Age rocks (Table I, Figure 9). The greatest thicknesses occur in the Lake Superior Basin, as shown by Table I (Michigan and Wisconsin).

Volume of the East Continent Basin

Much smaller than the Midcontinent Rift, the East Continent Basin is not as well understood. We recognize uncertainties in mapping its base and use the boundary of Moecher et al. (2018). Doing so yields a surface expression of 100,757 km^2, a little more than a third of the Midcontinent Rift and 4.39% of the study area. This is slightly larger than the boundary of Drahovzal et al. (1992), with less area in the south and more to the northwest, following the gravity anomaly reflecting the Fort Wayne Rift. We calculated that the total volume of the East Continent Basin is 238,435 km^3. This is a little more than 10% of the volume of the Midcontinent Rift and nearly 11% of the volume of the marine diluvial sediment in the study area. The average thickness of the basin is 7,764 ft. (2,366 m).

Together, the Midcontinent Rift and East Continent Basin total a little more than 2.5 million km^3 and exceed the volume of the total overlying marine post-rift diluvial and Ice Age sediments in the study area (Figure 10). This can be readily visualized in Figure 9. If the volumes of the Reelfoot Rift-Rough Creek Graben and Rome Trough were subtracted from the marine post-rift diluvial package and their volume combined with the northern rifts, the total *rift* volume for the study area would significantly exceed that of the overlying sedimentary record. When their areal extent is compared to the entire study area, their volumes suggest high energy levels very early in the Flood, with greater volumes of basalt emplaced in the northern rifts.

Midcontinent Rift Volcanics and Sediments

The Midcontinent Rift is an immense structure, infilled with volcanics—primarily basalt—and sediments. Estimating their relative volumes is difficult. Although the rift as a whole has been mapped, there are many uncertainties regarding the deep morphology of its sedimentary basins. There are also unknown volumes of sediment interbedded between basalt flows, varying fault angles between the volcanic horsts and the flanking sedimentary basins, and a lack of knowledge of the configuration of sedimentary basins in Michigan, if any. But like mapping the base of the rift to approximate the total volume of the rift fill, this helps constrain the volcanic/sediment ratio.

Two locations, illustrating different styles of sedimentation, can help. The first is the western Lake Superior Basin, where Oronto and Bayfield Group sediments overlie basalt flows. The second is in the Iowa/Nebraska segment, where Anderson (1990) reported volumes for sedimentary basins. Dickas and Mudrey (1999) mapped the base

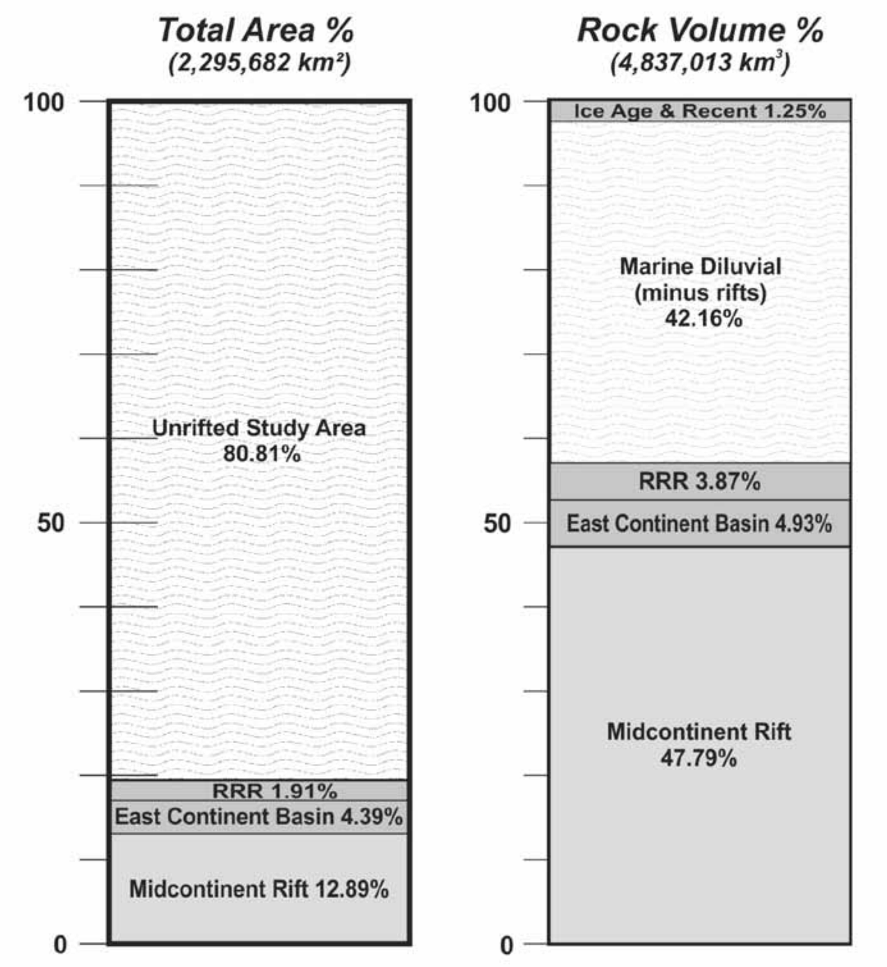

Figure 10. Area vs. volume of rifts in the Midcontinent study area. RRR means Reelfoot/Rough Creek/Rome rifts. Though the rifts occupy less than 20% of the study area, they comprise over 56% of its total rock volume.

of the Oronto Group in the western Lake Superior Basin. Using their map, a surface was gridded and a boundary drawn (Figure 11). The volume from the base of the Oronto Group to the sediment surface (this would include glacial and lake deposits) within this boundary is 144,084 km^3. Ice Age sediments make up 8,752 km^3 of that volume, leaving 135,332 km^3 of rift sediments. The volume of the underlying volcanics is 299,118 km^3. The Oronto and Bayfield sediments here are thus 31.15% of the total volume within the bounded area of the Lake Superior Basin (Figure 11).

In Iowa, Anderson (1990) calculated areas and volumes for the flanking and horst-top basins. He estimated a total of 49,500 km^3 for the western flanking basins, 99,700 km^3 for the eastern flanking basins, and 18,200 km^3 in the horst top basins, totaling 167,400 km^3. We compared this number to our total rift fill of the same segment, which is 423,750 km^3, and based on that comparison, sediment is 39.5% of the total fill. Based on our mapping (Figure 8), the volume for the flanking basins is 165,497 km^3, which is 11% greater than Anderson's (1990) number. Adding Anderson's (1990) number for the horst-top basins, the sediment in this segment totals 185,600 km^3 (24% greater than Anderson's total). This suggests that sediments could be as much as 48% of the rift fill (Figure 11). If these two locations are representative for the entire Midcontinent Rift, sedimentary facies comprise somewhere between a third and a half of the total volume of the rift.

Although imprecise, it is clear that the volume of Midcontinent Rift sedimentary rock is quite large. If even a third of the total fill is sedimentary, that would total over 824,000 km^3. That would be nearly 36% of the total Phanerozoic volume in the entire study area. The Midcontinent Rift occupies less than 13% of that area. Nor does this account for the volume of sediment (and basalt) eroded before the arrival of the post-rift sediments. In any case, the volume of sedimentary rock in the Midcontinent Rift is staggering.

Table II. Volume and average thickness of the study area rifts. See Figure 9.

RIFT BASIN	AREA (km^2)	VOLUME (km^3)	AVG THICK (m)	AVG THICK (ft.)
Midcontinent Rift	295,865	2,311,378	7,812	25,631
East Continent Basin	100,757	238,435	2,366	7,764
Reelfoot_Rough Creek	23,419	128,213	5,475	17,962
Rome Trough	20,171	59,166	2,933	9,623
TOTAL	440,212	2,737,192	6,218	20,400

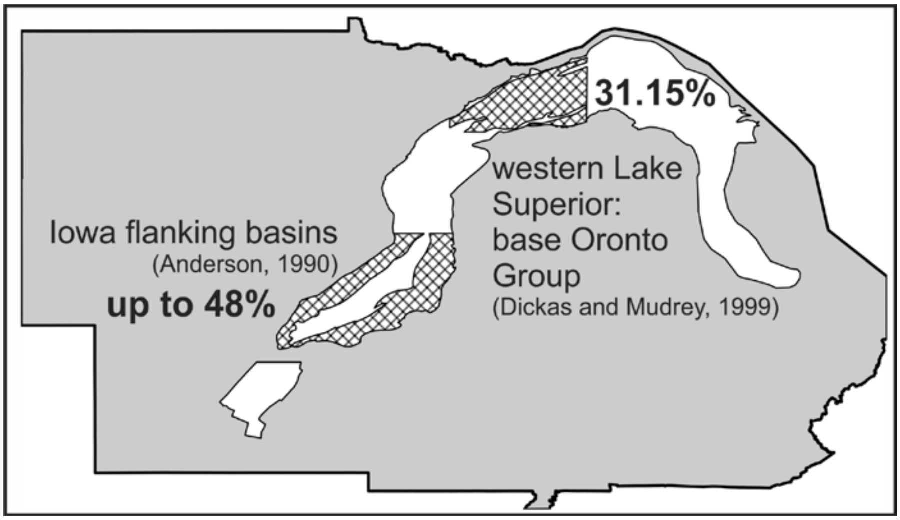

Figure 11. Two areas of the Midcontinent Rift allowed estimates of the sediment-to-volcanic rift fill ratio. In western Lake Superior, sediments of the Oronto and Bayfield groups overlying volcanics occupy nearly a third of the total volume there. In the flanking (and horst top) basins of Iowa, the sediments approach half the total volume.

Sudbury Impact and the Midcontinent Rift

Another interesting aspect of the Midcontinent Rift is its proximity to the Sudbury impact crater, located about 200 km from its present boundary. The Sudbury impact structure was controversial for a long time, but has since been accepted as an impact crater, meeting stringent criteria for identifying impacts. The crater has been greatly eroded (see below), which added to the problem of identifying it as an impact. Geologists think its original diameter was between 200 and 250 km (Huber et al., 2020). Adding a 200 km buffer to the present impact site slightly intersects the present Midcontinent Rift boundary (Figure 12) but they would overlap noticeably if the original rift boundary and the impact crater were both larger.

Based on Green et al. (1987) report that feeder dikes for the rift occur as much as 200 km out from its present location, it is reasonable to see the original rift as much larger. Recognizing that any pre-erosion boundary would not be a uniform distance from the present boundaries along the entire rift, we created a conservative uniform buffer 100 km from the present boundary. That increased the area covered significantly, to 821,691 km^2, or to nearly 36% of the total study area. However, the pre-eroded *volume* of the rift would probably not be proportionately greater since the greatest depths are found in the rift axis. Every 1,000 m of fill eroded from the buffer zone would represent nearly a half-million km^3 of volume.

Erosion at the nearby Sudbury feature is estimated at approximately 5,000 m (16,404 ft.) (Senft and Stewart, 2009). If erosion at the Midcontinent Rift was similar, the eroded thickness of 5,000 m multiplied by the ~800,000 km^2 would have been more than 4,000,000 km^3. Compare that to the current volume of the rift of less than 2,500,000 km^3. That would mean that over 60% of the original rift volume was eroded. This represents a vast sediment source for clastic rocks across central North America early in the Flood. The 4 million km^3 would represent a much greater volume of sediment than is found in the entire Phanerozoic record in the study area. Sourcing sediment for Flood deposits appears to have been no problem, given the energy of its erosion possibly reflected here.

Is there a link between the impact and rifting? Uniformitarians see the location as coincidental because they date Sudbury 700 million years before the rift. But to diluvialists, both could be related to the onset of the Flood. It is difficult to see one of the world's largest impact features in direct proximity to a massive rift and not think they were related. We could only speculate on the mechanics. Some very powerful force caused the rift, and the Sudbury impact was powerful. If they are connected, the 700-million-year error in dating is another indication that skepticism is warranted for the geological ages.

Precambrian Geology and the Base of the Flood

A century ago, the Precambrian was simply the doorway from a well-understood sedimentary record into a misty, speculative realm that inconveniently contained nearly 90% of deep time. That has changed. Precambrian geology has seen dramatic changes in two generations, as more data combined with mature narratives like plate tectonics have created a more complete Earth history extending far deeper into the uniformitarian past (e.g., Whitmire and Karlstrom, 2007; Miall, 2019).

Diluvialists have argued for some time over the basal diluvial boundary. Hunter (2022) has argued that it is the 660-km mantle seismic discontinuity (aka the 660-km phase transition).

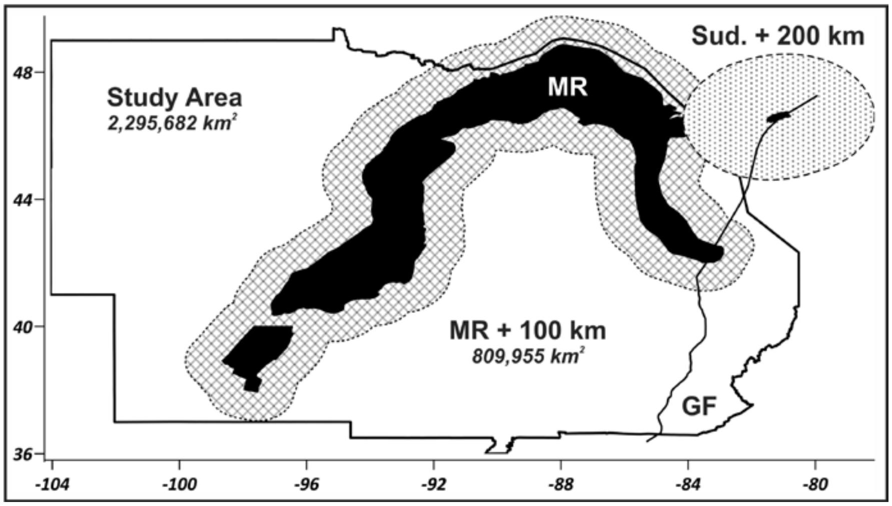

Figure 12. The relationship of the present Midcontinent Rift (black) to the present Sudbury Impact erosional remnant (also black). The Grenville Front (GF) also intersects the center of the Sudbury impact crater. A 200 km buffer of the Sudbury crater (stippled area) and a conservative 100 km buffer (hatched) of the Midcontinent Rift show the original impact zone would intersect with the eastern Lake Superior Basin part of the rift.

Others place it at various stratigraphic markers. Austin and Wise (1994), among others, believe that the basal diluvial boundary is just below the Precambrian/Cambrian contact in the Grand Canyon and well below the contact in the Mojave Desert. Dickens and Hutchinson (2021) place the lower diluvial boundary at the Mesoproterozoic/Neoproterozoic boundary. We suggest that most, if not all Precambrian sedimentary rocks are from the early Flood (Oard et al., 2023). Most today believe we must look past at least one cycle of plate tectonics (Snelling, 2009). But a common factor is the mantle's geological work during the Flood. The midcontinent rifts and their relationships to the large sedimentary basins provide an empirical test of these ideas.

What was the depth and nature of crustal erosion and tectonism at the beginning of the Flood? With regard to tectonism, CPT, HPT, and the Impact model (Oard, 2024) all picture an immediate catastrophic onset with upper-mantle involvement. Erosion is not specified. Perhaps it is more important to define criteria for setting a lower diluvial boundary. We suggest three Biblical ones: (1) an abrupt, clear, destructive signature in the rock record; (2) a significant and widespread erosional unconformity separating crystalline basement (which we assume to be antediluvian crust) from the sedimentary record; and (3) a global record of marine transgression and regression. Deeper crustal faulting, metamorphism, and intrusion are expected as a matter of course, but discovering those details is a forensic exercise, not a Biblical one.

For the central North American rifts described above, the first criterion certainly applies. The second is found at the Proterozoic/Phanerozoic unconformity outside of the Midcontinent Rift and East Continent Basin. Within those rifts, rapid sedimentation associated with the basalt flows certainly speaks to volcanism, erosion, and deposition at a scale achievable only during the Flood. The third is seen in the sedimentary sequence atop that unconformity, both outside and across the two rifts. Significant regional erosion is seen in the estimates of crustal removal from the nearby Sudbury impact crater, from the likely original size of the Midcontinent Rift, and in the ubiquitous presence of erosion of the surrounding crystalline basement, including erosional remnants in areas where sufficient well control exists to delineate them (Reed et al., 2024).

An Early Rifting Episode

The northern midcontinent of the United States is dominated by rifting (Figure 9). If gravity signatures farther south accurately outline rifts in Tennessee and Alabama (Stein et al., 2015), the area between the Appalachians and Rocky Mountains saw significant rifting prior to or coinciding with widespread post-rift marine sedimentation of the Flood Given the cross-cutting relationship with the crystalline basement, we speculate that the rifts in the subsurface are relicts of widespread and large-scale crustal disruption, probably marking the onset of the Flood. Most geologists attribute these rifts to plate tectonic episodes operating over millions of years. They are separated on the time scale by approximately a half-billion years. However, if rifting was an expression of crustal disruption during the early Flood, we would start with the assumption that all of the rifts are of similar ages, and that time is not the key factor in explaining differences in size, orientation, style, and fill. It is instead differences in local geological processes that must account for differences in size, orientation, style, and fill.

The Midcontinent Rift exhibits extensive vertical and lateral motion in its faults and the relative positions of its volcanics and sediments. Motion was initially extensional but the rift axis was inverted with compression afterwards, but prior to Flood post-rift marine sedimentation. This is more marked in the western arm of the rift than in the Lake Superior Basin. Reverse faulting occurred in the Lake Superior Basin, but its thicker sediments were preserved across the entire basin, not just in flanking and horst-top basins, as seen farther south. Little is known about the rift segment in Michigan.

What were the mechanics of rifting? On Earth's surface, the relationship between vertical motion and lateral separation or compression is geometrically equal to pi (ratio of circumference to radius). This is vastly complicated by the ability of rocks to deform locally by faulting or folding. Faulting may compensate for extension or compression, while folding will only accommodate compression. In general, compression of rocks results in relatively minor volume changes in the rock itself, and thermal expansion or contraction is of similar magnitude. However, mineral transformations at depth due to temperature or pressure changes can produce significant volume changes. For rough estimates such as described here, the ratio of pi is a good starting point. For every km of uplift, the crust will compensate by roughly 3 km of lateral separation, and the same for downwarping and compression. The Midcontinent Rift could have originally affected a region up to 500 km across, given the width of the present Lake Superior Basin and the estimate of Green et al. (1987) of its original extent.

Courtillot (1999) estimated 2 km of crustal uplift over a 1,000 km area prior to rifting. This is not enough to explain the lateral motion at the rift, which was estimated by Stein et al. (2015, their Figure 5) as 32 km at GLIMPCE Line A and 23 km at GLIMPCE Line C (both beneath Lake Superior). This would require a vertical uplift of nearly 10 km or another component of regional lateral motion. Rift dimensions are smaller in the southern arms (Figure 8), so the Lake Superior Basin probably represents the maximum disruption.

Basalt flooding was almost instantaneous with deformation (Reed, 2000) since the single largest constraint on the duration and volume of basalt emplacement is vent width. There was a smaller volume of basalt flows in the East Continent Basin and much less in the Reelfoot-Rough Creek-Rome complex. This may speak to crustal thickness or localized mantle activity. The volume of basalt in the rifts suggests an episode of severe decompression melting of the uppermost mantle. Basalt is concentrated in the rift axis, although it looks like a plateau basalt away from the center (Stein et al., 2015). There is also significant underplating of the crust along the rift (Reed, 2000).

Faults show that early extension was followed by compression, with up to 8 km of reverse motion (Reed, 2000) recorded at the major faults along the central basalt horst. So early Flood events included: crustal disruption with large normal faulting; flood basalt eruptions concentrated in a central axis; emplacement of intrusive bodies (e.g., the adjacent Duluth and Mellon complexes) with underplating of the crust at the rift axis; and then erosion and sedimentation, perhaps concurrent with the inversion of a solid horst. Reed (2000) argued that they were concurrent and that the relative volumes during the formation of the rift do not necessarily reflect changing sedimentation rates as much as they show rapid rifting and volcanism temporarily overwhelming erosion and sedimentation. This synchronicity, expected in the timeframe of the Flood, is evidenced by thin sediments beneath and between flows. Sedimentation continued well after, leaving up to 10 km in the Lake Superior Basin. Lower clastics were sourced from local erosion of volcanics and the surrounding granitic crust; later clastics appear to be sourced more from the granitic crust.

Differences and Similarities Between Rifts

The rifts in the study area share both similarities and differences. These include the northern rifts—the Midcontinent Rift and East Continent Basin—and the southern rifts—the Reelfoot Rift (or Mississippi Graben), the Rough Creek Graben, and the Rome Trough. In scale, the Midcontinent Rift dwarfs the others (Figure 7), both in size and depth. The orientations and stress vectors also vary. The Midcontinent Rift trends south/southwest in Kansas and arcs north/northeast to Lake Superior, where it bends under the lake, then pushes south through Michigan before turning southeast and terminating at either the Grenville Front or a little beyond. The Fort Wayne Rift parallels that segment. The East Continent Basin ranges roughly north-south. The Reelfoot Rift bends northeast at the southern boundary of the study area before curving east into the Rough Creek Graben. The Rome Trough runs east/northeast out of the study area, where it bends more north/northeast through West Virginia and Pennsylvania. These suggest a complex variety of lateral kinematic forces not easily explained. If these rifts formed concurrently, these differences are not easily explained by present models.

Uniformitarians attribute these differences to time. The Midcontinent Rift is dated at ~1.1 Ga, the East Continent Basin is thought to be approximately the same age, although the Middle Run litharenite has been dated at ~1.0 Ga (Moecher et al., 2018), leading them to see the East Continent Basin as a rift which evolved into a foreland basin dominated by Grenville thrusting. However, the Reelfoot-Rough Creek-

Rome rifts are dated as early Cambrian (Hickman, 2013). We think instead that the rifts are very similar in age.

The Lake Superior Basin shows two major types of sediment: (1) lithically and texturally immature volcanogenic clastics of the Oronto and Solor Church formations conformably overlying volcanic flows in the rift axis, and (2) more mature, more quartz-rich sediments of the Bayfield Group and Jacobsville Sandstone (and their equivalents) spreading out laterally. The Oronto Group reaches 5,500 m (18,044 ft.) in thickness and the nature of seismic reflectors suggests interbedded basalt flows and sediments at its base (Canon et al., 1989); there is not a profound erosional unconformity between them in the Lake Superior Basin. They are interpreted as having been deposited in alluvial fans and by braided streams. The relatively mature clastics of the Bayfield Group show more quartz and fewer volcanic clasts; these overlie the Oronto Group in the Lake Superior Basin and reach 5,000 m (16,404 ft.) in thickness. Both groups are unfossiliferous, with inversion of the volcanic horst occurring during Bayfield deposition along the original normal faults.

There is little data in Michigan but there are good descriptions of the flanking basin sediments in Iowa and Minnesota. The "red clastics" of Anderson (1990) are immature sandstones, siltstones, and shale. He divided them into a lower and upper unit, though they do not reflect the composition of the Lake Superior Basin sediments. In Kansas, similar sediments were called "arkose," "red clastics," and "granite wash" before Scott (1966) coined the term, "Rice Formation." These also appear unfossiliferous, and their base has not been penetrated. The Texaco Noel Poersch well encountered basalt flows over immature subarkose sediments, confirming reverse faulting there.

The East Continent Basin forms a shallower rift in western Ohio, eastern Indiana, and Kentucky. Drahovzal et al. (1992) posited a southern boundary into northern Tennessee. However, Moecher et al. (2018) terminated it at the Rough Creek Graben. Based on seismic data, Baranowski et al. (2009) extended the sedimentary basin west as far as Illinois. Basin fill, based on cores, drill samples, and geophysics is similar to the Midcontinent Rift, with bimodal volcanics dominated by continental flood basalts at its base and fewer felsic volcanics. These are overlain by unfossiliferous arkosic and lithic red-to-gray arenites of the Middle Run Formation. Cores and geophysics confirmed the presence of gabbro, flood basalt, felsic volcanics, and volcanic-to-feldspathic, lithic arenites (Shrake, 1991).

Based on radiometric dating of detrital zircons, Moecher et al. (2018) posit a two-stage basin formation: rifting as a southern extension of the Midcontinent Rift, followed by thrusting at the Grenville Front, resulting in a foreland basin receiving additional similar sediment from eroding orthogneissic basement, east of the Grenville Front. Drahovzal et al. (1992, p. 6) described the Middle Run Formation from the Ohio Geological Survey well No. 2627, which penetrated an 1800-foot (549 m) section of the Middle Run Formation, as "remarkably homogeneous, consisting of red to gray, fine- to medium-grained, thickly bedded lithic sandstones. It is estimated to contain less than 10 percent siltstones and shales." This reinforces the high-energy levels seen in sedimentation in the Lake Superior Basin. Those sediments are unconformably overlain by marine Cambrian Mount Simon sandstones.

The Fort Wayne Rift, a suspected northern extension of the East Continent Basin through northeast Indiana, and possibly extending as far as Lake Michigan, has been defined geophysically (Stein et al., 2018), but no wells have tested the extents of the rift, and we could find no description of its fill. Inference suggest basalts and sediments of the Middle Run Formation or its equivalent.

The southern rifts are distinct in their fill. Rifting coincides with sedimentation and much less basalt volcanism. Drahovzal (1997) described ultramafic intrusions which pointed to rifting. Hickman (2013) described the sedimentary sequence from the early Cambrian Reelfoot Arkose up through the Eau Claire Group, and the Knox Supergroup. By this point, the greatest thickness of rift sediment had been deposited, showing that these rifts were structurally most active early in the Flood. These were overlain by Lower Paleozoic strata through the Devonian New Albany Shale, and a few thousand feet of Mississippian through Permian sediment. The Gulf Coastal Plain extends up through western Kentucky with those strata onlapping over the rift fill.

Finally, if large-scale rifting represents a style of deformation associated with the onset of the Flood, then the rifts in the study area offer a problem for the geologic timescale. These rifts span 600 million years for uniformitarians, but would be, at most, forming within a few weeks of each other. If the relative dates of the chronostratigraphic time scale are accurate, then diluvialists need to explain why such similar features in the cratonic interior happened at such diverse times.

Erosion of the Basement

The basement in the northern study area was subjected to three episodes of erosion: (1) the top of the rift fill, (2) the late Flood regression after deposition of the Phanerozoic, marine sediments, and (3) the post-Flood, Ice Age glaciation. Basement erosional remnants in Minnesota and Wisconsin may reflect glaciation but the erosional remnants in Kansas, covered by thousands of feet of Flood sediments, show that erosion early in the Flood was significant.

Often, the identification of remnants is a function of well density. Contours are smooth in places where well control is sparse, but less so where well control is abundant. In the northern study area, this is especially seen in Minnesota and Wisconsin and on the Sioux Ridge (Reed et al., 2024). In the southern study area, it is seen most clearly in Kansas (see Figure A-4 in Part I). Cole (1976) mapped many pinnacles in the Kansas basement; some hundreds of feet high. It is hard to avoid the conclusion that these are erosional remnants from the early Flood, similar to those described by geomorphologists today that occurred during Late Flood regression (Oard, 2013).

Conclusion and Summary

If rifting across the study area occurred early in the Flood, then the scale of geological processes speaks to extremely high energy levels. One indicator of this energy would be the volume and distribution of the rift fill. We created a map of the base of the rifts in the study area and found that the sediment volume in the Midcontinent Rift alone was nearly half of that of the total Phanerozoic in the study area, even though the Midcontinent Rift occupies less than 13% of that area. An isopach map of the total diluvial rock record in the study area illustrates its importance and the significance of the other rifts and rift basins.

This mapping completes the necessary surfaces in the study area to define the volume and distribution of Ice Age and recent sediments, diluvial sediments deposited during and after the passage of the marine diluvial sediments, and diluvial sediments deposited as rift fill. As shown in Reed et al. (202x), marine diluvial sediments accumulated in cratonic basins, such as the Williston, Illinois, Michigan, Anadarko, and Appalachian Basins. But their volumes are easily exceeded by those of the rifts. The origin of the rifting is not known, but we find the congruence of the restored boundaries of the Midcontinent Rift and Sudbury Impact to be interesting and worthy of further investigation.

This paper summarizes a significant amount of regional data worth careful consideration by diluvialists. If the rifts represent the onset of the Flood, what mechanism(s) caused the rifting? Was the Midcontinent Rift related to the Sudbury impact? Is the estimated 5 km of erosion at Sudbury more widely applicable to the region? If so, what caused that erosion and where did the resulting sediment go? Why are the rift sedimentary basins different in the Lake Superior Basin and southern segments of the Midcontinent Rift? Why is the East Continent Basin more similar to the Lake Superior Basin than those southern limbs? Why were the southern rifts infilled by marine Phanerozoic sediments, as opposed to the Midcontinent Rift and East Continent Basin? How did the large cratonic basins, such as the Michigan, Williston, Illinois, and Anadarko form? What were their sediment sources and transport pathways? What volume of sediment and basalt was eroded from the Midcontinent Rift and East Continent Basin before the deposition of more widespread marine facies? With the volumes and distributions of the rift and basin fill presented in this study, diluvialists now have a more solid base of

Acknowledgments

We appreciate the help and professionalism of the state geological surveys, without which, the level of detail and accuracy of our mapping would have been impossible. Our maps exist as grids and shape files, and are available upon request (to the lead author) to creationist researchers.

References

Agena, W.F., M.W. Lee, D.R. Hutchinson, J.C. Behrendt, W.F. Cannon, and A.G. Green. 1988. 1986 GLIMPCE Seismic Reflection Survey Stacked Data. *USGS Open File Report 88–386*.

Allen, D.J., W.J. Hinze, A.B. Dickas, and M.G. Mudrey, Jr. 1997. Integrated geophysical modeling of the North American Midcontinent Rift System: New interpretations for western Lake Superior, northwestern Wisconsin, and eastern Minnesota. In Ojakangas, R.W., A.B. Dickas, and J.C. Green (editors). *Middle Proterozoic to Cambrian rifting, Central North America. GSA Special Paper 312*, pp. 47–72. Geological Society of America, Boulder, CO.

Anderson, R.R. 1990. The Amoco M.G. Eischeid #1 Deep Petroleum Test, Carroll County, Iowa—Preliminary investigations. *Iowa Geological Survey Special Report Series No. 2*.

Anderson, R.R. 1995. Structural configuration of the Precambrian surface of Iowa. *Iowa Geological Survey Open File Report 1995–2*.

Anderson, R.R. 2006. Geology of the Precambrian surface of Iowa and surrounding area. *Iowa Geological Survey Open File Map OFM-06–7*.

Austin, S.A., and K.P. Wise. 1994. The pre-Flood/Flood boundary: As defined in Grand Canyon, Arizona, and eastern Mojave Desert, California. In Walsh, R.E. (editor). *Proceedings of the Third International Conference on Creationism*, technical symposium sessions, pp. 37–47. Creation Science Fellowship, Pittsburgh, PA.

Bankey, V., et al. 2002. Digital data grids for the magnetic anomaly map of North America. *U.S. Geological Survey Open-File Report 02–414*. U.S. Geological Survey, Denver, CO.

Baranowski, M.T., S.L. Dean, J.L. Wicks, and V.M Brown. 2009. Unconformity-bounded seismic reflection sequences define Grenville-age rift system and foreland basins beneath the Phanerozoic in Ohio. *Geosphere* 5(2):140–151. DOI: 10.1130/GES00202.1.

Behrendt, J.C., A.G. Green, W.F. Cannon, D.R. Hutchinson, M.W. Lee, B. Milkereit, W.F. Agena, C. and Spencer. 1988. Crustal structure and deep rift basin of the Midcontinent Rift System—Results from GLIMPCE deep seismic reflection profile. *Geology* 16:81–85.

Berendsen, P. 1997. Tectonic evolution of the Midcontinent Rift system in Kansas. In Ojakangas, R.W., A.B. Dickas, and J.C. Green (editors). Middle Proterozoic to Cambrian rifting, Central North America. *GSA Special Paper 312*, pp. 235–241. Geological Society of America, Boulder, CO.

Berendsen, P., and K. Blair. 1996a. Structural configuration of the Precambrian basement. *Kansas Geological Survey Map M-45.1*.

Berendsen, P., and K. Blair. 1996b. Precambrian subcrop . *Kansas Geological Survey Map M-45.2*.

Berendsen, P., R.M. Borcherding, J. Doveton, L. Gerhard, K.D. Newell, D. Steeples, and W.L. Watney. 1988. Texaco Poersch #1, Washington County, Kansas—Preliminary geologic Report of the pre-Phanerozoic rocks. *Kansas Geological Survey Open File Report 88–22*.

Bickford, M.E., K.L. Harrower, R.L. Nusbaum, J.J. Thomas, and G.E. Nelson. 1979. Preliminary geologic map of the Precambrian basement rocks of Kansas. *Kansas Geological Survey Map M-9*.

Brown, L., L. Jensen, J. Oliver, S. Kaufman, and D. Steiner. 1982. Rift structure beneath the Michigan Basin from COCORP Profiling. *Geology* 10(12):645–649.

Burchett, R.R., and M.P. Carlson. 1986. Configuration of Precambrian surface in Nebraska. Nebraska Geological Survey, Lincoln, NE.

Cannon, W.F., A.G. Green, D.R. Hutchinson, M. Lee, B. Milkereit, J.C. Behrendt, H.C. Halls, J.C. Green, A. B. Dickas, G.B. Morey, R. Sutcliffe, and G. Spencer. 1989. The North American Midcontinent Rift beneath Lake Superior from GLIMPCE seismic reflection profile. *Tectonics* 8(2):305–332.

Cannon, W.F., M.W. Lee, W.J. Hinze, K.J. Schulz, A.G. Green. 1991. Deep crustal structure of the Precambrian basement beneath Northern Lake Michigan, midcontinent North America. *Geology* 19:207–210.

Chandler, V.W., P.L. McSwiggen, G.B. Morey, W.H. Hinze, and R.R. Anderson. 1989. Interpretation of seismic reflection, gravity, and magnetic data across Middle Proterozoic Mid-Continent Rift System, Northwestern Wisconsin, Eastern Minnesota, and Central Iowa. *AAPG Bulletin* 73(3):261–275.

Clarey, T. 2020. *Carved in Stone: Geological Evidence of the Worldwide Flood*. Institute for Creation Research, Dallas, TX.

Clay, J.M., D.P. Moecher, and J.R. Bowersox, 2021. Formation (Eastern North America Basement): Implications for Grenvillian foreland basin evolution and Midcontinent rifting. *Precambrian Research* 364(15). https://doi.org/10.1016/j.precamres.2021.106332.

Cole, V.B. 1976. Configuration of the top of Precambrian rocks in Kansas. *Kansas Geological Survey Map M-7*.

Coleman, J.L., Jr., and S.M. Cahan. 2012. Preliminary catalog of the sedimentary basins of the United States. *U.S. Geological Survey Open-File Report 2012–1111*, 27 p. (plus 4 figures and 1 table available as separate files). Available online at http://pubs.usgs.gov/of/2012/1111/.

Courtillot, V. 1999. *Evolutionary Catastrophes: The Science of Mass Extinction*. Cambridge University Press, New York, NY.

Csontos, R., R. Van Arsdale, R. Cox, and B. Waldron. 2008. Reelfoot Rift and its impact on Quaternary deformation in the Central Mississippi River valley. *Geosphere* 4(1):145–158.

Dart, R.L. 1995. Maps of Upper Mississippi Embayment Paleozoic and Precambrian Rocks. *USGS Miscellaneous Field Studies Map MF-2284*.

Dart, R.L., and H.S. Swolfs. 1998. Contour mapping of relic structures in the Precambrian basement of the Reelfoot Rift, North America Midcontinent. *Tectonics* 17(2):235–249.

Dickas, A.B., and M.G. Mudrey, Jr. 1997. The segmented nature of the Middle Proterozoic Midcontinent Rift System, North American. In Ojakangas, R.W., A.B. Dickas, and J.C. Green (editors). Middle Proterozoic to Cambrian Rifting, Central North America. *GSA Special Paper 312*, pp. 37–46. Geological Society of America, Boulder, CO.

Dickas, A.B., M.G. Mudrey, Jr., D.J. Allen, W.J. Hinze, P.A. Daniels, Jr., R.C. Burruss, J.G. Palacas, S.J. Uchytil, C.K. Stffensen, D.M. Jarvie, and R.G. Lindblom. 1999. Terra-Patrick #7–22 Deep Hydrocarbon Test, Bayfield County, Wisconsin: Investigations and Final Report. *Wisconsin Geological Survey Miscellaneous Paper 97–1*.

Dickens, H., and A. Hutchison. 2021. Geochemical and related evidence for early Noah's Flood Year. *Journal of Creation* 35(1):78–88.

Drahovzal, J.A. 1997. Proterozoic sequences and their implications for Precambrian and Cambrian geologic evolution of western Kentucky: Evidence from seismic-reflection data. *Seismological Research Letters* 68(4):553–566.

Drahovzal, J.A., D.C. Harris, L.H. Wickstrom, D. Walker, M.T. Baranowski, B. Keith, and L.C. Furer. 1992. The East Continent Rift Basin: A new discovery. *Ohio Geological Survey Information Circular 57*. Published by Kentucky Geological Survey, Lexington, KY. Also published as *Indiana Geological Survey Special Report 52* and *Kentucky Geological Survey Special Publication 18, Series XI.*

Drahovzal, J.H., and M.C. Noger. 1995. Preliminary map of the structure of the Precambrian surface in eastern Kentucky. *Kentucky Geological Survey Map and Chart Series 8*.

Fairchild, L.M., N.L. Swanson-Hysell, J. Ramezani, C.J. Sprain, and S.A. Bowring. 2017. The end of Midcontinent Rift magmatism and the paleogeography of Laurentia. *Lithosphere* 9(1):117–133.

Grauch, V.J.S., E.D. Anderson, S.J. Heller, E.K. Stewart, and L.G. Woodruff. 2020. Integrated geophysical analysis provides an alternate interpretation of the northern margin of the North American Midcontinent Rift System, Central Lake Superior. *Interpretation*. https://doi.org/10.1190/INT-2019–0262.1

Green, J.C., T.J. Bornhost, V.W. Chandler, M.G. Mudrey, Jr., P.R. Myers, L.J. Pesonen, and J.T. Wilbrand. 1987. Keweenawan dykes of the Lake Superior region: Evidence for evolution of the Middle Proterozoic Midcontinent Rift of North America. In Halls, H.C., and W.F. Fahrig (editors). *Mafic dyke swarms*. *Geological Association of Canada Special Paper 34*, pp. 289–302.

Halls, H.C. 1982. Crustal thickness in the Lake Superior region. In Wold, R.J., and W.J. Hinze (editors). *Geology and Tectonics of the Lake Superior Basin*. *GSA Memoir 156*, pp. 239–244. Geological Society of America, Boulder, CO.

Halls, H.C., and G.F. West. 1971. A seismic refraction survey in Lake Superior. *Canadian Journal of Earth Sciences* 8:610–630.

Hickman, J.C. 2011. *Structural evolution of an intracratonic rift system: Mississippi Valley Graben, Rough Creek Graben, and Rome Trough of Kentucky, USA*. University of Kentucky Doctoral Dissertation. https://uknowledge.uky.edu/gradschool_diss/144/. His plate 16 is PC Map 11.

Hickman, J.C. 2013. Rough Creek Graben Consortium Final Report. *Kentucky Geological Survey Contract Report 55, Series XII*.

Hinze, W.J., and V.W. Chandler. 2020. Reviewing the configuration and extent of the Midcontinent Rift System. *Precambrian Research* 342:105688.

Huber, M.S., E. Kovaleva, and U. Riller. 2020. Modeling the geochemical evolution of impact melts in terrestrial impact basins: Vredefort granophyre dikes and Sudbury offset dikes. *Meteoritics & Planetary Science* 55(10):2320–2337.

Hunter, M.J. 2022. The Precambrian: Globally correlated and all Flood-deposited. *Journal of Creation* 36(3):48–59.

Hutchinson, D.R., P. Morel-a-Huissier, H. Meyer, I. Asudeh, P. Ervin, Z. Hajnal, J. Karl, R. Mereu, R. Meyer, J. Sexton, C. Spencer, and A. Trehu. 1986. A Description of GLIMPCE, 1986, Large Offset Seismic Experiment from the Great Lakes. *USGS Open-file Report 88–431*.

Hutchinson, D.R., R.S. White, W.F. Cannon, and K.S. Schulz. 1990. Keweenaw hotspot: Geophysical evidence for a 1.1 Ga mantle plume beneath the MRS. *Journal of Geophysical Research* 95:10869–10884.

Jirsa, M.A., T.J. Boerboom, V.W. Chandler, John H. Mossler, A.C. Runkel, and D.R. Setterholm. 2011. Geologic Map of Minnesota Bedrock Geology. *Minnesota Geological Survey Map S-21*.

Kucks, R.P. 1999. Bouguer gravity anomaly data grid for the conterminous US. https://mrdata.usgs.gov/services/gravity?request=getcapabilities&service=WMS&version=1.3.0.

Luetgert, J.H., and R.P. Meyer. 1982. Structure of the western basin of Lake Superior from cross structure refraction profiles. *Geological Society of America Memoir 156*, pp. 245–255.

McGinnis, L.D., and M.G. Mudrey, Jr. 2003. Seismic reflection profiling and tectonic evolution of the Midcontinent Rift in Lake Superior. *Wisconsin Geological and Natural History Survey MP 91–2*.

Bedrock Geology of Michigan, 1987. Automated version, Michigan Department of Environmental Quality, Geological Survey Division. https://wmich.edu/sites/default/files/attachments/u263/2014/1987_Bedrock_Geology_Map.pdf.

Miller, J., S. Nicholson, R.M. Easton, E.M. Ripley, and J. Feinberg. 2013. The geology and mineral deposits of the 1.1 Ga Midcontinent Rift in the Lake Superior Region—An Overview. *USGS*. https://www.researchgate.net/publication/285968628_The_Geology_and_Mineral_Deposits_of_the_11Ga_Midcontinent_Rift_in_the_Lake_Superior_Region_-_An_Overview.

Moecher, D.P., J.R. Bowersox, and J.B. Hickman. 2018. Zircon U-Pb geochronology of two basement cores (Kentucky, USA): Implications for Late Mesoproterozoic sedimentation and tectonics in the eastern midcontinent. *Journal of Geology* 126:25–39.

Mudrey, Jr., M.G., B.A. Brown, and J.K. Greenberg. 1982. Bedrock geologic map of Wisconsin. University of Wisconsin *Extension Geological and Natural History Survey Map*.

Oard, M.J. (ebook). 2013. *Earth's Surface Shaped by Genesis Flood Runoff*. http://Michael.oards.net/GenesisFloodRunoff.htm.

Oard, M.J. (in preparation). An impact model or sub-model of the Flood.

Oard, M.J., J.K. Reed, and P. Klevberg. 2023. Suggested strategies for fitting Precambrian rocks into Biblical Earth history. *Creation Research Society Quarterly* 60(2):97–111.

Ojakangas, R.W., A.B. Dickas, and J.C. Green. 1997. Introduction: Middle Proterozoic to Cambrian rifting, central North America. In Ojakangas, R.W., A.B. Dickas, and J.C. Green (editors). Middle Proterozoic to Cambrian rifting, Central North America. *GSA Special Paper 312*, pp. 1–6. Geological Society of America. Boulder, CO.

Reed, J.K. 2000. *The North American Midcontinent Rift System: An Interpretation Within the Biblical Worldview*. CRS Books, Glendale, AZ.

Reed, J.K., M.J. Oard, and P. Klevberg. 2024. Mapping the Flood in the North American Midcontinent—Part I: Marine diluvial and Ice Age. *Creation Research Society Quarterly* 61(2):112–132.

Scott, R.W. 1966. New Precambrian(?) formation in Kansas. *American Association of Petroleum Geologists Bulletin* 50:380–384.

Senft, L.E., and S.T. Stewart. 2009. Dynamic fault weakening and the formation of large impact craters. *Earth and Planetary Science Letters* 287:471–482.

Serpa, L., T. Setzer, H. Farmer, L. Brown, J. Oliver, S. Kaufman, and J. Sharp. 1984. Structure of the southern Keweenawan Rift from COCORP surveys across the Midcontinent Geophysical Anomaly in Northeastern Kansas. *Tectonics* 3:367–384.

Shrake, D.L. 1991. The Middle Run Formation: A subsurface stratigraphic unit in southwestern Ohio. *Ohio Journal of Science* 91(1):49–55.

Sleep, N.H., and L.L. Sloss. 1978. A deep borehole in the Michigan Basin. *Journal of Geophysical Research* 45:125–154.

Snelling, A.A. 2009. *Earth's Catastrophic Past: Geology, Creation & the Flood*, Volumes 1 & 2. Institute for Creation Research, Dallas, TX.

Stein, C.A., J. Kley, S. Stein, D. Hindle, and G.R. Keller. 2015. North America's Midcontinent Rift: When rift met LIP. *Geosphere* 11(5):1607–1616. doi:10.1130/GES01183.1.

Stein, C.A., S. Stein, R. Elling, G.R. Keller, and J. Kley. 2018. Is the "Grenville Front" in the central United States really the Midcontinent Rift? *GSA Today* 28. doi: 10.1130/GSATG357.

Stein, S., et al. 2016. New insights into North America's Midcontinent Rift. *Eos* 97. https://doi.org/10.1029/2016EO056659.

Stein, S., C. Stein, R. Elling, J. Kley, R. Keller, M. Wysession, T. Rooney, A. Frederiksen, and R. Moucha. 2018. Insights from North America's failed Midcontinent Rift into the evolution of continental rifts and passive continental margins. *Tectonophysics* DOI: 10.1016/j.tecto.2018.07.021.

Whitmeyer, S.J., and K. Karlstrom. 2007. Tectonic model for the Proterozoic growth of North America. *Geosphere* 3(4):220, DOI: 10.1130/GES00055.1.

Woelke, T.S., and W.J. Hinze. 1991. Model of the Midcontinent Rift System in Kansas. *Geology* 19:277–280

Woelke, T.S., and W.J. Hinze. 2015. Midcontinent Rift System in Northeastern Kansas. *Kansas Geological Survey Bulletin 237*.

Woodruff, L.G., K.J. Schulz, S.W. Nicholson, and C.L. Dicken. 2021. Mineral deposits of the Mesoproterozoic Midcontinent Rift System in the Lake Superior region—Metallogeny of the prolifically mineralized Keweenawan LIP. *Large Igneous Provinces Commission LIP of the Month, February 2021*. http://www.largeigneousprovinces.org/21feb.

Zhu, T., and L. Brown. 1986. Consortium for continental reflection profiling Michigan surveys: Reprocessing and results. *Journal of Geophysical Research-Earth* 91:11477–11495.

Conference Reports

11th Annual CRS Conference Review

2024 CRS Conference Abstracts

The Creation Research Society held their 11th Annual Conference on July 25–27, 2024, at the Ark Encounter near Williamstown, KY.

It was the largest conference to date, with 210 in attendance. Workshops in the disciplines of astronomy, biology, education, and geology were held on the first day of the conference.

Ken Ham delivered the Henry Morris Memorial Lecture Friday evening, which was open to the general public as well as to attendees, and an optional field trip was also offered, led by Danny Faulkner.

Thirty research presentations were given on Friday and Saturday. The abstracts for these talks are listed below:

Steven Austin, Edmond Holroyd, Thomas Folks, Nathan Mogk, Joseph Austin, Peter Vanko

Shoreline Terraces Mark the Western Margin of Ancient Hopi Lake, Arizona

Terrace-like landforms are abundant at elevation 1750 m on the dipping Mogollon ramp structure of Kaibab Limestone 45 km ESE of Flagstaff, Arizona. Landforms were surveyed using photogrammetry combining tens of thousands of overlapping, low-altitude, aerial photos. The 25-square-km map produced is a 1.3-billion-pixel image with resolution expressed as ground surface distance (GSD) of 13.8 cm. Transects of landforms display phenomenal resolutions down to 3 cm GSD. Also, we explored the use of spectrographic analysis to distinguish rock types and elements of landforms, especially tufa-encrusted surfaces. Geologic structures and stratigraphy beneath landforms are well displayed on the dip-slope cross-section of the plunging syncline at Nate's Hill where landforms are inscribed upon the uppermost 6 m of the thin-bedded Harrisburg Limestone Member of Kaibab Formation. Aeolian soil, limestone gravel deposits and tufa encrustations were explored along another 130-m-long transect of landforms using ground penetrating radar (GPR) and sampling in shallow test pits (STP). Gravel appears to have been milled locally from the erosional scarp on the upslope side of the terrace, and deposited on the gravel-covered platform on the downslope side of the terrace. Tufa-encrusted surfaces on Harrisburg Limestone are thin (~2 cm) and resemble petrographically Lake Bonneville tufa of Utah. We interpret these landforms to be relict, transgressive shoreline terraces formed by rapid rise and abrupt disappearance of Pliocene Hopi Lake within Bidahochi Basin in northeastern Arizona and western New Mexico. We believe post-Flood spillover drainage of Hopi Lake at East Kaibab Monocline initiated rapid erosion in Grand Canyon.

Ralph Baeza

Interdisciplinary Arguments for God's Existence: A Challenge to Atheism

This article scrutinizes various arguments, claims, proofs, and evidence in favor of God's existence, drawing from classical natural philosophy, mathematics, physics, and engineering disciplines. Philosophical arguments spotlight cosmological and ontological perspectives from notable thinkers, including Aristotle, Thomas Aquinas, Descartes, and Geisler. Novel contributions include physics-based

Figure 1. Ken Ham delivering the Henry Morris Memorial Lecture.

arguments rooted in Hooke's Law, Einstein's General Theory of Relativity, and Cauchy's Law of Mechanics. The work also delves into Gödel's mathematical proof concerning God's existence. Moreover, a unique multi-objective design optimization process is introduced, which suggests that the emergence of a Pareto Frontier in multi-objective scenarios implies an external intelligence influencing the final design solution, given its constraints. It's essential to note that this article provides a select overview of arguments, not an exhaustive exploration. These philosophical insights, physics claims, mathematical proofs, and engineering evidence challenge atheistic stances. Collectively, they harmonize with historical cosmological and ontological reasonings from human history and Christendom, offering a comprehensive dissection of atheistic beliefs.

John Baumgardner

Physical Cause for the Megasequence Structure of the Fossil-Bearing Sediment Record during the Genesis Flood

Since in the 1960's data from the petroleum exploration community have revealed that the fossil-bearing sediment record displays a structure consisting of six massive sediment layer packages known as megasequences separated from one another by global-scale erosional unconformities. This talk offers an explanation for this structure in the framework of catastrophic plate tectonics (CPT). The explanation relates to a crucial aspect of that framework, namely, the imperative of rapid and extraordinary cooling of the newly forming ocean plates. In the CPT framework all the pre-Flood seafloor gets recycled into the mantle well before the continents reach their current locations. Without extra cooling of the newly forming ocean lithosphere, the runaway process would cease, and CPT would come to an abrupt halt. Since the first paper on CPT in 1986 it has been assumed that the enhanced cooling of the new oceanic lithosphere occurred at a steady and uniform rate. However, having this cooling instead occur in discrete episodes yields abrupt drops in global sea level and thereby provides a simple means for explaining the erosional unconformities. The new approach assumes episodes of cooling sufficient to cause a 700 m drop in average sea bottom height and produce the erosional unconformity observed at the base of each of the six megasequences. A final episode of cooling at the top of the sixth megasequence results in an additional 1,200 m of sea bottom drop, allowing the water that had covered the continent surfaces to drain rapidly back into the deepened ocean basins. The abrupt cooling event responsible for the Great Unconformity may well have been the trigger for CPT itself.

Kane Cariappa, Mark Horstemeyer, Stuart Burgess, Adriel Lau, Student Presentation

Why the Human Musculoskeletal System is an Optimal Design Engineering

We present a Creationeering® paradigm argument that illustrates the purposeful design of human body bones that distinguish the structure-function relationships of the upper and lower limbs. We conducted a comparative study of the mechanical stress-strain behavior of major skeletal bones in the upper and lower body because the design objectives of the upper and lower bodies are different. Our findings indicate that God's anatomical design is optimally suited to the various physiological functions of the human body. Because the compressive forces experienced by the lower body in standing, walking, running, and jumping conditions are greater than those in the upper body, our experimental data indicates that the lower body bones have greater compressive strength than the upper body bones. However, the bones of the upper body exhibit greater strength in tension when compared to the lower body bones. As such, each bone in the human body has a specific function in the body's overall performance, as intended by God. In contrast to evolutionary claims, which argue that monkeys evolved into humans, our analysis illustrates completely different structure-function relationships between monkeys and man. Evolutionists also argue that humans have bad designs. We counter these arguments in this presentation by demonstrating the efficacy and sophistication of the human skeletal design. We provide evidence supporting the superior functionality of these anatomical features. This approach underscores why the Creationeering® paradigm offers a more accurate and appreciative understanding of the human skeletal system's complexities and beauty as exhibited by the Fibonacci Sequence and Golden Ratio.

Robert Carter

Reassessing Human-Chimp Similarity

The evolutionary community is insistent that humans and chimpanzees are, genetically, highly similar. An accounting of the actual percent similarity, however, has been hard to come by. They require a high percent similarity because great differences cannot have accumulated since our claimed last common ancestor. Recently, they have pounced on the creationist claims that the similarity could be below 90%, carefully dissecting the methods of earlier work and pointing out any lapses or flaws (justified or not) they found. The situation has changed, however, with the recent publication of high-quality, full-length genomes for both species. Thus, a re-analysis is called for. To that end, custom Python programs were written to assess similarity, with extensive use of Blast (Basic Local Alignment Sequence Tool) to find 'seed' areas of high similarity. By extending to the left and right from those areas, basic statistics can be generated, like the range of lengths of perfect matches and the amount of DNA not shared between the species. Yes, there are many areas of extremely high similarity, but vast stretches of DNA that are not shared also exist. Two numbers are required here: the total percent similarity (~85%) and the similarity among shared sequences (~98%). Yet, since much of the difference can be accounted for in large steps (e.g., the insertion of long telomeric repeats), what is really needed is a third number: the number of mutational steps required. We are finally on the verge of being able to generate these statistics.

Matthew Cserhati

Baraminology of Cucurbitaceae Based on Chloroplast Genome Analysis

Chloroplast genome analysis represents a new area of molecular baraminology research, as plants are fairly underrepresented in this field. Analyzing the chloroplast genome is a good way of determining baraminic relationships between plant species due to its conserved nature. Chloroplasts are abundant in cells and are easy to isolate.

The chloroplast genomes for 30 Cucurbitaceae species and three outliers from Fagus and Lycopis were downloaded from the NCBI database and aligned using the MAFFT alignment tool. A sequence similarity matrix was created using the 'seqinr' package, and visualized using the 'heatmap' function in R. The Hopkins clustering statistic is 0.881, indicating very good clustering. Six putative cucurbit holobaramins were discovered: Gynostemma, Citrullus, Cucumis, Cucurbita, and a mixed group including Coccinia grandis, Hodgsonia macrocarpa, Lagenaria siceraria, Momordica charantia, Siraitia grosvernorii, and Trichosanthes kirilowii.

Previous hybridization data-based baraminology studies on Cucurbitaceae by Brophy et al. (2023) showed the holobaraminic status of Citrullus, Cucumis, and Cucurbita. They also unite several other cucurbit groups, including Sicyoeae, Bryonieae, and Momordiceae, based on their low genetic distance using the ITS regions of nuclear rRNA genes (Jobst et al., 1998). The upper boundary of this genetic distance is 0.142, which is the distance between Trichosanthes cucumerina and Momordica charantia, which hybridize with the same third species.

The present study supports previous findings on Cucurbitaceae based on hybridization, and discovered a new putative holobaramin, Gynostemma (jiaogulans). This is the second chloroplast genome-based baraminology study to date. Further plant groups could be analyzed based on chloroplast genome sequences.

Matthew Cserhati, David Cavanaugh

Machine Learning Tools for Baraminology

At present there exists only a small handful of online tools for analyzing baraminology data sets, such as the Molecular Baraminology Tool Suite and the Baraminology and Cluster Analysis tool. Machine learning (ML) refers to mathematical algorithms or procedures that identify groups within data. ML attempts to approximate humans' pattern recognition capabilities using computational methods. This is especially helpful if the data sets are either too large or too complex for humans to analyze (Greener et al., 2021).

ML tools have been used in DNA variant identification, protein structure prediction, and medical image classification. In the context of baraminology, ML tools could be

Figure 2. Conference attendees listening intently to the presentations.

used to classify a new unknown species into an existing baramin.

The present work has developed a website for doing just that. The Baraminology Machine Learning Tools (BMLT) website (https:// molbar.shinyapps.io/baraminology_machine_learning_tools) makes three ML tools available for users, including a Neural Network (NN), Support Vector Machine (SVM), and a Random Forest (RF). The user can upload a data matrix (a .csv file), with a list of species, morphological or molecular characters, and a classification scheme to classify a new species. Parameters specific to each of the three tools can also be set. The online tool produces output plots that are specific to each tool, such as a neural network plot, am SVM classification plot, and a Random Forest plot and a character importance plot. Furthermore, it also provides statistical results that describe the classification's accuracy.

Danny Faulkner

A New Theory for the Formation of Rock Bridge Arch in Red River Gorge of Eastern Kentucky

The formation of Rock Bridge, a true natural bridge in Eastern Kentucky's Red River Gorge, has been attributed to a remnant from a retreating waterfall. However, examination of the area around the arch reveals a normally dry U-shaped channel immediately to the west of the arch, suggesting that the this was the original stream, and that water cut through the rock to form the arch, leaving the abandoned U-shaped channel. I will discuss some difficulties with the current theory of Rock Bridge's formation, and I hope to share the results of a survey of the area in support of the new theory. This new formation theory for Rock Bridge has implications relevant to rapid, as opposed to gradual, formation of geological features. A further test of this proposal would be to drill or dig in either or both drainages to determine how deep bedrock is in the U-shaped channel. However, this would be expensive, and the National Forest Service may not approve such a research project in this protected part of Daniel Boone National Forest. Rock Bridge will be the second stop on the optional field trip after the Creation Research Society meeting concludes, so participants on the field trip can see the evidence for this proposal for themselves.

Gabriela Haynes, Joel Leineweber

Most Maniraptor Anatomy Shows Avian Form and Function

The idea of feathered dinosaurs has been popularized since the 1990s. This hypothesis relies on an evolutionary worldview that connects dinosaurs and birds. It is biblically understood that dinosaurs and birds are different kinds, created on different days of creation. However, several groups of animals, mostly classified as dinosaurs, such as oviraptorids, dromaeosaurs, troodontids, scansoriopterygids, and alvarezsaurids, include some genera that show evidence of avian features. The list of the features includes pennaceous feathers, an avian hand with a swivel wrist (semilunate bone present), lateral facing glenoid, a rectangular coracoid oriented at an angle to the scapula, occluded acetabulum, rear-facing pubic bones, low vertebrae caudal counts, pygostyle with varying types of fusion, absent femoral fourth trochanter, pre- and post-patagia, and more. The presence of those features in those groups was analyzed based on evolutionist reconstructions, secular Cladistics datasets, and a literature review. The distribution of these characteristics is discussed and visually demonstrated, highlighting that the reconstruction of these animals often displays them as transitional-like forms between dinosaurs and birds, not accounting for these avian features. Even though some scientists argue that accepting the feathered dinosaur's idea does not require believing in evolution, it is demonstrated that it is not reasonable to relate to this idea without relying on an evolutionary worldview.

Robert Hill

Bipolar Flows and Angular Momentum Transfer

"Creationist critiques of star formation in almost all instances use an outdated version of star formation. Critiquing an out of date model is not helpful to the creationist cause. A common creationist critique of evolutionary star formation models involves the conservation of angular momentum. Creationists point out that the angular momentum of the planets exceeds the angular momentum of the sun. That fact is then used to critique evolutionary star formation models.

The current evolutionary models of star formation have suggested mechanisms to shed angular momentum via bipolar flows. Doppler measurements of bipolar flows show that these flows are rotating. Therefore, they are transferring angular momentum away from the so called 'protostars.' The evidence for this angular momentum transferred is reviewed and evaluated.

This presentation will present an accurate presentation of the current evolutionary model of star formation that involves bipolar flows. Suggestions for creationist research involving angular momentum transfer will be discussed."

Kevin Horton

Aerial Videographic Survey of Geomorphological Structures Left Behind by the Glacial Lake Missoula Flood—Part 1 of 2

Oard suggested that the Glacial Lake Missoula Flood could be used as a model for understanding some of the geomorphological structures that massive flooding would produce thereby giving us a small-scale model for the Genesis Flood. In this 4-year study, the author collected extensive drone video captures of the topography of the Scablands of Washington state defining the common structures that massive flooding produced. These common structures were then collated, and standard findings were classified according to their common geomorphological shapes (topographic features.) This required extensive review of footage and multiple trips throughout Washington state for re-filming structures that needed refined examination. The relevant footage was then edited into short videos with instructional arrows and markers to aid in presentation. These videos had to be reduced to 1080p and a specialized laptop was required to handle the extensive video data. This study produced some dramatic footage of how floods change the landscape and give us standard geomorphological shapes that can easily be identified elsewhere in previously flooded landscape. These standardized findings will be compared to structures in 7 western states (part 2) resulting in profound evidence of the worldwide Genesis Flood. This section of the study will train the eyes of the audience to recognize the extensive Genesis Flood Evidence that is visible in plain sight.

Kevin Horton

Aerial Videographic Survey of Geomorphological Structures Left Behind by the Worldwide Genesis Flood—Part 2 of 2

In this second part of the study, the author captured many views, some of which that are inaccessible by terrestrial handheld photographic techniques, across multiple states demonstrating the same structures as identified in part one (The Glacial Lake Missoula Flood) but often on an even larger scale than seen in part 1. The findings were then collated according to common shapes that were previously identified and then edited for presentation. These clips provide visually stunning evidence of the massive flood-caused erosion from the receding phase of the Genesis Flood. Google Earth was also used to further the investigation by confirming the presence of structures visible from satellite images. A new model was developed for the formation of the Badlands of SD and the Sandhills of NE as the result of eddy formation due to the Black Hills of SD obstructing the flow off the rising Rocky Mountains. The author also discovered kolk lake (pothole lakes) evidence on the top of 700' mesas in Utah. This study also gives further evidence of how eddies led to arch and cone formations. Many people today are persuaded that the Genesis Flood is not to be taken literally. This study found abundant visual evidence of the massive runoff erosion as the Rocky Mountains rose out of the oceans. The primary intent of these presentations is to encourage the audience to fully trust the inspired Bible as written.

Marshall Jordan

A Biblical Radiocarbon Chronology for Dynastic Egypt

Secular radiocarbon dating supports a chronology of dynastic Egypt incompatible with the record of Genesis because it places the start of the Old Kingdom before the accepted Flood date of 2518 BC. This is from the faulty uniformitarian assumption that atmospheric C14 before 1000 BC was like that of today. But radiocarbon dating has been calibrated to a biblical timescale using the C14 content of coals as a proxy for atmospheric C14 levels at the time of the Flood. Here, the standard Egyptian radiocarbon-based chronology is recalibrated to this biblical timescale, compressing dynastic Egypt into the 2nd millennium BC. The resulting dated king list shows an overlap of dynasties due to concurrent sets (ranges) of C14 measurements. By this analysis, Joseph became a vizier near the start of the Old Kingdom before Djoser built the first great pyramid. Several assumptions make this biblical radiocarbon chronology uncertain. Both the Flood date and the beginning of Israel's sojourn in Egypt (1875 BC) are based on the Masoretic text. The recalibrated radiocarbon measurements are average, with large standard deviations, of those used for the construction of the secular chronology. Samples for radiocarbon measurement were taken from funerary contexts signifying dates of death, thus requiring the king's accession date to be calculated from the secular estimates of reign lengths. Given these assumptions and uncertainties, biblical radiocarbon dating should be considered ancillary to archaeological science, historiography, and biblical scholarship. Radiocarbon dating must be interpreted according to the Bible, the only inerrant historical record.

Marshall Jordan

Evidence for Patriarchal Drive on Iceman's Y Chromosome

The antediluvian longevity exhibited by Noah and his sons declined, according to the biblical record, in an exponential decay down to today's lifespan. Because older fathers pass on more mutations to their sons than younger fathers, a process known as "patriarchal drive," most mutations found on Y chromosomes today may have been added in the first few centuries after the Flood due to patriarchal drive. The recent publication of a high-coverage sequence of Otzi the Iceman's Y chromosome allows the rate of mutation accumulation to be tested by comparing Otzi's Y chromosome sequence to moderns in the same G2 haplogroup obtained from the dataset of Karmin et al. 2015. The mutations are single nucleotide differences from Noah's Y chromosome sequence as defined by Jeanson. Although Otzi lived in the late 19th century BC, the number of mutations on his Y chromosome is three-quarters of the total found on G2 haplogroup Y chromosomes today. This analysis gives evidence for patriarchal drive rather than the molecular clock hypothesis for determining the age of Y chromosome mutations. A computer simulation of artificial Y lineages descending from Noah shows Otzi's Y chromosome mutations occurring in 6 generations due to patriarchal drive. This model suggests that the remaining mutations on G2 haplogroup Y chromosomes have accumulated at a low rate of one every 5 generations over the past several thousands of years. Additional evidence for post-Flood patriarchal drive mutations awaits more high-coverage sequencing of ancient Y chromosomes.

Hannah Klein

The Role of Natural Law in Creation Week, and Implications for Astronomy

This presentation will investigate the relationship of natural process to the events of Creation Week, focusing on implications for creation astronomy and cosmology. Creationist thinking on the topic falls on a spectrum ranging from a strict emphasis on divine fiat, to recent literature emphasizing natural process and the scientific comprehensibility of Creation Week. Biblical and physical clues point to a middle-of-the-road approach, in which natural process are involved in Creation Week alongside acts of divine fiat. Specifically, the laws governing created entities were set in place simultaneously with the creation of those entities, and had a role in the rest of Creation Week processes. Central to this discussion is the distinction between God's creative and sustaining work. Just as there are clear examples of God's creative hand at work in the post-Creation Week world, it appears that God's sustaining hand was at work during the Creation Week. Literature from the creation geology community is reviewed for their perspectives on natural processes' relationship to Creation Week, and those perspectives are used to frame suggestions for the field of creation astronomy. The relationship of natural processes to Creation Week has implications for creationist understanding of stellar formation, stellar evolution, and evidence of astronomical processes.

Zachary Klein

The 38th Parallel Structures: Insights & Implications for Flood Geology

In the Midwest region of the United States, a series of enigmatic circular structures lie along the 38th Parallel for a span of more than 400 miles. Alternatively explained as cryptovolcanic structures or impact craters, the peculiar alignment of these structures has raised questions of their relationship and origin, especially following the 1994 Shoemaker-Levy 9 serial impact into Jupiter. Some geologists have proposed that a serial impact may be responsible for the arrangement of the 38th Parallel Structures. A challenge to this explanation is the varying stratigraphic levels of deformation within each structure, which range from the Late Cambrian to somewhere above the Permian. To date, three of the structures (all in the state of Missouri) have been confirmed to be impact craters: The Weaubleau Structure, the Decaturville Crater, and the Crooked Creek Crater. Of these, the Weaubleau is believed to be the oldest, the Decaturville the youngest, while the relative age of Crooked Creek is uncertain. Most Young Earth Creationists would assign all of these stratigraphic levels to the time of the Genesis Flood. From a Young Earth Creationist standpoint, the possibility of impact series that transgresses multiple geologic ages is an intriguing possibility, one that may offer useful insights into the nature and origin of the lithostratigraphic column, as well as a look into the role that impacts may have played in Flood sedimentation.

Tim Lewis, John Baumgardner

FEA Analysis of the Mechanics of the Tsunami Generation Process during the Genesis Flood

Within the framework of catastrophic plate tectonics, large tsunamis are a likely mechanism for producing both the fossil-bearing sediments of the Flood rock record and the many flat-topped seamounts in the world's oceans today. The focus of this research is to model the behavior of an overriding slab in response to a rapidly subducting plate with the aim of understanding in more detail the tsunami generation process. Key to this process is the locking and unlocking of the overriding and subducting slabs. The unlocking results in the rapid rise of the sea bottom and generation of a tsunami. Several key questions arise in this context that the model seeks to answer. What is the character of the friction for the plates to be locked sufficiently long to produce large tsunamis? What sort of stresses occur to keep the slabs locked together? How rapidly can the deformed overriding slab relax mechanically from its deformed shape? When the overriding slab undergoes strain, is the plastic portion of the strain sufficiently small to allow large numbers of repeated cycles? To address these questions in a quantitative manner, we apply the finite element code Ansys. Preliminary results show the relaxation time is sufficiently short and the plastic strain is sufficiently small to allow for large numbers of cycles.

Nate Loper

Post-Flood Formation for Grand Canyon as Evidenced by Geological and Paleoecological Data of the Lacustrine Bidahochi Formation in Northeastern Arizona

The geological community describes the Bidahochi Formation in Northeastern Arizona as a freshwater lacustrine sedimentary deposit from Hopi Lake (sometimes referred to as Lake Bidahochi). This formation is replete with abundant fossil flora and fauna ranging from the Neogene to the present. Fossils including freshwater lotic and lentic species, avian waterfowl bones and trackways, and preserved ice crystal casts are found within the confines and peripheries of Hopi Lake. The presence of the Bidahochi Formation at elevations far above the present Little Colorado River Gorge drainage provides data indicating it could not have been deposited in the Bidahochi Basin of the Little Colorado River if the Noachan Flood recession previously carved Grand Canyon. Rather, the presence of Hopi Lake within this basin must have existed for some time after the Noachan Flood to accumulate the lakebed formation and associated fossils. The Hopi Buttes Volcanic Field contains phreatomagmatic, Surtseyan, and other hydrovolcanic features that erupted through the Bidahochi Formation and into existing water, as we document by the presence of pillow lavas and columnar-jointed basalt caps. Our field studies of the upper Bidahochi Formation sediment data indicate it was deposited by a dramatic increase in freshet waters and fluvial sediment transport from the Upper Colorado River Basin subsequently draining into the Bidahochi Basin—creating an expansive lake system that preceded incursion across the Kaibab Plateau and rapid incision of the Grand Canyon through a breached dam mechanism.

Nate Loper

The Egyptian King Narmer Identified as the Biblical Nimrod

The biblical identification of Nimrod has perplexed historians and archaeologists alike in striving to identify him in the archaeological record. Similarly enigmatic, is the sudden arrival of written language, culture, and military might during the Early Dynastic Period in Ancient Egypt without precursory cultural development demonstrating an inherent source within existing Egyptian culture. This has led various Egyptologists, including the father of modern archeology, Flinders Petrie, to develop hypotheses such as the Dynastic Race Theory—speculating the arrival of a foreign group of people from Mesopotamia into Egypt, subsequently unifying both Upper and Lower Egypt, and establishing the Egyptian First Dynasty. Tradition states Nimrod was the builder of the Tower of Babel. If true, the downfall of Mesopotamian society following the Tower of Babel event would likely have seen Nimrod driven from his homeland and ruling leadership over the cities he established. Our studies for the past 10 years in Egypt and leading museums around the world find supporting evidence for linking the biblical Nimrod to the Egyptian king Narmer and his subjugation of the native Egyptian population, including the Badarian and Naqada I–II cultures likely descended from Mizraim. The evidence for this association comes from various biblical, etymological, and archaeological sources. What was the fate of the biblical Nimrod, and where did the inexplicable sudden rise of Dynastic Egypt come from? We see a correlation between Nimrod and Narmer that answers both of these questions.

Emerson Thomas McMullen

Mega Sheet and Channeled Flow: Formation of the Continental Shelf and Submarine Canyon Offshore Ventura, CA

During Noah's flood, Earth's crust may have broken into tectonic plates that eventually collided. If so, then the continents started to rise above the floodwaters. This caused a broad, wide, mega-sheet flow of the receding floodwaters over the relatively smooth land.

As the tectonic plates continued to collide, this forced mountains higher. The retreating floodwaters formed into channels, making creeks, rivers, and mega waterways. Rivers and mega waterways shaped both submarine and land canyons.

This paper presents scientific observations and data about the transverse mountains of the Santa Clara River watershed, the continental shelf offshore Ventura, and Hueneme Canyon. Analysis reveals how the watershed, river, continental shelf, and submarine canyon could and could not have formed.

Mega sheet flow from a catastrophic flood like Noah's is the best explanation for forming the continental shelf offshore Ventura. This shelf is too long and too continuous for uniformitarian dogma and its associated assumptions to properly explain.

The rising transverse mountains channeled floodwaters into a mega waterway that ran through Port Hueneme. From there it quickly and easily cut through the newly formed continental shelf, carving out Hueneme Canyon and generating its delta. This submarine canyon is too deep and its walls are too steep for gradualist explanations.

Noah Nicklas, Nathaniel Jeanson Student Presentation

Analysis of Middle Eastern Genetic Lineages Through the Y-Chromosome

The aim of this project is to begin cataloguing and searching for distinguishable events in history that might isolate an identifiable people group in the Middle East to establish a biblical timeline of middle eastern genetic origins. Haplogroup data collected from genetic databases already had global location and evolutionary time points of when divisions may have occurred between haplogroups. Conversion factors for the rate of mutational change were derived using modern mutation rates to derive haplogroup formation dates from a young earth perspective. The frequency of a haplogroup was determined by dividing the number of individuals in a haplogroup specific to a country by the number of total testers in that haplogroup. This ratio was then used to plot the relative frequencies of the haplogroups per country at a specific time to determine when and where haplogroups were to see migration patterns. Splits in haplogroup branches are assumed to be either population expansions or migrations and correlating evidence is sought after in frequency plots. The results of this study began to map out specific lineages of Arabs and Africans. It also gives a possible ancestry of Arabic descent to Somalis, rather than African. This information provides increasing data for tracing mankind's lineage back to Noah and his three sons.

Mike Oard

When Was the Belt Supergroup Deposited in Biblical History

The Belt Supergroup is located in the northwest United States and adjacent Canada. It covers an area of 197,000 km^2. It is slightly metamorphosed forming quartzite and argillite. Based on folds, the greatest depth at present is 20 km, a minimum depth for the original Belt basin. The Belt Supergroup is divided into four groups and 25 formations, but it is difficult to correlate strata across the basin. Some geologists early on thought the Belt basin was a filled-in impact crater. The Belt Supergroup has several unusual, unexplained features such as molar-tooth structures, found only in the Precambrian, and abundant syneresis cracks and ripple marks. It also has "stromatolites," raindrop imprints, and dolomite that requires hot temperatures to form. Paleocurrent indicators show the sediments came mostly from the west. Conventional scientists date it as early Mesoproterozoic, 1,470–1,400 Ma, based on U-Pb dating. There are three options for its placement within Biblical earth history: (1) Creation Week, (2) between Creation and the Flood, and (3) early in the Flood. After several reconnaissance trips, I have come to believe that the Belt Supergroup was deposited early in the Flood. This is based on the mostly conformable contacts between the Belt Supergroup and the overlying Cambrian Flathead Sandstone, which most creation scientists believe was deposited during the Flood. An early Flood placement for the Belt Supergroup has significant implications for a Flood model.

Michael Oard, John Reed, Peter Klevberg

The Flood Sediments Research Project

An important constraint on Flood models is the global distribution and volume of Flood sediments. Projects of that scale tend to obscure important detail, which is why we have developed a state-by-state GIS method. We map a basal diluvial surface, which can often be differenced from a DEM to generate isopach maps and volumes of sediments. Mapping is the heart of geology and our grids are offered to creationist researchers. The volume and distribution of sediments constrains ideas concerning erosion, deposition, source areas, and timing. The NOAA GlobSed project provides oceanic data. For example, continental margin volumes suggest erosion of nearly 2,000 m from North America during the Recessive Stage of the Flood. With more precise mapping, more accurate estimates can be made. Also, we have submitted an original map of the base of the Midcontinent Rift, showing the power of the Flood's earliest stages. Eventually, we will have detailed maps of the pre-Flood boundary for much of North America and our work can be replicated on other continents. We work at the state level, since state surveys often have detailed maps prepared by local experts and provide access to basic data. States vary: in the midcontinent, control in Iowa is dictated by fifty wells; in Minnesota, by over sixty thousand. Our work yields basic, yet necessary, constraints for global Flood models, as well as uncovering local and regional puzzles for research and publication.

Sarah Petersen, John Baumgardner

Terra3D Models Provide Insights into Catastrophic Plate Tectonics and Western North American Tectonics

A significant challenge for the secular earth science community has been accounting for the major tectonic changes in western North America since the mid-Cretaceous part of the rock record. These changes include the formation of the Western Interior Seaway, involving depression of a large swath of western North America, up to a km in depth and 1,000 km in width, extending from the Arctic Ocean in the north to the Gulf of Mexico in the south. This region subsequently rose, the seaway disappeared, and the Colorado Plateau and Great Plains regions rose by more than a km and the Rocky Mountain region by several. We apply the geodynamics code Terra to gain insight into processes responsible for these dramatic changes in the context of catastrophic plate tectonics and the Genesis Flood. The Terra calculations show clearly that the surface of western North America is drawn sharply downward as North America migrates westward over the subduction zone where the eastward moving Farallon plate is plunging into the mantle. We will show how Terra readily accounts for the Western Interior Seaway. We are currently working to improve Terra's ability to resolve the layer of continental crust at the earth's surface to be able understand how the interactions between the westward-moving North

American plate and the eastward-moving Farallon plate left behind a zone of thickened continental crust that then rose isostatically to form the Rocky Mountains.

John Rajca

Elucidating Pre-Flood Atmospheres using Living Flora and Fauna

The fossil record contains several species that seem to be nearly identical to present day organisms in every way except size and/or growth rate. The literature suggests one of the reasons for the larger size in the past for dragonflies, for instance, was that the atmosphere had considerably higher levels of CO^2. As a standard practice, some greenhouses artificially raise the level of CO^2 in order to make plants grow faster and larger. Also, the increasing atmospheric CO^2 within the last few decades seems to be responsible for a remarkable increase of plant growth worldwide. The literature seems to in indicate that the present CO^2 in the atmosphere is very low relative to levels in the fossil record. Based on these findings, it is that proposed that, simulating different atmospheric conditions, such as different concentrations of CO^2, in controlled environments, using organisms which have exhibited increased size in the fossil record (e.g., dragonflies, tree ferns and Equisetum) would perhaps lead to a more focused understanding the pre-flood atmosphere. There are other atmospheric gases and perhaps a higher atmospheric pressure that could contribute to this phenomenon. Several different facilities could run similar experiments with various parameters to compare and expedite results.

Harry Sanders

A Model of the Founder Effect and Post-Flood Dispersal in Ark Kinds

In the aftermath of the flood, the animals emerged from the Ark and had to repopulate the world. Depending on the kind and the translation, two, seven, or fourteen of each kind represented a founding population. Each of these kinds had gone through a bottleneck and represented a case of the founder effect. As the founding populations grew and spread out, they diversified and formed new populations and species. To simulate this process, a preliminary model was developed in Python called Founder Effect, Diversification, and Dispersal (FEDD), including selection, genetic drift, assortative mating, migration, mutation, and other important factors. This model can track the changes in a kind's population, and its diversification can be predicted. 100 simulations were run using a long-living slow-reproducing kind as one model and a short-lived, fast-reproducing kind as the second. Based on this model, it is theoretically possible to model the dispersal and diversification of any of the Ark Kinds after the Ark landed, provided certain variables are known. However, the model is still preliminary and will need fine-tuning to align more closely with the biological world.

Harry Sanders, Brian Thomas

An Initial Analysis of the Biochemistry of "Dinofuzz"

Descriptions of supposedly feathered dinosaurs have increased exponentially in recent years. Interest has correspondingly increased in the molecular content of "dinofuzz," the ambiguous material often found surrounding feathered dinosaur skeletons. Some have called this fuzz either feathers or proto-feathers due to the presence of beta-keratin and melanosomes in them. The claims about the material being either feathers or proto-feathers have been widely accepted, even within creationist circles. However, there are reasons to doubt the prevailing narrative. Those reasons have caused some evolutionary researchers to contest the feather claim, preferring to simply call them dino-fuzz or collagen fibers. There have been few studies on the protein structure of the dino-fuzz, nor the melanosomes found in the structures, and none from a creationist perspective. This study reviews those studies with emphasis on the underlying biochemistry. We conclude that, while existing evidence surrounding dino-fuzz is consistent with what would be expected of decayed skin fragments, much more biochemical analysis is needed to confirm this hypothesis.

Carissa Shipman

Pioneering Molecular Paleontology: Visualizing and Sequencing Dinosaur DNA

Knowing that secular scientists have isolated soft-tissue from dinosaurs, it is abundantly obvious DNA can also be isolated. A few recent secular publications have upset their own notion of 'millions of years' through the successful visualization of dinosaur nuclear DNA. Therefore, it is only a matter of time before someone sequences the first dinosaur genome. To pioneer molecular paleontology, we propose to be the first to pursue the following research aims: 1. Visualize nuclear DNA in dinosaur chondrocytes and osteocytes using propidium iodide and DAPI from multiple, well-characterized, accessioned fossils. 2. Stain mitochondria in dinosaur cells using the JC-1 mitochondrial fluorescent probe 3. Sequence nuclear and mitochondrial DNA of dinosaur chondrocytes and osteocytes using Next Generation Sequencing from the highest quality fossils identified in specific aims 1 and 2 4. The mitochondrial and nuclear DNA sequences obtained would be compared to many taxonomic groups, including birds, to determine which group dinosaurs are most similar to genetically or if they are altogether dissimilar to extant taxa. 5. Visualize nuclear DNA from different cells of various dinosaur and non-dinosaur fossils obtained throughout the geologic column, thereby eliminating the argument that DNA can survive deep time. If successful, this novel research would be a world first for biblical creation science. Our results will provide further strong evidence for the creation model of earth's history: recent creation followed by a cataclysmic worldwide flood which laid down the fossils in a short (1 year) timeframe. To complete this paradigm-shifting research, significant funds are needed.

Letters to the Editor

Structure of the Cosmos

Dear Editor,

Michael A. Harbin’s article, “Has God Said?,” in the Summer 2024 issue of *CRSQ*, describes the philosophical ins and outs of developing a proper hermeneutic for Genesis 1:1–2:3. He says much about the nature of miracles that might apply to the question of age and the days of Creation. It is the linguistic part of his discussion, *vis-a-vis* the physical possibilities on Creation Days One and Two, that come into focus. While God does not command us to make up scientific theories to explain the “missing details” of Genesis 1, many readers of *CRSQ* probably do just that. The writer is satisfied with the “how” part: “He spoke...and it was.’’ The “what” that was involved is that which seems most interesting; because most of the speculations about the missing details are based on presuppositions that are probably not true at all. Harbin’s tone exhibits a blessed open-mindedness that one should follow up with positive suggestions. Our only requirements are that whatever one cooks up in the way of physical science must be allowed by Scripture and not conjectured by special pleading.

Harbin *really* hits the nail on the head when he says, ”The basic problem that tends to be overlooked is that when one looks at an event and attempts to describe a process which led up to the situation at hand, any number of possible processes may be given, some more feasible than others—with feasibility determined by one’s world view.” Indeed, the writer argued just this point with a physicist propounding an alternate theory of cosmology, based on a mathematical model of “dark matter” he constructed and worked out carefully at great length on his own, and published in a long series of papers. He made many good arguments defending his model. Since it is a mathematical model, the criticism (besides rejecting Scripture and scientific facts) was from the Lowenheim-Skolem Corollary, which may be summarized in layman’s terms: There may be a great many, or even an infinite number of ways to skin a complicated creature like a cat. But as there is only *one* cat, it can only be skinned *once* in *one* way. So much for mathematical models without a *physical model* that agrees with observation and experiment.

Let’s begin with Harbin’s statement, “God spoke and it existed in a fully functioning completed state. However, that completed state was not static, but one which was highly dynamic from the beginning.” Now, imagine that God first creates the electromagnetic field pervading all of space, *along with* the basic laws governing electrodynamics that make the field work. The metric of space is defined by these laws and the speed of propagation of electromagnetic waves in the medium of the field, *c*. Note: Hebrew scholars allow “fluid” as alternative to “water” in translation.

Next, God stirs up the field, creating “light,” which is then *divided* from the darkness. One way to separate light from “darkness” requires something to *absorb* the light, what we call *matter*, which will be formed out of the excited medium. Hebrew scholars roughly allow “unformed substance out of which physical structures could be formed” as an alternative to “earth” in translation. An alternative translation of Genesis 1:4 is given as, “...divided *between* the light and *between* the darkness.” One could also interpret separation in a different sense: removing light sources from each other or removing oneself by such great distance from the source that the amount of ambient light isn’t sufficient to see one’s hand in front of one’s face. In Genesis 1:5, God called the *light* “Day,” and the *darkness*, “Night.” It had nothing to do with time, just light or the absence thereof. Because we live on a rotating Earth and have the sun and moon and stars to declare time, our notion of day and night is always intimately associated with time, and the rotation of Earth. Imagine one is floating out in space. In one direction he sees bright light, in the opposite direction, darkness. Isn’t he going to say “day” is over there where the light is; and night is over there where it’s dark? Perhaps we could better interpret this verse of Scripture if we were Eskimos, living at the North Pole. Joe Eskimo comes out of his igloo, sees bright light and declares, “Oh! It must be day.” But the day never ends (for 6 mos.), even though 24-hour periods keep going by; because, light = day. Our language and everyday experience can cause us to approach Biblical interpretation with unacknowledged presuppositions, which could lead us astray. It is not time that makes it day or night.

If these latter ideas are more relevant than light being absorbed by matter, it follows naturally into the action of Day Two, where matter is divided from matter by an *expansion*, as one Hebrew translation puts it. John 1:5 may give a further hint with a translation that says the darkness could not *overcome* the light. All the darkness can do with light is *flee* from it. These words we are trying to translate clearly have meaning depending on context; and in both Genesis 1:6–8 and John 1:5 we may have a case of *shifting context*, which is common in Scripture. In the first case, transitioning the scene of action from the cosmos in general down to Earth. In the second case, going from one level of meaning, spiritual (heavenly), to a literal meaning of "light" in physicality, with reference back to the parallel chapter in Genesis.

The electromagnetic field is like a fluid. But, what is *matter*? In fluids like air or water, one can form *solitons* (solitary waves that keep their shape like "particles"). For example, this happens when one blows smoke rings. One can see the process in water or fluids in videos on the internet. Note that smoke rings often assume not just a round shape, but a helical shape as well. What kind of soliton do we get if the electromagnetic field is stirred the right way? It is a unit charge of electricity, moving at the speed of light in a circular ring, which may become helical as more energy is added by absorption of certain wavelengths of light. This is a stable arrangement due to the magnetic force. Higher energies can also cause the unit charge ring to divide into 3 rings of 1/3 unit charge, intertwined around the helix. Rings of charge, circulating at the speed of light are what we call *fundamental particles*, the basic building blocks of matter, having real size and shape.

Once God has made the fundamental particles in this way, there is no problem (for God!) to fashion them into atoms, molecules, plasma, or bulk matter, as necessary to complete the creation. Of course, there is a lot more to this model which has been carefully worked out for several decades. For example, using positive and negative, right-handed and left-handed, 1/3-charge rings that appear in high energy experiments, it is possible to construct the zoo of all 100 fundamental particles and anti-particles of the Standard Model. There is still the mystery of the rarity of anti-particles, except to ask what would happen if particles and anti-particles had equal distribution? God favored us by stirring the field one way.

The particle rings are of size, shape, and charge distribution consistent with scattering experiments of Compton and Hofstadter. At that scale, the electric and magnetic forces are enormous. The particle rings are very powerful ring magnets that can lock into minimum energy, magic number, configurations to form atomic nucleii and atoms. Molecules form from the atoms according to the magic numbers. The magnetic field pinch on the charge ring balances the repulsion of electric force within the charge ring. Further, plasma confinement experiments by Winston Bostick demonstrated the natural tendencies of charge to form soliton configurations that had tensile strength. And, experiments by Hooper proved that the field always remains attached to the particles, just as Alfven, at the presentation of his Nobel Prize, disowned his earlier idea of magnetic separation and re-connection, now maintaining that the magnetic field is always continuous and connected. These results fit well with the idea that particles and charge *are* the field made into solitons. Unfortunately, theories, even wrong ones, get published and acquire a life of their own, such that astronomy texts and many astronomers still labor under the theory Alfven disowned as wrong.

The initially static, formless, and dark electromagnetic field, void of matter, would fill with light as soon as God made waves in it. (Depending on intensity, this compares with the Big Bang idea of so much energy, only electromagnetic waves would exist. Not saying that was the case; since we don't subscribe to the BB hypothesis.) God speaks to the field to form solitons, creating at once, both electric charge and what we call "matter." (This compares with some establishment theories about multiple dimensions balled up in tiny knots. Conjectures about extra dimensions are unnecessary, being replaced in providing necessary degrees of freedom by the actual 3-D geometry of the ring model.) [Now, you're the first kid on your block to know what matter *is*: electric charge moving in closed helical paths around a toroid at the speed of light! Even more fundamentally, it *is* the electromagnetic field, in the geometric form of solitons. However, you still don't know what that pesky "*m*" in Newton's equations *is*. Hint: *Mass* is *not* a fundamental property of "matter."]

Understanding the issue of separating light from darkness doesn't seem so straightforward as creation of light and matter. But, let's consider what astronomers have learned by surveys of vast areas of the cosmos. They've found galaxies along the surface of gigantic bubbles, with vast volumes inside the bubbles showing very little content. This lines up with plasma theory that bodies of plasma with different net charge form double layers around themselves to isolate the bodies electrically. from one another. In such a case, all the electrical action, the flows of charge in vast currents occur between the different bodies within the double layers. In Plasma Universe theory, these Birkeland currents can entrain huge amounts of matter, many times the amount actually ionized, due to the extremely strong electromagnetic force, compared to gravity. Parallel currents attract and twist around each other due to magnetic attraction, producing a pinch effect, which in astro-photos, gives the impression they could compress matter sufficiently to form galaxies and stars along the lines of the currents. Or, is it possible, the stars and galaxies are just bodies God created that are lit up by the Birkeland currents, as an outside power supply? Might look the same either way. Either way, we have the phenomenon of separation of charge causing currents to flow.

Consider a thunderstorm. A natural generator that ionizes *water*, separates charge, and lightning strikes! At night, one can see it separates light from dark. So, for the ancient people in the desert, God describes what He did in the cosmos, in terms familiar to them, speaking of water, to indicate matter and/or electric charge, and of light, to indicate electromagnetic radiation and/or electric charge, which appear together in a storm—because they had no understanding of electricity or plasma.

God divides opposite charges (charge = light) to create distinct bodies of plasma so that currents could flow to light up stars and nebulae. But as far as first mention of day and night, it might be well to compare the end of Revelation, where there's no need for the sun: as God is the light. Then, the "evening and the morning" merism could simply indicate the start and end of daily activity, with everything done in between as signifying which day it was.

Day Two is a very sparse description of creating a great expanse...in what? The plasma? To what end? Were the waters (matter, plasma) above (outside?) the expanse used to make the stars and other related things, while the waters (water, plasma?) beneath (inside?) used to make the Earth? Everything after Day Two seems rather down to earth, or seen from Earthly perspective. But what happened on the second day while all the "expanding" was going on? Did it have to do with forming a giant plasma bubble, or lesser plasma body around Earth, or the whole cellular structure of the universe? If so, *double layers* might be called the firmament? This idea is different from, but inclusive of, the usual perspective Harbin gives. Space probes have reached beyond the heliopause and confirmed the change in electrical status. Is all the expanding causing the red shift; or, is that just due to the extinction effect and the fact that light has to travel a long way through plasma? More questions than answers.

All that has been lacking to start analyses such as suggested in Harbin's (and Andrew Repp's, "Groundwork for Creation Cosmology," in this same issue of *CRSQ*, which support each other so well they're like Luke and Acts) has been a physical model of the fundamental particles working under classical Laws of Electrodynamics, to *unite* the smallest and largest scales of God's Work in Creation. The writer hopes this physical model and how it might fit into the first two creation days does justice to the authors' hermeneutical standard, without conflict to acceptable translations of Genesis 1.

Many of the disputes about the timing and order of the Genesis 1 account that the Creation community has endured over decades may be due to different levels of literal meaning that can be legitimately attached to various Scripture passages. This is not simply about different translations or interpretations, but the fact that Scripture given by God can have multiple actual meanings, both literal and metaphorical, embedded in the writing. The writer noticed this in studying John 1 intensively, and that is the parallel passage to Genesis 1—so why shouldn't it exhibit the same property? Consider how Dr. John Sanford has teased out different connections between the genes in DNA when it gets wrapped up in three dimensions. God created the DNA, which bears a language of its own. Thus, reasonable to expect that Scripture passages could all be related in different ways, not to equivocate, but to enhance with more understanding. This is not about supposed "Bible codes," but, as an example, it could be about information theory, such as offered by Dr. Werner Gitt, with its five levels of meaning. Or, different types of knowledge, as described by philosophers, like Dr. J.P. Moreland, et al.

Structure is another consideration that ties in with multiple meanings. The authors say that Genesis 1:1 is a summary statement packed with meaning. But, it also stands on its own, packed with meaning. As the start of an inclusio, which the writer takes to end with Genesis 2:1, it has one function as summary. On its own, Genesis 1 is a powerful blast of an announcement in Heaven and Earth, that the old Satanic order is done! Keep in mind that Genesis 1 was written as a refutation of the cosmology and the supposed power of the pantheon of gods worshiped by the pagans all over the earth, but especially those of Egypt, from which the soon-to-be Israelites had just come. As each day is enumerated, this or that pagan god is renounced and True God glorified.

Ancient literature was not necessarily written in chronological order, even as an historical account, such as this. Until the fourth day, when dynamical time was established, one might ask if God used an atomic clock to measure the same amount of time as a solar or siderial day, or if the "day" was established, not by "absolute time," but characterized by the activity done in it. That could seem a shorter or longer time if we had been there—but we weren't. Chapter 2 fills out details of creation—but not in the same chronological order as Chapter 1. Could some of the activities ascribed to a particular day in Genesis 1 actually overlap with parts of other days? The whole of Scripture militates for a short age, stating that life is temporal and fleeting, and that things are wearing out. Thus, the writer will not be arguing that the days of Genesis 1 are any long time in a meaningful sense, such as, if we could have been there to experience them.

There is a supposed problem with entropy, whether the 2nd Law was in effect from the beginning, or instituted on one of the days of creation, or only at the time of the Fall. Since God gave every green plant to be food for man and beast in Genesis 1:30, does the process of digestion and nourishment imply the 2nd Law was in effect before the Fall? Yes, and the Fall was a spiritual death, judging by the fact Adam lived over 900 years. The curse was not the 2nd Law, but removal from access to the Tree of Life, which appears again in Revelation 2 and 22, stated to be for the healing of the nations. Thus, until the new Heaven and new Earth arrived, men were not permitted to live too long accumulating sins to their detriment. Ultimately, it was for their benefit, and the salvation of mankind. Apparently, in the "very good" original creation, no one had to worry about the 2nd Law; because they had the Tree of Life to counteract its effects.

Historically, men might have envisioned God first creating little round balls called "atoms," then commanding the atoms to obey the laws of physics. Electric charge on atoms, or "particles" was then seen as an accident, or epiphenomenal to the particles. The electromagnetic field was seen as contingent on the particles. Why the laws would work on the particles was mysterious. The classical particle theory described above is radically different from that outlook, and the magnificent creative genius of Our Creator much magnified by it. God makes one essence, one substance, the electromagnetic field, such that it obeys its own laws of electrodynamics, co-extant with it, and from which everything in the physical universe is made, and from which all the forces are derived. The particles are contingent on the field and its laws, *not* the other way around. Ultimate intelligence makes everything from the one simplest thing. All forces derive from the complete set of independent laws of electrodynamics and the geometry of particles formed from the field.

It is interesting to note that unlike the laws of electrodynamics, which were discovered and tested experimentally in an active, precise, and positive sense in the laboratory, the laws of thermodynamics are tested passively by statistical means. As Dr. Hugh Ross once put it to the writer, "The 2nd Law is not proven by deduction, but by the fact that all the air molecules in the room don't run over to the corner and suffocate us." So, the 2nd Law is in a different class than the laws of electrodynamics, not being made to govern itself, but to observe the traffic. Whether and how it might have been involved with Creation is beside the point. The laws of electrodynamics are sufficient to predict the heat death because charged particles in motion radiate electromagnetic energy which gets dispersed.

The bugaboos about special relativity making problems for cause and effect, light travel time and other related things are negated. God's omnipresence is taken to mean that we are all immediately in God's presence, no matter where we are; hence, the entire physical universe is also immediately under His supervision. God can act *at the same moment of time* all over the universe. If He can create the *most complicated* thing in the universe, mankind, "while we wait," as it were, can He not, at the same time, be filling up those large, but *very simple* gas bags we call stars?

The writer wishes to thank those who labored so long with Common Sense Science, Inc., to work out and present the concepts upon which the above-described model is based, especially Dr. Charles William Lucas, Jr., the late David Bergman, Greg D. Volk, and others, not to mention the plasma physicists of renown. The result of their combined efforts is a worldview with sensible physical and cosmological models far more satisfying to mind and spirit than the academic establishment has so far entertained. Also, to be thanked are authors Harbin and Repp for their excellent articles inspiring this discussion.

George P. Drake
California City, CA

Media Reviews

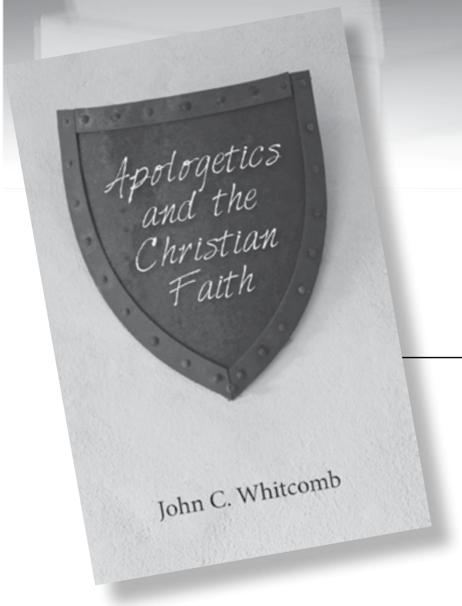

Apologetics and the Christian Faith

by John C. Whitcomb

Whitcombministries.org,
2024, 77 pages, $7.99

Theologian John Whitcomb (1924–2020) was a pioneer in the modern creation movement. He also helped guide the CRS board during the early decades of the Society. This short book is the text of lectures Whitcomb gave at Dallas Seminary during 1977. That same year the material was also published in the Dallas journal *Bibliotheca Sacra*. Today, 50 years later, Whitcomb's words remain relevant in evaluating our creation research efforts.

Whitcomb promotes an approach to evangelism called presuppositional apologetics. He was in turn a student of the Dutch-American theologian Cornelius Van Til (1895–1987). The presuppositional label comes from the central tenet that we must presuppose the supernatural revelation of Scripture as the final arbiter of truth. This approach contrasts with rational and semi-rational (evidential) apologetics in which human intellect and reasoning are used in the effort to demonstrate God's existence.

In this book the term *Christian evidences* refers to the rich treasury of data which supports the Biblical worldview, including the 50-year archive of the *CRS Quarterly*. Evidences include archaeological, historical, philosophical, psychological, and scientific findings. Whitcomb makes two compelling statements regarding this information. First, it alone is incapable of guiding a person into the kingdom of God. No matter how convincing may be such data, even including Biblical miracles, people simply are non-rational in evaluating the evidence. "Not only does the unbeliever not seek and practice truth, he consistently suppresses whatever truth he does receive" (p. 19). In other words, for the nonbeliever, Christian evidences alone cannot lead to saving faith (p. 56).

Whitcomb's second statement is that God's Word along with the work of the Holy Spirit are essential to spiritual regeneration. "The biblical method of winning men to Christ, including the intellectuals of our day, is to lovingly, patiently and prayerfully present the true Gospel according to the Scriptures" (p. 24). On a personal note, Whitcomb explains that in his early efforts to win souls while a student at Princeton University, "I had underestimated the depth of man's rebellion against God, and I was unaware of the absolutely crucial part which the Word of God must have, through the convicting and illuminating work of the Holy Spirit, in bringing sinful men to Christ" (p. 16).

What then is the value of Christian apologetics? After all, Whitcomb claims that evidences alone "can neither create, sustain, not increase true faith in God," (p. 56) for otherwise the greatest faith would be shown by those who have been exposed to such evidence (p. 56). Still, there remains great value in Christian evidences: "For the believer, they can provide a certain degree of intellectual satisfaction, deeper appreciation for the marvels and complexities of God's universe, and helpful background materials for the study of various aspects of biblical revelation. And for the unbeliever, they can be used to rouse interest and hold attention, if carefully handled by the Christian in conjunction with a true gospel witness" (p. 56). Some readers may not agree with Whitcomb's strong conclusions. It should be remembered, however, that Whitcomb dedicated his life to supporting the creation research efforts of the Creation Research Society.

The book provides detailed Scripture analysis in support of presuppositional apologetics. There are also provided a glossary of terms, Scripture index, and a Study Guide. The publisher distributes a variety of Whitcomb materials including his books, lectures, Bible charts, and seminary course packages.

Don DeYoung

Instructions to Authors

Submission

Electronic submissions of all manuscripts and graphics are preferred and should be sent to the editor of the *Creation Research Society Quarterly* in Word, WordPerfect, or Star-Office/Open Office (see the inside front cover for address). Printed copies also are accepted. If submitting a printed copy, an original plus two copies of each manuscript should be sent to the editor. The manuscript and copies will not be returned to authors unless a stamped, self-addressed envelope accompanies submission. If submitting a manuscript electronically, a printed copy is not necessary unless specifically requested by the *Quarterly* editor. Manuscripts containing more than 35 pages (double-spaced and including references, tables, and figure legends) are discouraged. An author who determines that the topic cannot be adequately covered within this number of pages is encouraged to submit separate papers that can be serialized.

All submitted manuscripts will be reviewed by two or more technical referees. However, each section editor of the *Quarterly* has final authority regarding the acceptance of a manuscript for publication. While some manuscripts may be accepted with little or no modification, typically editors will seek specific revisions of the manuscript before acceptance. Authors will then be asked to submit revisions based upon comments made by the referees. In these instances, authors are encouraged to submit a detailed letter explaining changes made in the revision, and, if necessary, give reasons for not incorporating specific changes suggested by the editor or reviewer. If an author believes the rejection of a manuscript was not justified, an appeal may be made to the *Quarterly* editor (details of appeal process at the Society's web site, www.creationresearch.org).

Authors who are unsure of proper English usage should have their manuscripts checked by someone proficient in the English language. Also, authors should endeavor to make certain the manuscript (particularly the references) conforms to the style and format of the *Quarterly*. Manuscripts may be rejected on the basis of poor English or lack of conformity to the proper format.

The *Quarterly* is a journal of original writings, and only under unusual circumstances will previously published material be reprinted. Questions regarding this should be submitted to the Editor (CRSQeditor@creationresearch.org) prior to submitting any previously published material. In addition, manuscripts submitted to the *Quarterly* should not be concurrently submitted to another journal. Violation of this will result in immediate rejection of the submitted manuscript. Also, if an author uses copyrighted photographs or other material, a release from the copyright holder should be submitted.

Appearance

Manuscripts shall be computer-printed or neatly typed. Lines should be double-spaced, including figure legends, table footnotes, and references. All pages should be sequentially numbered. Upon acceptance of the manuscript for publication, an electronic version is requested (Word, WordPerfect, or Star-Office/Open Office), with the graphics in separate electronic files. However, if submission of an electronic final version is not possible for the author, then a cleanly printed or typed copy is acceptable.

Submitted manuscripts should have the following organizational format:

1. Title page. This page should contain the title of the manuscript, the author's name, and all relevant contact information (including mailing address, telephone number, fax number, and e-mail address). If the manuscript is submitted by multiple authors, one author should serve as the corresponding author, and this should be noted on the title page.

2. Abstract page. This is page 1 of the manuscript, and should contain the article title at the top, followed by the abstract for the article. Abstracts should be between 100 and 250 words in length and present an overview of the material discussed in the article, including all major conclusions. Use of abbreviations and references in the abstract should be avoided. This page should also contain at least five key words appropriate for identifying this article via a computer search.

3. Introduction. The introduction should provide sufficient background information to allow the reader to understand the relevance and significance of the article for creation science.

4. Body of the text. Two types of headings are typically used by the *CRSQ*. A major heading consists of a large font bold print that is centered in column, and is used for each major change of focus or topic. A minor heading consists of a regular font bold print that is flush to the left margin, and is used following a major heading and helps to organize points within each major topic. Do not split words with hyphens, or use all capital letters for any words. Also, do not use bold type, except for headings (italics can be occasionally used to draw distinction to specific words). Italics should not be used for foreign words in common usage, e.g., "et al.", "ibid.", "ca." and "ad infinitum." Previously published literature should be cited using the author's last name(s) and the year of publication (ex. Smith, 2003; Smith and Jones, 2003). If the citation has more than two authors, only the first author's name should appear (ex. Smith et al., 2003). Contributing authors should examine this issue of the *CRSQ* or consult the Society's web site for specific examples as well as a more detailed explanation of manuscript preparation.

Frequently-used terms can be abbreviated by placing abbreviations in parentheses following the first usage of the term in the text, for example, polyacrylamide gel electrophoresis (PAGE) or catastrophic plate tectonics (CPT). Only the abbreviation need be used afterward. If numerous abbreviations are used, authors should consider providing a list of abbreviations. Also, because of the variable usage of the terms "microevolution" and "macroevolution," authors should clearly define how they are specifically using these terms. Use of the term "creationism" should be avoided. All figures and tables should be cited in the body of the text, and be numbered in the sequential order that they appear in the text (figures and tables are numbered separately with Arabic and Roman numerals, respectively).

5. Summary. A summary paragraph(s) is often useful for readers. The summary should provide the reader an overview of the material just presented, and often helps the reader to summarize the salient points and conclusions the author has made throughout the text.

6. References. Authors should take extra measures to be certain that all references cited within the text are documented in the reference section. These references should be formatted in the current *CRSQ* style. (When the *Quarterly* appears in the references multiple times, then an abbreviation to *CRSQ* is acceptable.) The examples below cover the most common types of references:

Robinson, D.A., and D.P. Cavanaugh. 1998. A quantitative approach to baraminology with examples from the catarrhine primates. *CRSQ* 34:196–208.

Lipman, E.A., B. Schuler, O. Bakajin, and W.A. Eaton. 2003. Single-molecule measurement of protein folding kinetics. *Science* 301:1233–1235.

Margulis, L. 1971a. The origin of plant and animal cells. *American Scientific* 59:230–235.

Margulis, L. 1971b. *Origin of Eukaryotic Cells*. Yale University Press, New Haven, CT.

Hitchcock, A.S. 1971. *Manual of Grasses of the United States*. Dover Publications, New York, NY.

Walker, T.B. 1994. A biblical geologic model. In Walsh, R.E. (editor), *Proceedings of the Third International Conference on Creationism* (technical symposium sessions), pp. 581–592. Creation Science Fellowship, Pittsburgh, PA.

7. Tables. All tables cited in the text should be individually placed in numerical order following the reference section, and not embedded in the text. Each table should have a header statement that serves as a title for that table (see a current issue of the *Quarterly* for specific examples). Use tabs, rather than multiple spaces, in aligning columns within a table. Tables should be composed with *14-point type* to insure proper appearance in the columns of the *CRSQ*.

8. Figures. All figures cited in the text should be individually placed in numerical order, and placed after the tables. Do not embed figures in the text. Each figure should contain a legend that provides sufficient description to enable the reader to understand the basic concepts of the figure without needing to refer to the text. Legends should be on a separate page from the figure. All figures and drawings should be of high quality (hand-drawn illustrations and lettering should be professionally done). Images are to be a minimum resolution of 300 dpi at 100% size. Patterns, not shading, should be used to distinguish areas within graphs or other figures. Unacceptable illustrations will result in rejection of the manuscript. Authors are also strongly encouraged to submit an electronic version (.cdr, .cpt, .gif, .jpg, and .tif formats) of all figures in individual files that are separate from the electronic file containing the text and tables.

Special Sections

Letters to the Editor:

Submission of letters regarding topics relevant to the Society or creation science is encouraged. Submission of letters commenting upon articles published in the *Quarterly* will be published two issues after the article's original publication date. Authors will be given an opportunity for a concurrent response. No further letters referring to a specific *Quarterly* article will be published.

Editor's Forum:

Occasionally, the editor will invite individuals to submit differing opinions on specific topics relevant to the *Quarterly*. Each author will have opportunity to present a position paper (2000 words), and one response (1000 words) to the differing position paper. In all matters, the editor will have final and complete editorial control. Topics for these forums will be solely at the editor's discretion, but suggestions of topics are welcome.

Book Reviews:

All book reviews should be submitted to the book review editor, who will determine the acceptability of each submitted review. Book reviews should be limited to 1000 words. Following the style of reviews printed in this issue, all book reviews should contain the following information: book title, author, publisher, publication date, number of pages, and retail cost. Reviews should endeavor to present the salient points of the book that are relevant to the issues of creation/evolution. Typically, such points are accompanied by the reviewer's analysis of the book's content, clarity, and relevance to the creation issue.

Author Copies:

CRSQ policy is that authors get 10 free copies of the issue containing their article, regardless of the number of co-authors. These free copies must be pre-ordered before the issue goes to press.

Creation Research Society
Membership/Subscription Application and Renewal Form

The membership/subscription categories are defined below:

1. **Voting Member** ....Those having at least an earned master's degree in a recognized area of science.
2. **Sustaining Member** ....Those without an advanced degree in science, but who are interested in and support the work of the Society.
3. **Student Member** ....Those who are enrolled full time in high schools, undergraduate colleges, or postgraduate science programs (e.g., MS, PhD, MD, and DVM). Those holding post-doctoral positions are not eligible. A graduate student with a MS degree may request voting member status while enrolled as a student member.
4. **Senior Member** ....Voting or sustaining members who are age 65 or older.
5. **Life Member** ....A special category for voting and sustaining members, entitling them to a lifetime membership in the Society.
6. **Subscriber** ....Libraries, churches, schools, etc., and individuals who do not subscribe to the Statement of Belief.

All members (categories 1–5 above) must subscribe to the Statement of Belief as defined on the next page.

Please complete the lower portion of this form and mail it with payment to CRS Membership Secretary, 1 W. Firestorm Way #145, Glendale, AZ 85306, or fax for credit card payment to (928) 636-1153. Applications may also be completed online at creationresearch.org.

This is a ☐ new ☐ renewal application for the subscription year beginning Summer 20____. *(Please type or print legibly.)*

Name ______________________________ Address ______________________________

City ____________________ State ________ Postal/Zip code ________ Country ______________

Phone (optional) ______________________ Email ______________________________

Degree ______________________________ Field ______________________________

Year granted ______________ Institution ______________________________

Presently associated with ____

I have read and subscribe to the CRS Statement of Belief. Signature ______________________________

For foreign orders, including Canadian, payment must be made in U.S. dollars by a check drawn on a U.S. bank, international money order, or credit card. *Please do not send cash.*

Indicate applicable category ⬇	*Indicate payment* ⬇			
	Paper**			
☐ Voting ☐ Sustaining	USA	Canada Mexico	Other countries	**Paper-less‡**
☐ Regular [per year]	☐ $53	☐ $73	☐ $93	☐ $35
☐ Senior [per year]	☐ $48	☐ $68	☐ $85	☐ $30
☐ Life member	☐ $600	☐ $600	☐ $600	☐ $600
☐ Student* [per year]	☐ $48	☐ $68	☐ $85	☐ $30
☐ Subscriber [per year]	☐ $56	☐ $76	☐ $96	☐ $38

* Student members are required to complete the bottom portion of this form.
NOTE: Student members may qualify for the *Future Leaders Sponsorship* program.
See the CRS website at www.creationresearch.org for details.
** Rates for the paper option include postage for First Class Mail International

‡ **PAPERLESS option:** You may opt out of receiving paper copies of the CRS periodicals (*CRS Quarterly* and *Creation Matters*). By choosing this option you may register for access to the Premium Area of the website, where you may view or download electronic (PDF) versions of these publications. Of course, regular members and subscribers may also have access to the Premium Area. Only members, however, will have access to the Members Exclusive Area of the website.

Member/Subscriber $_____ per year
x ______ years
SUBTOTAL $__________
Optional contribution + $__________
Life membership + $__________
TOTAL $__________

☐ Visa ☐ MasterCard ☐ Discover
☐ American Express ☐ Check/money order
Card number ______________________
Expiration date (mo/yr) ______________
Phone number (_____) ______________
Signature ______________________

Student Members **are required to complete the following:**

School or institution now attending ______________________
____

Your current student status: ☐ high school; ☐ undergraduate;
graduate program ☐ MS ☐ PhD; ☐ other ______________

Year you expect to graduate or complete your degree ____________

Major, if college or graduate student ______________________

Signature ______________________________

Order Blank for Past Issues

Cost of complete volumes (per volume):	members (all categories) – $18.00 + S/H
	nonmembers and subscribers (libraries, schools, churches, etc.) – $25.00 + S/H
Cost of single issues (per issue):	members (all categories) – $5.00 + S/H
	nonmembers and subscribers (libraries, schools, churches, etc.) – $7.00 + S/H

	Number			
Volume	**1**	**2**	**3**	**4**
23	☐	☐	☐	☐
24	☐	☐	☐	☐
25	☐	☐	☐	☐
26	☐	☐	☐	☐
27	☐	☐	☐	☐
28	☐	☐	☐	☐
29	☐	☐	☐	☐
30	☐	☐	☐	☐
31	☐	☐	☐	☐
32	☐	☐	☐	☐
33	☐	☐	☐	☐
34	☐	☐	☐	☐
35	☐	☐	☐	☐

	Number			
Volume	**1**	**2**	**3**	**4**
36	☐	☐	☐	☐
37	☐	☐	☐	☐
38	☐	☐	☐	☐
39	☐	☐	☐	☐
40	☐	☐	☐	☐
41	☐	☐	☐	☐
42	☐	☐	☐	☐
43	☐	☐	☐	☐
44	☐	☐	☐	☐
45	☐	☐	☐	☐
46	☐	☐	☐	☐
47	☐	☐	☐	☐
48	☐	☐	☐	☐

	Number			
Volume	**1**	**2**	**3**	**4**
49	☐	☐	☐	☐
50	☐	☐	☐	☐
51	☐	☐	☐	☐
52	☐	☐	☐	☐
53	☐	☐	☐	☐
54	☐	☐	☐	☐
55	☐	☐	☐	☐
56	☐	☐	☐	☐
57	☐	☐	☐	☐
58	☐	☐	☐	☐
59	☐	☐	☐	☐
60	☐	☐	☐	☐
61	☐	☐	☐	

Add 20% for postage (**for U.S. orders:** min. $6, max. $18; **for Canadian orders:** min. $10, no max.; **for other foreign orders:** min. $15, no max.)

Total enclosed: $______________

Make check or money order payable to Creation Research Society. Please do not send cash. For foreign orders, including Canadian, please use a check in U.S. funds drawn on a U.S. bank, an international money order, or a credit card.

(Please type or print legibly)

Name ______________________________ Address ____

City ____________________________ State _______ Zip _____________ Country _____________________

☐ Visa ☐ MasterCard ☐ Discover ☐ American Express Card number ___________________________________

Expiration date (mo/yr) ____________ Signature ____

Mail to: Creation Research Society, 1 W. Firestorm Way #145, Glendale, AZ 85306, USA

Creation Research Society

History—The Creation Research Society was organized in 1963, with Dr. Walter E. Lammerts as first president and editor of a quarterly publication. Initially started as an informal committee of 10 scientists, it has grown rapidly, evidently filling a need for an association devoted to research and publication in the field of scientific creation, with a current membership of over 600 voting members (graduate degrees in science) and about 1000 non-voting members. The *Creation Research Society Quarterly* is a peer-reviewed technical journal. It has been gradually enlarged and modified, and is currently recognized as one of the outstanding publications in the field. In 1996 the *CRSQ* was joined by the newsletter *Creation Matters* as a source of information of interest to creationists.

Activities—The Society is a research and publication society, and also engages in various meetings and promotional activities. There is no affiliation with any other scientific or religious organizations. Its members conduct research on problems related to its purposes, and a research fund and research center are maintained to assist in such projects. Contributions to the research fund for these purposes are tax deductible. As part of its vigorous research and field study programs, the Society operates the Van Andel Creation Research Center in Glendale, Arizona.

Membership—Voting membership is limited to scientists who have at least an earned graduate degree in a natural or applied science and subscribe to the Statement of Belief. Sustaining membership is available for those who do not meet the academic criterion for voting membership, but do subscribe to the Statement of Belief.

Statement of Belief—Members of the Creation Research Society, which include research scientists representing various fields of scientific inquiry, are committed to full belief in the biblical record of creation and early history, and thus to a concept of dynamic special creation (as opposed to evolution) both of the universe and the earth with its complexity of living forms. We propose to re-evaluate science from this viewpoint, and since 1964 have published a quarterly of research articles in this field. *All members of the Society subscribe to the following statement of belief:*

1. The Bible is the written Word of God, and because it is inspired throughout, all its assertions are historically and scientifically true in all the original autographs. To the student of nature this means that the account of origins in Genesis is a factual presentation of simple historical truths.
2. All basic types of living things, including humans, were made by direct creative acts of God during the Creation Week described in Genesis. Whatever biological changes have occurred since Creation Week have accomplished only changes within the original created kinds.
3. The Great Flood described in Genesis, commonly referred to as the Noachian Flood, was a historical event worldwide in its extent and effect.
4. We are an organization of Christian men and women of science who accept Jesus Christ as our Lord and Savior. The act of the special creation of Adam and Eve as one man and woman and their subsequent fall into sin is the basis for our belief in the necessity of a Savior for all people. Therefore, salvation can come only through accepting Jesus Christ as our Savior.

iDINO II

Investigation of Dinosaur Intact Natural Osteo-tissue

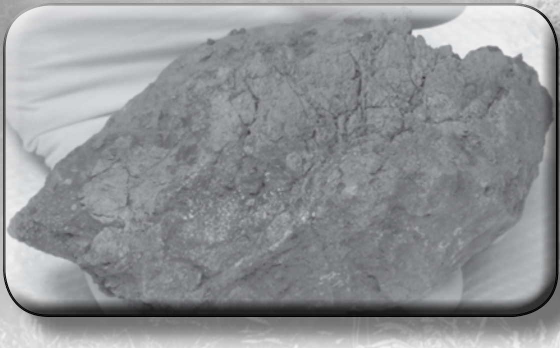

A fragment of the *Triceratops* brow horn. Fragments, such as this one, still contain tissue and cells.

How can pliable, stretchable tissue survive inside dinosaur fossils for over 65 million years?

How can this tissue still contain intact cells and even dinosaur proteins?

How can this fragile biological material survive for so long?

The answer to these questions directly challenges the current, evolutionary-biased, geologic timescale.

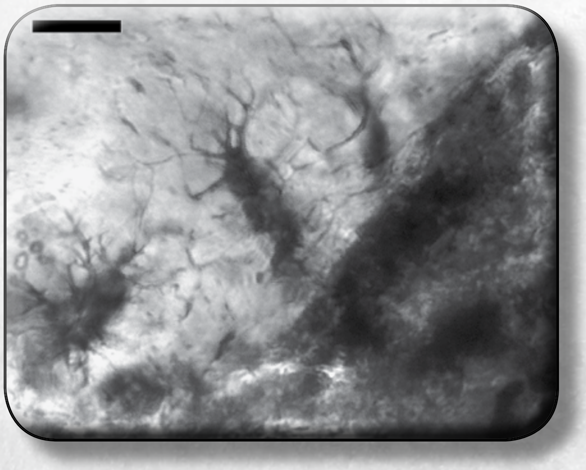

Microscopic examination of tissue extracted from a *Triceratops* horn reveals bone cells still present.

The Creation Research Society began its iDINO research initiative for the purpose of studying soft tissue in dinosaur fossils. The first phase of the project detected pliable, unfossilized tissue in a brow horn of a *Triceratops*. Within this tissue were intact osteocytes (bone cells). Some results from the iDINO project have been published in a technical microscopy journal and presented at an international microscopy conference. The Spring 2015 issue of the *Creation Research Society Quarterly* also features a special report of the iDINO project. Plus, to further spread the important information about soft tissue, the Society is developing a video (Echoes of the Jurassic).

The **second phase** of the project (iDINO II) will look more extensively at the process of tissue preservation. Evolutionists have offered various theories of how this tissue could survive for millions of years. iDINO II will methodically investigate these preservation claims, assessing their plausibility.

The iDINO results have already provided a strong challenge to the evolutionary worldview. More extensive and detailed examination may provide even stronger evidence that the age of dinosaur fossils is far less than 65 million years. To this end, the Society continues to seek those willing to fund this project with either one-time gifts or monthly donations.

For more information contact us at (928) 636-1153 or crsvarc@crsvarc.com.

Also visit http://tinyurl.com/nphm2c4 for project updates and details.

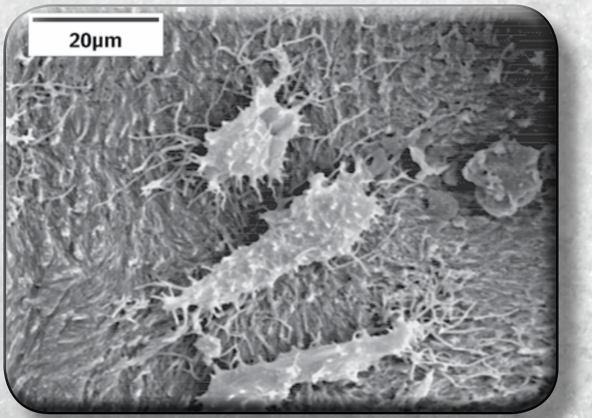

Electron microscope picture of intact bone cells still in tissue extracted from a *Triceratops* horn.

V61N3